ACS SyntheticBiology

Research Article

pubs.acs.org/synthbio

The All *E. coli* TX-TL Toolbox 2.0: A Platform for Cell-Free Synthetic Biology

Jonathan Garamella,[†] Ryan Marshall,[†] Mark Rustad,[†] and Vincent Noireaux*

School of Physics and Astronomy, University of Minnesota, 115 Union Street SE, Minneapolis, Minnesota 55455, United States

Supporting Information

ABSTRACT: We report on and provide a detailed characterization of the performance and properties of a recently developed, all *Escherichia coli*, cell-free transcription and translation system. Gene expression is entirely based on the endogenous translation components and transcription machinery provided by an *E. coli* cytoplasmic extract, thus expanding the repertoire of regulatory parts to hundreds of elements. We use a powerful metabolism for ATP regeneration to achieve more than 2 mg/mL of protein synthesis in batch mode reactions, and more than 6 mg/mL in semicontinuous mode. While the strength of cell-free expression is increased by a factor of 3 on average, the output signal of simple gene circuits and the synthesis of entire bacteriophages are increased by orders of magnitude compared to previous results. Messenger RNAs and protein degradation, respectively tuned using *E. coli* MazF interferase and ClpXP AAA+ proteases, are characterized over a much wider range of rates than the first version of the cell-free toolbox. This system is a highly versatile cell-free platform to construct complex biological systems through the execution of DNA programs composed of synthetic and natural bacterial regulatory parts.

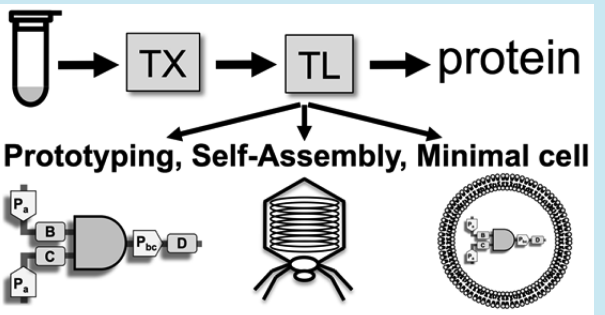

KEYWORDS: *cell-free transcription−translation, gene circuits prototyping, biosynthesis, self-assembly, minimal cell*

Cell-free transcription−translation is becoming an effective technology for *in vitro* synthetic biology and bioengineering. In recent years, DNA-dependent *in vitro* protein synthesis has rapidly expanded its range of applications to research areas such as biological network prototyping by accelerating the build−design−test cycle,[1−7] artificial cell systems and biological physics,[8−16] nanotechnologies,[17−19] metabolic and chemical engineering,[20−23] medicine,[24−27] and the production of functional membrane proteins.[28−30] *In vitro* protein synthesis is increasingly employed as a means to construct, understand and interrogate complex biochemical systems, from molecular to cell-sized scales.

The hybrid bacteriophage-*Escherichia coli* system, invented in the 90s, is the most popular cell-free TX-TL platform.[31] Commercially available, this system is useful as an alternative to recombinant protein expression and for molecular applications such as protein evolution,[32−34] proteomics,[35−37] and production of therapeutics.[38] Transcription is performed by a bacteriophage RNA polymerase with its promoter, usually T7, due to its simplicity, high specificity, and strength. The translation machinery is provided by a cytoplasmic extract, often from *E. coli*. In those systems, protein synthesis can reach more than 1 mg/mL. The PURE system, also based on T7, allows working in a simpler environment than extract-based systems.[39] While hybrid T7 systems are useful for a vast array of applications, their transcription consists of only a few elements−a serious limitation in a thriving era of synthetic biology and gene circuit engineering. Elementary gene circuits have been executed in bacteriophage cell-free systems,[1,5] but those platforms are not well suited for the construction of complex *in vitro* dynamical systems programmed with DNA as working with so few promoters is too limiting. The development of a synthetic T7 transcription toolbox could provide an alternative to this limitation,[40] although it has to be tested in cell-free conditions.

In that perspective, the development of an all *E. coli* cell-free TX-TL system that recapitulates the entire sigma factor transcription scheme was a major improvement to the existing *in vitro* protein synthesis technology.[41] By expanding transcription to hundreds of regulatory elements, from *E. coli* and other bacteria, this platform has proven useful for numerous applications, especially for testing synthetic and natural genetic parts,[2] for prototyping gene circuits[42] and for constructing minimal cell systems.[8] In this work, we build on the first all *E. coli* platform[41] to deliver the toolbox 2.0, a unique cell-free TX-TL portal for the construction of complex biochemical systems through the execution of DNA programs *in vitro*. We characterize the performance of this improved cell-free platform for elementary gene circuits, phage synthesis and bottom-up minimal cells.

The regeneration of ATP in cell-free TX-TL systems is one of the key components directly related to protein synthesis. The process of protein translation is highly demanding in chemical energy, with an equivalent of four ATP per amino acid added to

Received: December 21, 2015

DOI: 10.1021/acssynbio.5b00296
ACS Synth. Biol. XXXX, XXX, XXX−XXX

the primary chain. The all *E. coli* system reported in this work integrates a novel metabolism for ATP regeneration. This metabolism, based on a phosphate donor and a carbon source,[43] extends the kinetics of TX-TL by activating the glycolysis pathway and by recycling inorganic phosphate, a reaction byproduct that inhibits expression. Cell-free protein synthesis yields are increased by a factor of 2 to 3 on average, depending on the expressed *E. coli* sigma transcription factor. In batch mode reaction, the production of a reporter protein can reach more than 2 mg/mL (active fluorescent). Surprisingly, output signals of simple gene circuits[41] and the synthesis of coliphages[19] are increased by orders of magnitude. We describe in detail methods to accelerate and quantify mRNA degradation with the interferase MazF, as well as achieve high protein degradation with the ClpXP proteases, over a much larger range of rates compared to our previous approaches.[44] Finally, we show that the cell-free reactions can be encapsulated in cell-sized liposomes for synthetic cell applications. Our results demonstrate how essential the metabolism supporting *in vitro* protein synthesis is to create a powerful, versatile, and easy to use all *E. coli* cell-free TX-TL toolbox.[43]

RESULTS AND DISCUSSION

Overview of the Platform. The goal of this work was first to construct the most versatile and powerful all *E. coli* cell-free TX-TL systems for *in vitro* synthetic biology. We worked on four parts of the TX-TL reaction: transcription, translation, mRNA degradation and protein degradation (Figure 1a). In doing so, we aimed to deliver a quantitative and highly flexible platform, with maximum modularity, capable of carrying out complex dynamical behaviors and active self-assemblies through the execution of synthetic or natural DNA programs.

An *E. coli* cytoplasmic extract, absent any remaining living *E. coli* cells (Supplementary Figure S1), provides the TX-TL molecular machineries. One of the unique features of this platform is at the level of transcription. Unlike conventional hybrid bacteriophage systems, transcription is solely based on the endogenous core RNA polymerase with the primary sigma factor 70 (σ_{70}).[45] The major advantage is the extension of the transcription repertoire to hundreds of regulatory parts from *E. coli* and other bacteria. To achieve more than 2 mg/mL of reporter protein synthesized in batch mode reactions through an *E. coli* promoter specific to σ_{70}, a novel metabolism based on a phosphate donor and a carbon source energizes translation. This metabolism couples ATP regeneration and inorganic phosphate recycling.[43] Concentrations of the cell-free TX-TL components are estimated based on the dilution factor of the *E. coli* cytoplasm (Supplementary Table S1).

To emulate dynamical systems coded by genetic circuits *in vitro*, tuning the degradation rates of mRNAs and proteins is as important as strong synthesis, especially in batch mode reactions with fixed-volume. As previously demonstrated for this system, mRNA and protein degradation is described by a first and a zeroth order chemical kinetic, respectively.[46] Using the *E. coli* mRNA interferase MazF,[44] we can adjust transcript degradation rates at will in a wide range of lifetimes (18 to 0 min for deGFP mRNA). The degradation of proteins tagged with ClpXP specific degrons can be accelerated up to 250 nM/min (based on deGFP measurements).

In addition to deGFP, eight reporter proteins were expressed: deCFP, deYFP, dmVenus, dTomato, TagRFP-T, mApple, mRuby, mmCherry. The DNA sequence of some of those reporters has been modified in N and/or C terminal to increase

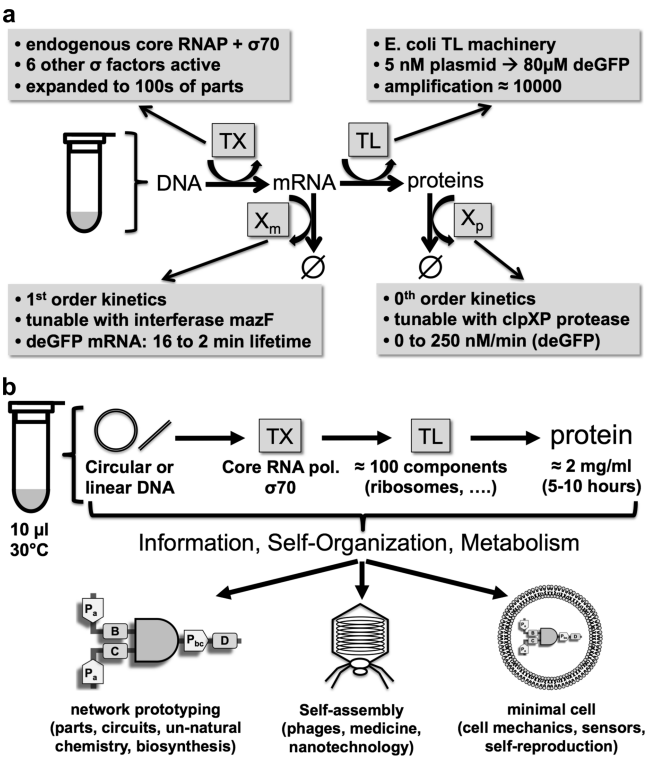

Figure 1. Overview of the all *E. coli* cell-free toolbox 2.0 characteristics and scope of application. (a) The four parts of the protein synthesis reactions (TX: transcription, TL: translation, X_m: mRNA degradation, X_p: protein degradation) were characterized and engineered so as to provide a powerful system. (b) The toolbox 2.0 is a highly flexible, easy-to-use cell-free platform for applications at molecular (network prototyping), supra-molecular (self-assembly) and cell-sized scales (minimal cell, microfluidics).

translation, according to our earlier findings with deGFP (Supplementary Table S2). The maturation time of deGFP, a more translatable, truncated version of eGFP,[45] was estimated to be 16.2 min using a new fluorescence-based assay (Supplementary Figure S2). deGFP has the shortest maturation time among the nine reporter proteins tested, as observed from the kinetics of expression (Supplementary Figure S3). In contrast, the maturation of red reporter proteins is slow, in agreement with other *in vitro* measurements.[47] The excitation and emission spectra of all the reporter proteins were determined (Supplementary Figure S4 and S5), and their respective fluorescence intensity was measured at their optimum excitation/emission wavelengths (Supplementary Table S3).

The scope of toolbox 2.0 applications ranges from molecular scales to minimal cell systems (Figure 1b). Applications in each of those research areas have already been shown and are cited in this article. Cell-free expression is compatible with various setups: 1.5 mL tubes, well plates, semi- continuous systems, microfluidics, and liposomes. In large volumes of 5−20 μL, reactions are performed at 29−30 °C, an optimum temperature for synthesis, in either 384 or V-bottom 96 well plates.

Cell-Free Synthesis: Strength and Repertoire. A specific set of plasmids "pTXTL" has been devised for toolbox 2.0. These plasmids are amplified through *E. coli* using standard procedures. The design is highly modular so as to easily change either promoter, UTR, gene or terminator (Supplementary Figure S6). About one hundred ready-to-use plasmids are available (Supplementary Table S4).

DOI: 10.1021/acssynbio.5b00296
ACS Synth. Biol. XXXX, XXX, XXX−XXX

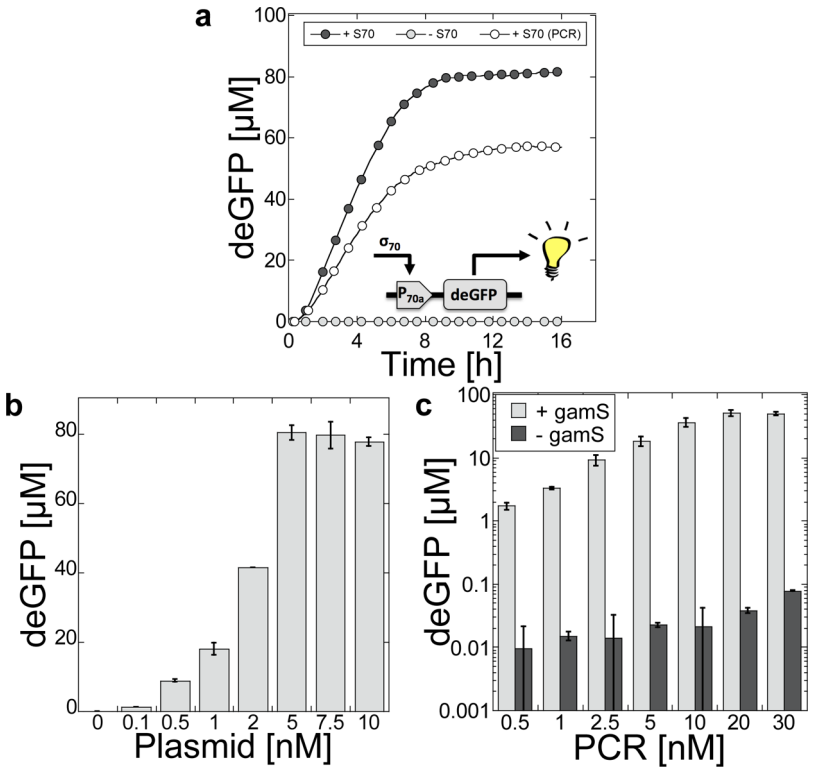

Figure 2. Characterization of deGFP cell-free expression with an *E. coli* promoter specific to the housekeeping σ_{70}. (a) Kinetics of expression. Plasmid P_{70a}-deGFP fixed at 5 nM and PCR at 20 nM. Negative control: addition of Rifampicin, an inhibitor of the *E. coli* RNA polymerase. Inset: schematic of the circuit. Both circular plasmid and linear PCR product of the plasmid can be used. (b) Synthesis of active fluorescent deGFP *versus* plasmid concentration. Response is linear up to 2−3 nM plasmid and saturates above 5 nM. (c) Synthesis of active fluorescent deGFP *versus* PCR product concentration. In the presence of gamS, response is linear up to 10 nM PCR and saturates above 20 nM. Protein synthesis is negligible when gamS is not added to the reaction.

Table 1. Batch Mode Cell-Free Expression for 14 Transcription Factors[a]

transcription factor	Mg-glutamate [mM]	K-glutamate [mM]	plasmid encoding the transcription factor [nM]	reporter plasmid [nM]	deGFP [μM] (mg/mL)	
			Plasmids			
σ_{70}	3−4	80	N/A	5	81	(2.05)
σ_{19}	3	80	2	15	35	(0.89)
σ_{19}-ssrA	3	80	5	15	52	(1.32)
σ_{24}	3	120	1	20	70	(1.78)
ompA-σ_{24}	3	120	5	20	55	(1.40)
σ_{28}	3	80	0.5	15	77	(1.95)
σ_{28}-ssrA	3	80	0.5	15	81	(2.05)
σ_{32}	3−5	80	0.1	15	89	(2.26)
σ_{32}-ssrA	3	80	0.1	15	84	(2.13)
σ_{38}	4	80	0.5	20	75	(1.90)
ompA-σ_{38}	4	80	0.5	20	63	(1.60)
σ_{54}/NtrC	7	80	1/0.1	20	27	(0.68)
T3 RNAP	4	100	0.2	2	74	(1.88)
T7 RNAP	4	100	0.2	2	87	(2.35)
			PCR			
σ_{70}	5	60	N/A	20	50.5	(1.28)
T7 RNAP	3	80	1	10	36	(0.91)

[a]Except for the endogenous σ_{70}, deGFP was synthesized through two-stage transcriptional activation cascades (Supplementary Figure S8a-i). The optimum magnesium glutamate, potassium glutamate, and plasmid concentrations were determined (end-point measurements). 1 mg/mL deGFP = 39.4 μM, 1 mg/mL His-deGFP = 36.76 μM.

Transcription is based on the core RNA polymerase and the primary sigma factor σ_{70} present in the cytoplasmic extract. All of the circuitries start with σ_{70} specific promoters. Cell-free expression was first characterized with the plasmid P_{70a}-deGFP and a linear PCR product of this plasmid, with about 200−300 bases upstream and downstream of the coding parts. In the case of using PCR products, the lambda gamS protein is added to the reaction (3−5 μM) to block degradation of the linear DNA by

DOI: 10.1021/acssynbio.5b00296
ACS Synth. Biol. XXXX, XXX, XXX−XXX

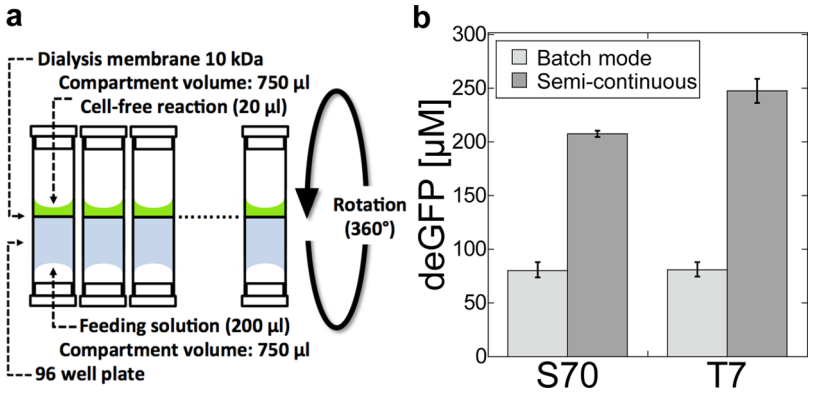

Figure 3. Cell-free expression of deGFP in semicontinuous mode. (a) Schematic of the system. A 96 well plate with two compartments separated by a dialysis membrane (MWCO 10 kDa) was used. The plate was rotated for mixing while incubated at 29 °C. (b) Synthesis of deGFP through P_{70a}-deGFP and the cascade P_{70a}-T7rnap → $T7P_{14}$-deGFP. After 24 h of incubation, more than 5 mg/mL (P_{70a}-deGFP) and 6 mg/mL (P_{70a}-T7rnap → $T7P_{14}$-deGFP) were produced.

the recBCD complex, the major DNA exonuclease present in the extract. The promoter P_{70a}, previously described as P_{70},[45] originates from the lambda phage repressor Cro promoter with the two operators sites OR_2 and OR_1 overlapping the −10 and −35 sequences. This σ_{70} *E. coli* promoter is the strongest so far reported. Unless otherwise stated, plasmids contain the untranslated region UTR1 from bacteriophage T7,[45] one of the strongest bacterial untranslated regions, routinely used in recombinant protein expression. In batch mode, cell-free expression lasts about 8−10 h (Figure 2a), at the end of which 2 and 1.3 mg/mL of active (fluorescent) reporter proteins are produced with plasmid and linear DNA, respectively. Protein production increases linearly within the first 4−5 h. Protein synthesis as a function of DNA template is linear up to 2−3 nM plasmid and up to 10 nM for PCR product (Figure 2b and 2c). With no gamS added to the reaction, protein synthesis is negligible. The saturation observed above those concentrations is due to a depletion of TX-TL machineries onto either DNA (RNA polymerase) or messengers (ribosomes).[48] Cell-free expression from batch to batch, using the same biochemical settings (reaction composition is the same except for the four different extracts), shows excellent reproducibility and consistency (Supplementary Figure S7).

We then characterized a dozen transcriptional activation cascades (Table 1, Supplementary Figures S8a-i) including: the six other *E. coli* sigma factors, which reconstitutes the entire *E. coli* sigma factors transcription scheme, and the two bacteriophage RNA polymerases T7 and T3. Five degradable versions were constructed: σ_{19}-ssrA, ompA-σ_{32}, σ_{28}-ssrA, σ_{32}-ssrA, ompA-σ_{38}, where ompA and ssrA are specific degrons of the ClpXP complex. Optimum magnesium and potassium settings fall into a rather small range of concentrations for the entire set of transcription factors. In batch mode reactions, more than 2 mg/mL of fluorescent reporter proteins are synthesized in the case of σ_{70}, σ_{28}-ssrA, σ_{32}, σ_{32}-ssrA, and T7, reaching 2.35 mg/mL of active fluorescent reporter protein for T7. Only σ_{19} and σ_{54}/NtrC have yields smaller than 1 mg/mL. At low transcription factor plasmid concentration, expression with σ_{19}-ssrA, ompA-σ_{32}, σ_{28}-ssrA, σ_{32}-ssrA is lower due to degradation. Only expression with σ_{32} and σ_{38} and their degradable counterparts are similar at low plasmid concentration, which indicates that σ_{32}−ssrA and ompA-σ_{38} are not significantly degraded by ClpXP. Kinetics of deGFP expression are similar for most of the transcription factors, with about 8−10 h of protein accumulation, except for T7 and T3 which are shorter, and σ_{38} which is slightly longer. A marked leak is observed for the promoter P_{32a} only (Supplementary Figure S8e). Without adding P_{70a}-σ_{32}, about 20 μM of deGFP is produced. It is known that σ_{32} is slightly expressed in *E. coli* at 37 °C.[49] To determine whether the leak comes from σ_{70} through the P_{32a} promoter or from the presence of σ_{32} in the extract, we cloned the anti σ_{70} gene asiA[50] from the bacteriophage T4 under a T7 promoter. A decrease of deGFP expression through the promoter P_{70a} is observed when Asia is expressed (Supplementary Figure S9), as opposed to the expression through the promoter P_{32a}. Consequently, σ_{32} is the only sigma factor other than σ_{70} present in the reaction.

The crosstalks between transcriptional activation units were characterized at fixed plasmid concentrations in the linear regime of protein synthesis (Supplementary Table S5). Our observations are in agreement with previous measurements[41] and with the affinity of each sigma factor for the core RNA polymerase.[51] Sigma factors σ_{28} and σ_{38} are the strongest and weakest competitors, respectively.

The all *E. coli* cell-free toolbox 2.0 can be used either as a separate-component system where the reaction is composed manually from each component (cytoplasmic extract, energy mixture, amino acid mixture, magnesium and potassium glutamate, PEG, DNA and water), or as a prepackaged reaction that just requires the addition of DNA and water. No difference is observed between these two packaging formulations (Supplementary Figure S10).

Semicontinuous Cell-Free TX-TL. To increase protein synthesis yields and extend the reaction lifetime, a semicontinuous system is created by feeding the reaction with nutrients through a dialysis membrane of molecular mass cutoff 10 kDa. Such setups have already been demonstrated.[41,52,53] To show that toolbox 2.0 can be used in semicontinuous mode, we used a commercial dialysis 96-well plate, with 20 μL cell-free reaction on one side and 200 μL feeding solution on the other side (Figure 3a). The feeding solution has an identical composition to the reaction, except for the extract and plasmid, which are replaced by the S30B buffer[43] and water, respectively. We measured concentrations of 5.25 mg/mL (207 μM) and 6.25 mg/mL (247 μM) of deGFP with plasmids P_{70a}-deGFP and $T7P_{14}$-deGFP, respectively, after 24 h of incubation (Figure 3b).

DOI: 10.1021/acssynbio.5b00296
ACS Synth. Biol. XXXX, XXX, XXX−XXX

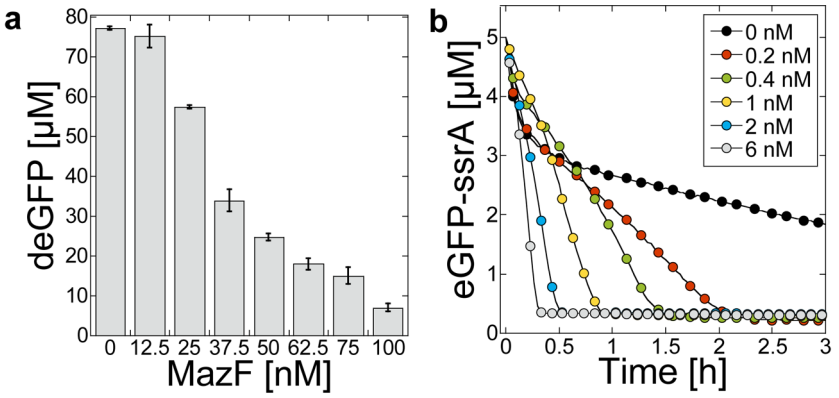

MazF [nM]	deGFP mRNA mean lifetime (min)
0	17.45 ± 0.23
25	10.54 ± 0.53
50	6.39 ± 1.55
75	4.33 ± 1.41
100	2.65 ± 1.67

clpXP [nM]	eGFP degradation rate (nM/min)
0	6.51 ± 1.25
0.2	28.04 ± 3.87
0.4	48.24 ± 8.06
1	88.32 ± 17.71
2	159.13 ± 21.92
6	256.07 ± 38.24

Figure 4. Characterization of mRNA and protein degradation in toolbox 2.0. (a) Synthesis of deGFP through P_{70a}-deGFP as a function of the *E. coli* MazF interferase concentration. Table: acceleration of mRNA degradation rate (1st order kinetics) with various concentration of MazF. (b) Degradation of His-eGFP-ssrA by the *E. coli* complex ClpXP. The pure protein (5 μM) was added to a cell-free reaction preincubated with P_{70a}-clpXP for 1 h. The linear kinetics is characteristic of a 0th order chemical reaction (constant rate). Table: acceleration of His-eGFP-ssrA as a function of P_{70a}-clpXP concentration.

Adjustable mRNA Degradation. While it is important to have a strong TX-TL and a broad transcription repertoire, it is also essential to implement strong, tunable degradation of the synthesized messengers and proteins to emulate complex dynamical behaviors through gene circuit programming, especially in reactions with fixed volume. The *E. coli* MazF interferase has already been shown to be a useful tool to accelerate the degradation of transcripts.[44] MazF only cleaves mRNA at the ACA sequence, without degrading ribosomes or tRNA.[54] We prepared a cytoplasmic extract containing the toxin by overexpressing it and estimated its concentration at 2 μM with the antitoxin MazE.[44] We applied a range of MazF to a cell-free reaction containing 5 nM P_{70a}-deGFP (Figure 4a) and observed, as expected, a decrease in deGFP synthesis. To determine the deGFP mRNA mean lifetime at different MazF concentrations, we developed a new assay based on transcription arrest and modeled the subsequent increase in fluorescence with a simple set of eqs (Supplementary Figure S11). With no MazF added to the reaction, the deGFP messenger mean lifetime is 17.45 min, compared to 9.8 min in *E. coli*.[55] The mean lifetime, which can be easily estimated from gene expression data (Supplementary Figure S12), was determined for four concentrations of MazF, accelerating degradation down to a mean lifetime of 2.65 min with 100 nM MazF (Figure 4a). We concluded that using MazF within 0−100 nM allows setting mRNA mean lifetime in a large and convenient range from 17.45 to 2.65 min.

Control of Protein Degradation. The *E. coli* complex ClpXP, a protease from the AAA+ family, is an ideal system to achieve targeted protein degradation in cell-free reactions by adding, either to the N-terminus or C-terminus, a specific degron typically 10−12 amino acids long.[56] In cell-free systems,[46] as well as in *E. coli*,[57] protein degradation by ClpXP is a zeroth order reaction with constant rate. Previously we showed that degradation of His-eGFP-ssrA using the endogenous ClpXP found in the extract works, but the constant rate, 5−15 nM/min, is too small to create an efficient protein degradation in cell-free TX-TL reactions.[44] The maximum rate of deGFP synthesis after 2 h of expression (linear accumulation) is on the order of 150 nM/min (Supplementary Table S6). To achieve powerful protein degradation by ClpXP, we cloned the tandem clpP-clpX genes from *E. coli* under the P_{70a} promoter. Then, we added pure His-eGFP-ssrA to a concentration of 5 μM in cell-free reactions and determined its rate of degradation by measuring the constant linear slopes, following three approaches: (i) adding pre-expressed ClpXP to a reaction (Supplementary Figure S13), (ii) expressing ClpXP in a cell-free reaction (Supplementary Figure S13) and (iii) preincubating for 1 h the expression of ClpXP (Figure 4b). The third method delivers the largest rate of protein degradation, up to 250 nM/min when 6 nM plasmid P_{70a}-clpXP is used. At low plasmid concentration (0 and 0.2 nM) a fast degradation is observed during the first 15 min that switches quickly to a low constant rate, indicating that the endogenous ClpXP machinery present in the extract is rapidly saturated. With no preincubation, a maximum rate of about 130 nM/min is obtained, while adding pre-expressed ClpXP to a cell-free reaction is less efficient. We concluded that expressing ClpXP in a cell-free reaction, with and without preincubating, allows setting protein degradation at sufficient rates with respect to the synthesis rate.

Examples of Circuits. The all *E. coli* toolbox 1.0 has already been used by many other groups for applications in synthetic biology and biological physics, at molecular, supra-molecular and cell-sized scales. This unique cell-free system facilitates prototyping of gene circuitries by accelerating the design-build-cycle to just 1 day compared to a few days *in vivo*; it is a platform to achieve complex self-assemblies and to construct synthetic cells. The cell-free toolbox has proven useful for testing simple genetic parts such as promoters,[2] riboregulators,[3] and small gene circuits.[41,42] It also enables self-assemblies in test tubes,[19] liposomes,[8] and supported phospholipid bilayers[58] along with the construction of oscillators and spatiotemporal patterns into microfluidic devices.[59] The system has been adapted to other *E. coli* strains so as to synthesize proteins with non-natural amino acids.[22,60]

DOI: 10.1021/acssynbio.5b00296
ACS Synth. Biol. XXXX, XXX, XXX−XXX

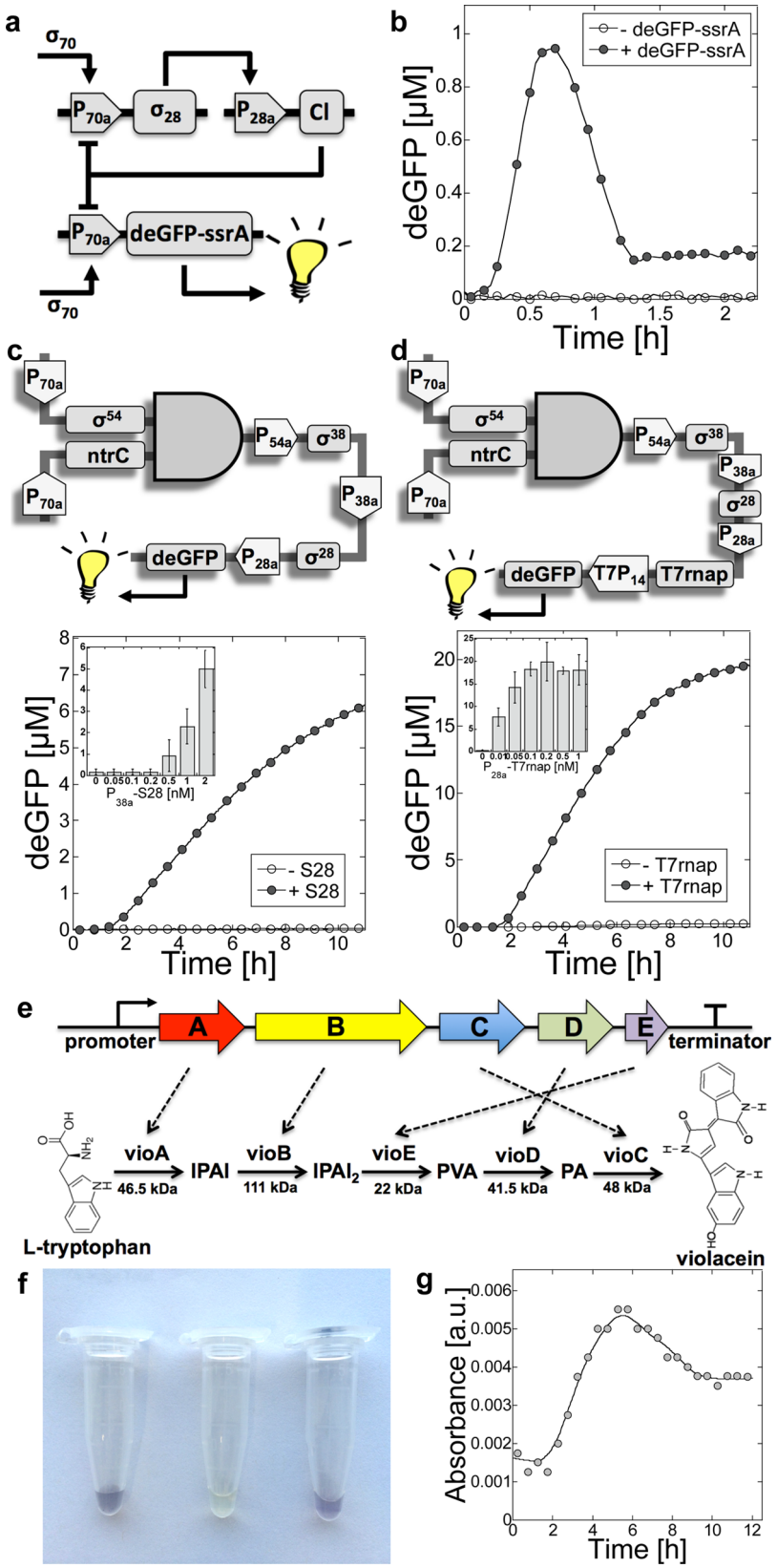

Figure 5. Examples of synthetic regulatory and biosynthesis circuits executed in toolbox 2.0. (a) Schematic of a pulse circuit. The lambda repressor Cl is expressed through the transcriptional activation cascade σ_{28} to turn off transcription of the first stage (the promoter P_{70a} has two operators specific to Cl). (b) Kinetics of expression in presence and absence of the reporter gene. Settings: P_{70a}-σ_{28} (0.1 nM), P_{28a}-Cl (1 nM), P70a-deGFP-ssrA (8 nM or 0 nM). (c) A 5-gene transcriptional activation cascades composed of *E. coli* transcription factors. Up to 6 μM deGFP was produced. The specificity of the circuit is tested by removing the second to last stage of the circuit (inset: range of P_{38a}-S_{28} plasmid). (d) A 6-gene transcriptional activation cascades constructed form the 5-gene cascade by adding a T7 stage at the end. Up to 20 μM deGFP (0.5 mg/mL) was produced. The specificity of the circuit is tested by removing the second to last stage of the circuit (inset: range of P_{28a}-T7rnap plasmid). (e) The violacein biosynthesis pathway from

DOI: 10.1021/acssynbio.5b00296
ACS Synth. Biol. XXXX, XXX, XXX−XXX

Figure 5. continued

Chromobacterium violaceum, composed of five genes. Synthesis of deoxyviolacein (not shown in the schematic) is achieved by the four enzymes vioABCE. (f) Photos of *E. coli* culture producing violacein (left), cell-free reaction with no plasmid (center, negative control), cell-free reaction containing the plasmid with the vioABCDE operon (right), after 12 h of incubation. (g) Kinetics of violacein production (after background subtraction) measured in a cell-free reaction by following the absorbance at 570 nm. The decrease of signal after 6 h of incubation is due to the precipitation of violacein, which is poorly soluble in aqueous solutions.

a

	Phage characteristics			Ref.
	T7	ΦX174	MS2	
Genome type	linear dsDNA	ssDNA (Group II)	ssRNA	
Genome size (bp or b)	39937	5386	3569	(70,71)
# genes	57	11	4	(72,73)
# promoters	3 *E. coli*, 17 T7	5	NA	(71)
Life cycle	30 min (30°C)	40 min	60 min	(73)
Viral type	lytic	lytic	lytic	
Physical size	60 nm	32 nm	27 nm	(74-76)
Host	*E. coli* Host B	HF 4704	*E. coli* C-1	
	Cell-free synthesis			
# Phage/ml	$3.35\ 10^{11}$	$1.9\ 10^{12}$	$4.23\ 10^{12}$	This work
# Phage/genome	2.2	0.6	0.047	This work
Optimum [Genome]	0.25 nM	5 nM	150 nM	This work
Genome replication	Yes	No	undetermined	This work

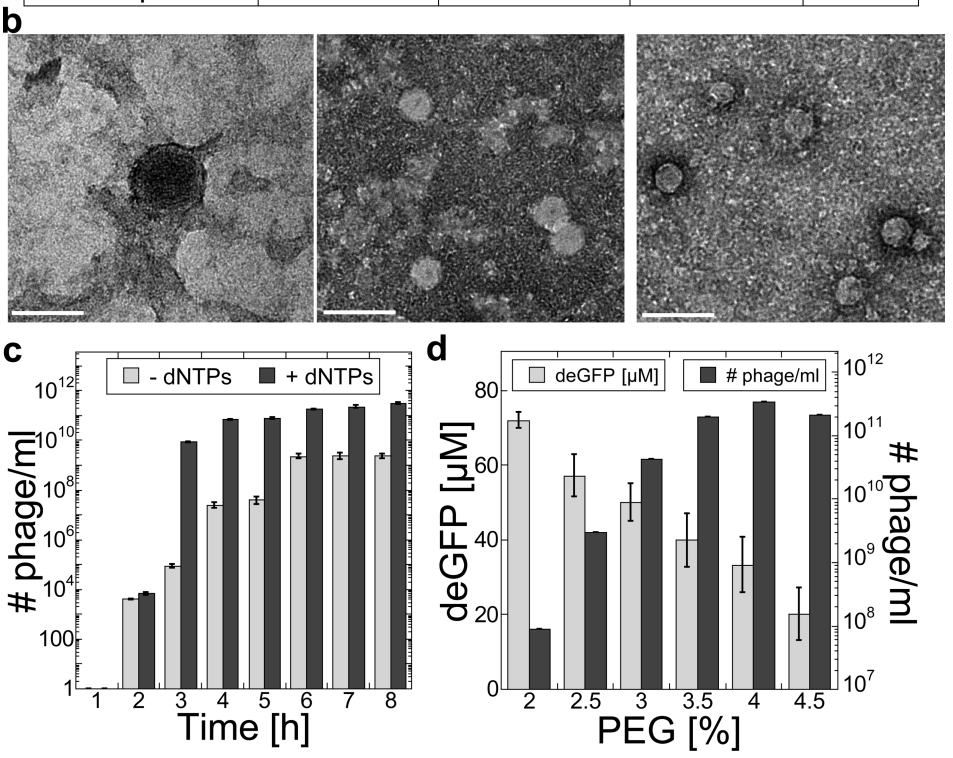

Figure 6. Cell-free synthesis of the bacteriophages T7, ΦX174 and MS2. (a) Characteristics of the three phages and their cell-free synthesis. (b) From left to right, electron microscopy images of T7, ΦX174 and MS2 (scale bar: 60 nm). (c) Kinetics of phage T7 synthesis with and without dNTPs added to the reaction. In both cases, phage synthesis plateaus after 6 h. (d) Effect of molecular crowding on the synthesis of T7 and the expression from one of its regulatory parts.

Here, we show several examples of synthetic circuits. First, we created a pulse through a cascading negative feedback loop circuit, similar to an incoherent feed-forward loop circuit motif[61] (Figure 5a). The lambda phage repressor Cl is expressed through a sigma factor σ_{28} transcriptional activation cascade to turn off transcription of the first gene. The pulse is created by adding the reporter gene deGFP-ssrA in the first stage. The protein is first expressed, and then degraded once transcription is turned off by the repressor (Figure 5b). We then constructed two long transcriptional activation cascades, composed of 5 and 6 genes, and compared the magnitude of the output signals to similar circuits described previously[41] (Figure 5c and 5d). These two long cascades are assembled in a series-like circuit based on the strength of the transcription factor and on the competition between sigma factors for the core RNA polymerase: from the weakest to the strongest and from the least competitive to the most competitive. The objective was to get a strong and specific output signal that is not due to transcriptional leaks of sigma factors through nonspecific promoters. The AND gate σ_{54}/NtrC is placed at the beginning of the cascades, followed by σ_{38} (a

DOI: 10.1021/acssynbio.5b00296
ACS Synth. Biol. XXXX, XXX, XXX−XXX

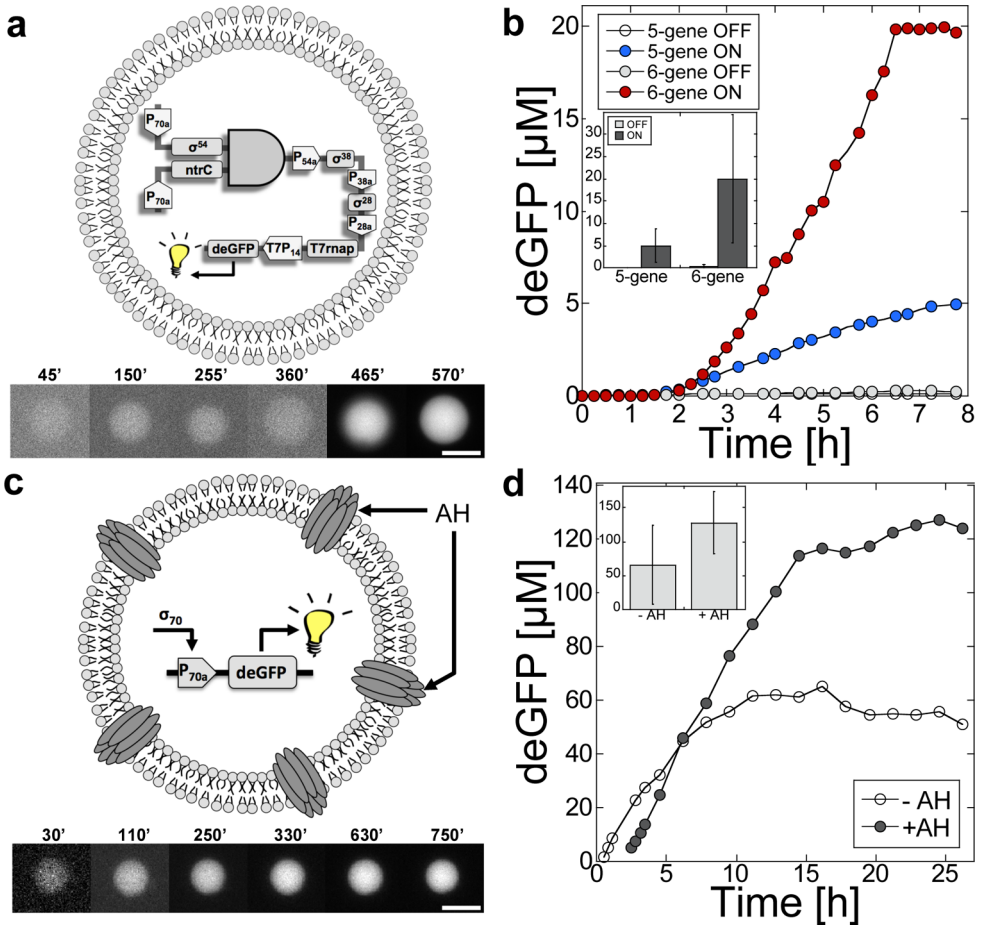

Figure 7. Cell-free expression with toolbox 2.0 inside cell-sized liposomes. (a) Schematic showing the 6-gene circuit inside a phospholipid vesicle. The 5-gene circuit was also expressed inside liposomes (See Figure 5d). Below: a series of photos showing deGFP fluorescence intensity (time in minutes, scale bar: 10 μm). (b) Kinetics of expression of deGFP expressed through the 5-gene and 6-gene circuit inside liposomes. 5-gene: the OFF state is minus the plasmid P_{38a}-σ_{28} (liposome of diameter 5.5 μm), the ON state was monitored for a liposome of diameter 7.3 μm. 6-gene: the OFF state is minus the plasmid P_{28a}-T7rnap (liposome of diameter 6.6 μm), the ON state was monitored for a liposome of diameter 6.2 μm. Inset: end point measurements of the 5-gene and 6-gene circuit measured for 20−30 liposomes. The kinetics were rescaled to the average values of the histogram shown in the inset. (c) Schematic showing a cell-free reaction (plasmid P_{70a}-deGFP) inside a liposome. The toxin alpha-hemolysin (AH) was added to the encapsulated reaction. Below: a series of photos showing deGFP fluorescence intensity (time in minutes, scale bar: 10 μm), when AH was added to the reaction. (d) Kinetics of expression of deGFP (P_{70a}-deGFP) inside liposomes with (liposome of diameter 11.5 μm and without AH (liposome of diameter 7.3 μm). Inset: statistics of deGFP fluorescence after 12 h of incubation with and without AH. The kinetics were rescaled to the average values of the histogram showed in the inset. The negative control with no plasmid did not show any signal (not shown).

weak competitor), σ_{28} (a strong competitor) and finally T7 in the case of the 6-gene circuit. Each gene was cloned into a separate plasmid so as to freely set the stoichiometry of each part, which was adjusted stepwise for both circuits. We found settings so that the leak is at background level when the second to last stage is removed (Figure 5c and 5d). For the full circuits, we observe output signals more than 2 orders of magnitude larger than previous similar circuits.

In addition, we tested the ability of toolbox 2.0 to achieve the biosynthesis of the metabolite violacein, whose pathway is from *Chromobacterium violaceum*. Testing and prototyping metabolic pathways is another promising application of cell-free systems. We chose violacein because it has been synthesized *in vitro* from pure proteins[62] (expressed and purified from *E. coli*), it has a characteristic color that can be easily measured by absorbance at 570 nm, the five genes are in a single operon (Figure 5e), and the precursor is simply the amino acid L-tryptophan present in the reaction at 2 mM. We used the plasmid #40782 from Addgene that contains the violacein biosynthesis pathway operon with optimized expression level.[63] Violacein (full pathway) and deoxyviolacein (full pathway minus VioD) are produced with the same characteristic purple color. The two cofactors necessary for violacein and deoxyviolacein biosynthesis, NADH (nicotinamide adenine dinucleotide, 100 μM) and FAD (flavin adenine dinucleotide, 5 μM), were added to the reaction. A net production of the metabolites is observed with a characteristic purple color (Figure 5f). The time course of production (absorbance at 570 nm) shows that the metabolites are produced after 2 h of incubations with a maximum at 6 h (Figure 5g). The absorbance spectra from *E. coli* cultures producing violacein and deoxyviolacein and from cell-free reactions were identical, with a characteristic peak between 570 and 580 nm (Supplementary Figure S14).

Cell-Free Synthesis of Phages. While toolbox 2.0 proves to be a powerful system to prototype genetic parts and circuits, the platform can also complete complex self-assembly processes. We previously showed, with the cell-free toolbox 1.0, that bacteriophages T7 (dsDNA) and ΦX174 (ssDNA) can be entirely resynthesized *in vitro* from their genome.[19] With the new system, we show that the synthesis of these two phages is

DOI: 10.1021/acssynbio.5b00296
ACS Synth. Biol. XXXX, XXX, XXX−XXX

increased by several orders of magnitude, and that the bacteriophage MS2 (RNA) is also successfully synthesized *in vitro* (Figure 6a, Supplementary Figure S15). The three phages were visualized by electron microscopy to confirm their presence and physical sizes (Figure 6b). For bacteriophage T7—in the presence of dNTPs to stimulate DNA replication—we observe an increased phage production by a factor of 100 as about 2 phages per genome added to the reaction are produced, compared to only 0.02 phages produced per genome in our first work. With no addition of dNTPs to the reactions, 10−100× less phages are produced under the same reaction conditions (Figure 6c). In the case of ΦX174, we observe a maximum of 1.9×10^{12} phages per milliliter of reaction, compared to about 10^5 previously reported.[19]

The complete cell-free synthesis of phages from their genome provides a unique means to interrogate the biochemistry and the biophysics of this complex process. Here, as a simple insight, we show the enormous effect of molecular crowding on the synthesis of phage T7. We chose phage T7 because it is the most recapitulated of the three phages: TX-TL and DNA replication happen concurrently, with more phages produced than genomes added to the reaction. Molecular crowding is known to promote and accelerate the self-assembly of macro-molecular complexes[64−66] and has been shown to affect simple biochemical reactions such as the transcription rates in cell-free TX-TL.[67] The cytoplasmic extract is diluted 25−30 times compared to the *E. coli* cytoplasm: the cell-free reactions contain 9.5−10 mg/mL of proteins, compared to 250−300 mg/mL (4−5 mM) in *E. coli*. To emulate molecular crowding, we used PEG8000, a typical molecular crowder present in most cell-free TX-TL systems. The reporter protein deGFP was cloned under the regulatory part encoding for the major capsid protein 10A of phage T7 (promoter-UTR number 14). We then measured the number of phages produced and the expression of deGFP as a function of PEG8000 concentration. Remarkably, over the same PEG8000 concentration range, the expression of deGFP decreases 3-fold while the synthesis of phages increases by a factor of 4000 (Figure 6d). We determined the kinetics of T7 phage synthesis with and without dNTPs and observed that the major difference appears in the first 2−3 h of incubation (Figure 6c), while no phages are produced in the first hour. With DNA replication, almost 100 000× more phages are produced after 3 h, and between 10 and 100 times at plateau. A comprehensive characterization of T7 phage synthesis is currently being performed in our laboratory to determine the magnitude of molecular crowding on the different parts of this process and gene expression patterns during synthesis.

Minimal Cell System. Cell-free expression is one of the most interesting technologies to construct minimal cells using a bottom-up approach. The proof of concept of cell-free TX-TL based synthetic cells has already been demonstrated.[11,12,68] The objective is to program phospholipid vesicles with synthetic or natural gene circuits to construct complex biological functions, such as membrane channels to control the in and out diffusion of nutrients. Here, in addition to describing cell-free expression inside cell-sized liposomes with a single reporter gene, we characterized the performance of toolbox 2.0 using the 5 and 6-gene circuits to demonstrate that relatively large circuits can be executed in minimal cell systems. First, we calibrated deGFP fluorescence intensity in liposome populations as a function of size (Supplementary Figure S16). Then, we encapsulated both the 5 and 6-gene circuits into liposomes (Figure 7a) and measured the kinetics of expression (Figure 7b). The expression of a single reporter gene in liposomes is known to show large fluctuations due to a nonuniform encapsulation process, in particular of the DNA template.[10,69] As expected, with 5 and 6-gene circuits, we observe large fluctuations in signal among the same population of liposomes. Yet, the negative controls for both circuits (no σ_{28} and no T7 rnap plasmids, respectively) are at background level. The kinetics of expression in liposomes are similar to the expression in batch mode reactions, with the signal rising after 90 min. Expression of deGFP (P_{70a}-deGFP) and the membrane channel AH-eGFP ($T7P_{14}$-AH-eGFP) inside cell-sized liposomes is easily observed under the microscope (Supplementary Figure S17).

To create long-lived expression inside the vesicles, we permeabilized the membrane using the pore-forming toxin alpha-hemolysin (AH) from *Staphylococcus aureus*[68] that self-assembles into membrane channels of molecular mass cutoff 3 kDa. This approach has already proven useful to create free diffusion of small nutrients through the lipidic bilayer necessary for TX-TL, and thus extend the kinetics of protein synthesis.[68] Rather than using pure AH or coexpressing AH in the reaction, we first expressed the toxin in a cell-free reaction (Supplementary Figure S18). Then, we diluted this reaction 15-fold into a reaction containing the plasmid P_{70a}-deGFP (Figure 7c) and prepared liposomes. After 24 h of incubation, we measured a 2-fold increase of deGFP expression when AH was used, reaching 3.2 mg/mL in liposomes (Figure 7d). It is not clear why this is less than in batch semicontinuous cell-free reactions. The amount of reporter protein expressed is much larger than in previous, similar setups made with a T7-based cell-free system.[68] The level of expression without the addition of AH in the external solution was comparable to batch mode reactions in test tubes (about 1.5−2 mg/mL of fluorescent deGFP). We monitored the kinetics of deGFP expression with and without AH and observed an extension of expression in the presence of the toxin (Figure 7d). To complete the characterization of this system, we monitored the leak of UTP-fluorescein from liposomes, with and without adding AH in the external solutions (Supplementary Figure S19). It takes a few hours to observe a complete leak of 5 μM of the fluorescent probe, while with no addition of AH no leak is observed. Toolbox 2.0 allows two major improvements for minimal cell systems: greater cell-free protein synthesis in liposomes and execution of larger gene circuits, both being an essential steps toward the construction of synthetic cells capable of self-reproduction.

CONCLUSION

The construction of complex biochemical systems *in vitro*, programmed with genetic information, requires the development of novel experimental platforms that offer broad capabilities and enough flexibility so as to change and investigate biochemical and biophysical parameters that are hardly or not accessible *in vivo*. In this work, we presented a unique all *E. coli* cell-free expression toolbox specifically optimized for synthetic biology and biological physics. This platform is designed to be generic at the level of transcription, and compatible with various setups, from batch reactions to microfluidics to liposomes.

Our work demonstrates how essential energy regeneration is to build a powerful long-lived expression system and to increase the performance of gene circuits and larger systems, such as phages. Surprisingly, expression from *E. coli* promoters can be as strong as expression from bacteriophage promoters. This toolbox comes with assays to measure maturation time of fluorescent proteins, mRNA and protein degradation rates. In

DOI: 10.1021/acssynbio.5b00296
ACS Synth. Biol. XXXX, XXX, XXX−XXX

the linear regime of plasmid concentrations and expression kinetics, TX-TL reactions are well modeled with simple equation sets,[46] another advantage of this system. Because of its simple use and unique versatility, the all *E. coli* toolbox 2.0 is also well adapted for education purposes. This platform could also reveal useful to define biological metrics and standards.

METHODS

Cell-Free Reaction. Transcription and translation are performed by endogenous molecular components provided by an *E. coli* cytoplasmic extract, without addition of exogenous purified TX-TL enzymes. *E. coli* cells are grown in 2xYT medium supplemented with phosphates.[70] Lysis is performed either by bead beating[45,70] or with a cell-press,[43] followed by the typical steps: centrifugation, recovery and preincubation of the supernatant at 37 °C for 80 min, centrifugation, dialysis of supernatant at 4 °C for 3 h, centrifugation, aliquoting the supernatant, storage at −80 °C. The extract is stable for more than a year at −80 °C. In addition to the extract, the reaction is composed of an energy mixture[43] and amino acids.[71] The reaction buffer is composed of 50 mM Hepes pH 8, 1.5 mM ATP and GTP, 0.9 mM CTP and UTP, 0.2 mg/mL tRNA, 0.26 mM coenzyme A, 0.33 mM NAD, 0.75 mM cAMP, 0.068 mM folinic acid, 1 mM spermidine, 30 mM 3-PGA, 1 mM DTT, 2% PEG8000, either 10−15 mM maltose or 20−40 mM maltodextrin. A typical cell-free reaction is composed of 33% (volume) *E. coli* crude extract. The other 66% of the reaction volume are composed of the plasmids and the reaction buffer containing the nutrients. The amino acid concentration was adjusted between 1.5 mM and 3 mM of each of the 20 amino acids. Mg-glutamate and K-glutamate concentrations were adjusted according to the plasmids used (typically 60 mM K-glutamate and 5 mM Mg-glutamate for P_{70a}-deGFP, 20 mM K-glutamate and 5 mM Mg glutamate for the T7 cascade). The toolbox 2.0 will be commercialized under the name "MYtxtl" by the company MYcroarray (Michigan, USA). Cell-free reactions are carried out in a volume of 5 μL to 20 μL at 29−30 °C. Semicontinuous cell-free reactions were carried out using a 96-well equilibrium dialyzer plate (Harvard Apparatus, MWCO 10 kDa), with 20 μL reaction on one side and 200 μL feeding solution on the other side. The feeding solution has a similar composition to the reaction, minus the extract and the plasmid. The plate was incubated at 29−30 °C with constant rotation (0.125 Hz), on a rotary axis.

DNA Part List and Plasmid Preparation. The DNA parts used in this work are reported in Supplementary Table S7. Unless specified, the plasmids contain the highly efficient untranslated region named UTR1. Plasmid names: P_{38a}-S_{28} or P_{38a}-σ_{28} refers to the same plasmid with a promoter specific to σ_{38} and the gene σ_{28}.

Liposome Preparation and Observations. The encapsulation of cell-free reactions into large unilamellar phospholipid vesicles is based on the water-in-oil emulsion transfer method.[68,72,73] Briefly, phospholipids (egg PC, Avanti Polar Lipids) are dissolved in mineral oil (Sigma-Aldrich) at 2 mg/mL. A few microliters of cell-free reaction are added to 0.5 mL of the phospholipid solution. This solution is vortexed for a few seconds to create an emulsion. 100−250 μL of the emulsion are placed on top of 20 μL of feeding solution. The vesicles are formed by centrifugation of the biphasic solution for 20 s at 4000 rpm. The phospholipid vesicles were observed with a CCD camera mounted on an inverted microscope (Olympus IX-81) equipped with the proper set of fluorescence filters.

Measurements of Batch Mode Cell-Free TX-TL Reactions. Quantitative measurements were carried out with either the reporter protein deGFP (25.4 kDa, 1 mg/mL = 39.37 μM) or His-deGFP (27.2 kDa, 1 mg/mL = 36.76 μM). deGFP is a variant of the reporter eGFP that is more translatable in cell-free systems. The excitation and emission spectra as well as fluorescence properties of deGFP and eGFP are identical, as reported before.[41] The fluorescence of deGFP produced in batch mode cell-free reaction was measured on an H1m plate reader (Biotek Instruments, 384-well plate). End-point measurements were carried out after 8−12 h of incubation. Pure recombinant eGFP with His tags (from two sources: Cell Biolabs Inc. and Biovision) was used for quantification (linear calibration on plate reader). Error bars are the standard deviations from multiple repeats. An example measurement is shown in Supplementary Figure S20.

Protein Purification. The reporter protein His-eGFP-ssrA (N-terminal His-tag and C-terminal ssrA degron) and His-GamS (6His tag in N-terminal) from lambda phage were overexpressed in *E. coli* and purified on nickel beads using standard procedures. His-eGFP-ssrA was quantified using pure recombinant His-eGFP (Cell Biolabs Inc. or Biovision), His-GamS was quantified by Bradford assay.

Bacteriophage Titration and Imaging. Bacteriophages were counted by the standard plaque forming assay using the following strains: *E. coli* B for T7, *E. coli* HF4714 for ΦX174 (Yale Genetic Stock Center), and *E. coli* 4401 for MS2 (Yale Genetic Stock Center). Cells were grown in Luria−Bertani (LB) broth at 37 °C. The plates were prepared as follow: each sample was added to a solution composed of 5 mL of 0.6% liquid LB-agar (45 °C) and 50 μL of cell culture, poured on a 1.1% solid LB-agar plate. Plates were incubated at 37 °C and plaques counted after 6 h. Transmission electron microscopy (TEM) was performed with a FEI Tecna F30 (300 kV, negative staining, carbon-coated TEM grid).

ASSOCIATED CONTENT

Supporting Information

The Supporting Information is available free of charge on the ACS Publications website at DOI: 10.1021/acssynbio.5b00296.

Cytoplasmic extract control plates, determination of deGFP maturation time, eight reporter proteins kinetics, nine reporter proteins excitation and emission spectra, photos of nine reporter proteins produced using Toolbox 2.0, example of two pTXTL plasmids, batch to batch cell-free reaction reproducibility, two-stage transcriptional activation cascade characterization, anti σ_{70} protein Asia tests, prepackaged *vs* separate performance (Plasmid P_{70a}-deGFP), mRNA mean lifetime determination (MazF), setting mRNA mean lifetime with MazF, eGFP-ssrA degradation by clpXP (no preincubation, pre-expressed), violacein absorbance spectrum from *E. coli* culture, images of plaque assay, calibration of deGFP concentration in liposomes, fluorescence image of liposomes (deGFP and AH-eGFP), SDS-PAGE of alpha-hemolysin synthesis, AH leak tests in liposomes, calibration and measurements (Figures S1−S20). Component concentrations, cDNA sequences of nine reporter proteins, Relative intensity of nine reporter proteins, pTXTL plasmid list, Crosstalk between transcriptional activation units, deGFP synthesis rate (plasmid P_{70a}-deGFP) as a function of MazF, DNA part list (Tables S1−S7). (PDF)

DOI: 10.1021/acssynbio.5b00296
ACS Synth. Biol. XXXX, XXX, XXX−XXX

AUTHOR INFORMATION

Corresponding Author

*Tel: +1-612-624-6589. Fax: +1-612-624-4578. E-mail: noireaux@umn.edu.

Author Contributions

†J.G., R.M., and M.R. contributed equally to this work.

Notes

The authors declare the following competing financial interest(s): Noireaux laboratory receives research funds from MYcroarray, a distributor of MYtxtl cell-free protein expression kit.

ACKNOWLEDGMENTS

We thank Filippo Caschera, without whom this work would have not been possible. We are grateful to Claudia Schmidt-Dannert for technical help, Natalie Ma for discussions on MS2 phage, John Wertz at CGSC (Yale), Wei Zhang for TEM performed at the Characterization Facility at the University of Minnesota, which receives partial support from NSF through the MRSEC program. This work was supported by the Office of Naval Research award number N00014-13-1-0074, by MYcroarray as part of the Defense Advanced Research Projects Agency (DARPA) and the Army Contracting Command—Aberdeen Proving Grounds (ACC-APG) under Contract/Purchase Order number W911NF-15-P-0027, and by the Human Frontier Science Program grant number RGP0037/2015.

REFERENCES

(1) Noireaux, V., Bar-Ziv, R., and Libchaber, A. (2003) Principles of cell-free genetic circuit assembly. *Proc. Natl. Acad. Sci. U. S. A. 100*, 12672−12677.

(2) Sun, Z. Z., Yeung, E., Hayes, C. A., Noireaux, V., and Murray, R. M. (2014) Linear DNA for Rapid Prototyping of Synthetic Biological Circuits in an Escherichia coli Based TX-TL Cell-Free System. *ACS Synth. Biol. 3*, 387−397.

(3) Takahashi, M. K., Chappell, J., Hayes, C. A., Sun, Z. Z., Kim, J., Singhal, V., Spring, K. J., Al-Khabouri, S., Fall, C. P., Noireaux, V., Murray, R. M., and Lucks, J. B. (2015) Rapidly Characterizing the Fast Dynamics of RNA Genetic Circuitry with Cell-Free Transcription-Translation (TX-TL) Systems. *ACS Synth. Biol. 4*, 503−515.

(4) Chappell, J., Jensen, K., and Freemont, P. S. (2013) Validation of an entirely in vitro approach for rapid prototyping of DNA regulatory elements for synthetic biology. *Nucleic Acids Res. 41*, 3471−3481.

(5) Karig, D. K., Iyer, S., Simpson, M. L., and Doktycz, M. J. (2012) Expression optimization and synthetic gene networks in cell-free systems. *Nucleic Acids Res. 40*, 3763−3774.

(6) Niederholtmeyer, H., Stepanova, V., and Maerkl, S. J. (2013) Implementation of cell-free biological networks at steady state. *Proc. Natl. Acad. Sci. U. S. A. 110*, 15985−15990.

(7) Niederholtmeyer, H., Sun, Z. Z., Hori, Y., Yeung, E., Verpoorte, A., Murray, R. M., and Maerkl, S. J. (2015) Rapid cell-free forward engineering of novel genetic ring oscillators. *eLife*, DOI: 10.7554/eLife.09771.

(8) Maeda, Y. T., Nakadai, T., Shin, J., Uryu, K., Noireaux, V., and Libchaber, A. (2012) Assembly of MreB Filaments on Liposome Membranes: A Synthetic Biology Approach. *ACS Synth. Biol. 1*, 53−59.

(9) Noireaux, V., Maeda, Y. T., and Libchaber, A. (2011) Development of an artificial cell, from self-organization to computation and self-reproduction. *Proc. Natl. Acad. Sci. U. S. A. 108*, 3473−3480.

(10) Nourian, Z., and Danelon, C. (2013) Linking Genotype and Phenotype in Protein Synthesizing Liposomes with External Supply of Resources. *ACS Synth. Biol. 2*, 186−193.

(11) Ishikawa, K., Sato, K., Shima, Y., Urabe, I., and Yomo, T. (2004) Expression of a cascading genetic network within liposomes. *FEBS Lett. 576*, 387−390.

(12) Stano, P., Kuruma, Y., Souza, T. P., and Luisi, P. L. (2010) Biosynthesis of proteins inside liposomes. *Methods Mol. Biol. 606*, 127−145.

(13) Matsubayashi, H., Kuruma, Y., and Ueda, T. (2014) In Vitro Synthesis of the E. coli Sec Translocon from DNA. *Angew. Chem., Int. Ed. 53*, 7535−7538.

(14) Liu, Y. J., Hansen, G. P., Venancio-Marques, A., and Baigl, D. (2013) Cell-free preparation of functional and triggerable giant proteoliposomes. *ChemBioChem 14*, 2243−2247.

(15) Forlin, M., Lentini, R., and Mansy, S. S. (2012) Cellular imitations. *Curr. Opin. Chem. Biol. 16*, 586−592.

(16) Caschera, F., and Noireaux, V. (2014) Integration of biological parts toward the synthesis of a minimal cell. *Curr. Opin. Chem. Biol. 22*, 85−91.

(17) Daube, S. S., Arad, T., and Bar-Ziv, R. (2007) Cell-free co-synthesis of protein nanoassemblies: tubes, rings, and doughnuts. *Nano Lett. 7*, 638−641.

(18) Heyman, Y., Buxboim, A., Wolf, S. G., Daube, S. S., and Bar-Ziv, R. H. (2012) Cell-free protein synthesis and assembly on a biochip. *Nat. Nanotechnol. 7*, 374−378.

(19) Shin, J., Jardine, P., and Noireaux, V. (2012) Genome Replication, Synthesis, and Assembly of the Bacteriophage T7 in a Single Cell-Free Reaction. *ACS Synth. Biol. 1*, 408−413.

(20) Jewett, M. C., Fritz, B. R., Timmerman, L. E., and Church, G. M. (2013) In vitro integration of ribosomal RNA synthesis, ribosome assembly, and translation. *Mol. Syst. Biol. 9*, 678.

(21) Hong, S. H., Kwon, Y. C., and Jewett, M. C. (2014) Non-standard amino acid incorporation into proteins using Escherichia coli cell-free protein synthesis. *Front. Chem. 2*, 34.

(22) Chemla, Y., Ozer, E., Schlesinger, O., Noireaux, V., and Alfonta, L. (2015) Genetically expanded cell-free protein synthesis using endogenous pyrrolysyl orthogonal translation system. *Biotechnol. Bioeng. 112*, 1663.

(23) Albayrak, C., and Swartz, J. R. (2014) Direct polymerization of proteins. *ACS Synth. Biol. 3*, 353−362.

(24) Bundy, B. C., Franciszkowicz, M. J., and Swartz, J. R. (2008) Escherichia coli-based cell-free synthesis of virus-like particles. *Biotechnol. Bioeng. 100*, 28−37.

(25) Kanter, G., Yang, J., Voloshin, A., Levy, S., Swartz, J. R., and Levy, R. (2007) Cell-free production of scFv fusion proteins: an efficient approach for personalized lymphoma vaccines. *Blood 109*, 3393−3399.

(26) Lu, Y., Welsh, J. P., Chan, W., and Swartz, J. R. (2013) Escherichia coli-based cell free production of flagellin and ordered flagellin display on virus-like particles. *Biotechnol. Bioeng. 110*, 2073−2085.

(27) Pardee, K., Green, A. A., Ferrante, T., Cameron, D. E., DaleyKeyser, A., Yin, P., and Collins, J. J. (2014) Paper-based synthetic gene networks. *Cell 159*, 940−954.

(28) Hovijitra, N. T., Wuu, J. J., Peaker, B., and Swartz, J. R. (2009) Cell-free synthesis of functional aquaporin Z in synthetic liposomes. *Biotechnol. Bioeng. 104*, 40−49.

(29) Matthies, D., Haberstock, S., Joos, F., Dotsch, V., Vonck, J., Bernhard, F., and Meier, T. (2011) Cell-free expression and assembly of ATP synthase. *J. Mol. Biol. 413*, 593−603.

(30) Roos, C., Kai, L., Proverbio, D., Ghoshdastider, U., Filipek, S., Dotsch, V., and Bernhard, F. (2013) Co-translational association of cell-free expressed membrane proteins with supplied lipid bilayers. *Mol. Membr. Biol. 30*, 75−89.

(31) Nevin, D. E., and Pratt, J. M. (1991) A coupled in vitro transcription-translation system for the exclusive synthesis of polypeptides expressed from the T7 promoter. *FEBS Lett. 291*, 259−263.

(32) Hanes, J., and Pluckthun, A. (1997) In vitro selection and evolution of functional proteins by using ribosome display. *Proc. Natl. Acad. Sci. U. S. A. 94*, 4937−4942.

DOI: 10.1021/acssynbio.5b00296
ACS Synth. Biol. XXXX, XXX, XXX−XXX

(33) Tawfik, D. S., and Griffiths, A. D. (1998) Man-made cell-like compartments for molecular evolution. *Nat. Biotechnol. 16*, 652−656.
(34) Fallah-Araghi, A., Baret, J. C., Ryckelynck, M., and Griffiths, A. D. (2012) A completely in vitro ultrahigh-throughput droplet-based microfluidic screening system for protein engineering and directed evolution. *Lab Chip 12*, 882−891.
(35) He, M. (2008) Cell-free protein synthesis: applications in proteomics and biotechnology. *New Biotechnol. 25*, 126−132.
(36) Sawasaki, T., Ogasawara, T., Morishita, R., and Endo, Y. (2002) A cell-free protein synthesis system for high-throughput proteomics. *Proc. Natl. Acad. Sci. U. S. A. 99*, 14652−14657.
(37) Vinarov, D. A., Lytle, B. L., Peterson, F. C., Tyler, E. M., Volkman, B. F., and Markley, J. L. (2004) Cell-free protein production and labeling protocol for NMR-based structural proteomics. *Nat. Methods 1*, 149−153.
(38) Cai, Q., Hanson, J. A., Steiner, A. R., Tran, C., Masikat, M. R., Chen, R., Zawada, J. F., Sato, A. K., Hallam, T. J., and Yin, G. (2015) A simplified and robust protocol for immunoglobulin expression in Escherichia coli cell-free protein synthesis systems. *Biotechnol. Prog. 31*, 823.
(39) Shimizu, Y., Kanamori, T., and Ueda, T. (2005) Protein synthesis by pure translation systems. *Methods 36*, 299−304.
(40) Segall-Shapiro, T. H., Meyer, A. J., Ellington, A. D., Sontag, E. D., and Voigt, C. A. (2014) A 'resource allocator' for transcription based on a highly fragmented T7 RNA polymerase. *Mol. Syst. Biol. 10*, 742.
(41) Shin, J., and Noireaux, V. (2012) An E. coli cell-free expression toolbox: application to synthetic gene circuits and artificial cells. *ACS Synth. Biol. 1*, 29−41.
(42) Takahashi, M. K., Hayes, C. A., Chappell, J., Sun, Z. Z., Murray, R. M., Noireaux, V., and Lucks, J. B. (2015) Characterizing and prototyping genetic networks with cell-free transcription-translation reactions. *Methods 86*, 60.
(43) Caschera, F., and Noireaux, V. (2014) Synthesis of 2.3 mg/mL of protein with an all Escherichia coli cell-free transcription-translation system. *Biochimie 99*, 162−168.
(44) Shin, J., and Noireaux, V. (2010) Study of messenger RNA inactivation and protein degradation in an Escherichia coli cell-free expression system. *J. Biol. Eng. 4*, 9.
(45) Shin, J., and Noireaux, V. (2010) *J. Biol. Eng. 4*, 8.
(46) Karzbrun, E., Shin, J., Bar-Ziv, R. H., and Noireaux, V. (2011) Coarse-grained dynamics of protein synthesis in a cell-free system. *Phys. Rev. Lett. 106*, 048104.
(47) Lentini, R., Forlin, M., Martini, L., Del Bianco, C., Spencer, A. C., Torino, D., and Mansy, S. S. (2013) Fluorescent proteins and in vitro genetic organization for cell-free synthetic biology. *ACS Synth. Biol. 2*, 482−489.
(48) Siegal-Gaskins, D., Tuza, Z. A., Kim, J., Noireaux, V., and Murray, R. M. (2014) Gene circuit performance characterization and resource usage in a cell-free "breadboard". *ACS Synth. Biol. 3*, 416−425.
(49) Straus, D. B., Walter, W. A., and Gross, C. A. (1987) The heat shock response of E. coli is regulated by changes in the concentration of sigma 32. *Nature 329*, 348−351.
(50) Orsini, G., Ouhammouch, M., Le Caer, J. P., and Brody, E. N. (1993) The asiA gene of bacteriophage T4 codes for the anti-sigma 70 protein. *J. Bacteriol. 175*, 85−93.
(51) Maeda, H., Fujita, N., and Ishihama, A. (2000) Competition among seven Escherichia coli sigma subunits: relative binding affinities to the core RNA polymerase. *Nucleic Acids Res. 28*, 3497−3503.
(52) Spirin, A. S., Baranov, V. I., Ryabova, L. A., Ovodov, S. Y., and Alakhov, Y. B. (1988) A continuous cell-free translation system capable of producing polypeptides in high yield. *Science 242*, 1162−1164.
(53) Kigawa, T., and Yokoyama, S. (1991) A continuous cell-free protein synthesis system for coupled transcription-translation. *J. Biochem. 110*, 166−168.
(54) Zhang, J., Zhang, Y., and Inouye, M. (2003) Characterization of the interactions within the mazEF addiction module of Escherichia coli. *J. Biol. Chem. 278*, 32300−32306.
(55) Selinger, D. W., Saxena, R. M., Cheung, K. J., Church, G. M., and Rosenow, C. (2003) Global RNA half-life analysis in Escherichia coli reveals positional patterns of transcript degradation. *Genome Res. 13*, 216−223.
(56) Flynn, J. M., Neher, S. B., Kim, Y. I., Sauer, R. T., and Baker, T. A. (2003) Proteomic discovery of cellular substrates of the ClpXP protease reveals five classes of ClpX-recognition signals. *Mol. Cell 11*, 671−683.
(57) Wong, W. W., Tsai, T. Y., and Liao, J. C. (2007) Single-cell zeroth-order protein degradation enhances the robustness of synthetic oscillator. *Mol. Syst. Biol. 3*, 130.
(58) Chalmeau, J., Monina, N., Shin, J., Vieu, C., and Noireaux, V. (2011) alpha-Hemolysin pore formation into a supported phospholipid bilayer using cell-free expression. *Biochim. Biophys. Acta, Biomembr. 1808*, 271−278.
(59) Karzbrun, E., Tayar, A. M., Noireaux, V., and Bar-Ziv, R. H. (2014) Programmable on-chip DNA compartments as artificial cells. *Science 345*, 829−832.
(60) Worst, E. G., Exner, M. P., De Simone, A., Schenkelberger, M., Noireaux, V., Budisa, N., and Ott, A. (2015) Cell-free expression with the toxic amino acid canavanine. *Bioorg. Med. Chem. Lett. 25*, 3658−3660.
(61) Alon, U. (2007) Network motifs: theory and experimental approaches. *Nat. Rev. Genet. 8*, 450−461.
(62) Balibar, C. J., and Walsh, C. T. (2006) In vitro biosynthesis of violacein from L-tryptophan by the enzymes VioA-E from Chromobacterium violaceum. *Biochemistry 45*, 15444−15457.
(63) Kittleson, J. T., DeLoache, W., Cheng, H. Y., and Anderson, J. C. (2012) Scalable plasmid transfer using engineered P1-based phagemids. *ACS Synth. Biol. 1*, 583−589.
(64) Zimmerman, S. B., and Minton, A. P. (1993) Macromolecular crowding: biochemical, biophysical, and physiological consequences. *Annu. Rev. Biophys. Biomol. Struct. 22*, 27−65.
(65) Minton, A. P. (2000) Implications of macromolecular crowding for protein assembly. *Curr. Opin. Struct. Biol. 10*, 34−39.
(66) Minton, A. P. (2006) How can biochemical reactions within cells differ from those in test tubes? *J. Cell Sci. 119*, 2863−2869.
(67) Sokolova, E., Spruijt, E., Hansen, M. M. K., Dubuc, E., Groen, J., Chokkalingam, V., Piruska, A., Heus, H. A., and Huck, W. T. S. (2013) Enhanced transcription rates in membrane-free protocells formed by coacervation of cell lysate. *Proc. Natl. Acad. Sci. U. S. A. 110*, 11692−11697.
(68) Noireaux, V., and Libchaber, A. (2004) A vesicle bioreactor as a step toward an artificial cell assembly. *Proc. Natl. Acad. Sci. U. S. A. 101*, 17669−17674.
(69) Pereira de Souza, T., Stano, P., and Luisi, P. L. (2009) The minimal size of liposome-based model cells brings about a remarkably enhanced entrapment and protein synthesis. *ChemBioChem 10*, 1056−1063.
(70) Sun, Z. Z., Hayes, C. A., Shin, J., Caschera, F., Murray, R. M., and Noireaux, V. (2013) Protocols for implementing an Escherichia coli based TX-TL cell-free expression system for synthetic biology. *J. Visualized Exp.*, e50762.
(71) Caschera, F., and Noireaux, V. (2015) Preparation of amino acid mixtures for cell-free expression systems. *BioTechniques 58*, 40−43.
(72) Pautot, S., Frisken, B. J., and Weitz, D. A. (2003) Engineering asymmetric vesicles. *Proc. Natl. Acad. Sci. U. S. A. 100*, 10718−10721.
(73) Noireaux, V., Bar-Ziv, R., Godefroy, J., Salman, H., and Libchaber, A. (2005) Toward an artificial cell based on gene expression in vesicles. *Phys. Biol. 2*, P1−8.

DOI: 10.1021/acssynbio.5b00296
ACS Synth. Biol. XXXX, XXX, XXX−XXX

Supporting Information

The all *E. coli* TX-TL Toolbox 2.0: a platform for cell-free synthetic biology

Jonathan Garamella[†], Ryan Marshall[†], Mark Rustad[†] and Vincent Noireaux*
School of Physics and Astronomy, University of Minnesota, 115 Union Street SE, Minneapolis, 55455 Minnesota, United States of America.

[†]Contributed equally to this work.
*Corresponding author: noireaux@umn.edu

Content:

Parameter	*In vivo*	Cell-free reaction	Ratio *in vivo*/cell-free	Footnote
Protein concentration [mg/ml]	200-320	9-10	20-32	a, b
Transcription				
Free core RNA polymerase per cell [nM]	1900	60-75	20-32	c
σ_{70} [nM]	730	< 35	20-32	d
σ_{19} [nM]	< 1	< 0.05	20-32	d
σ_{24} [nM]	< 10	< 0.5	20-32	d
σ_{28} [nM]	385	< 20	20-32	d
σ_{32} [nM]	< 10	< 0.5	20-32	d
σ_{38} [nM]	< 1	< 0.05	20-32	d
σ_{54} [nM]	115	< 6	20-32	d
NtrC [nM]	73	< 4	20-32	e
Average mRNA elongation rate [nuc/s]	39-55	> 5	$\leq$ 10	f
Global mRNA mean lifetime [min]	9.8	16-17	1.65	g
Translation				
Ribosome [nM]	46500	< 2300	20-30	h
Peptide chain elongation rate [AA/s]	18	> 1.5	$\approx$ 10	i
Doubling time [h]	0.5	50 (semi-continuous)	$\approx$ 100	j

Table S1. Gene expression numbers *in vivo* and *in vitro* (Toolbox 2.0 estimates).

[a] *In vivo* refers to *E. coli* and cell-free reaction to *E. coli* cell-free expression reaction. *E. coli* numbers have been calculated for a division time of 30 minutes at 37°C[1]. The protein concentration in *E. coli* was obtained from[2-4].

[b] Most of the cell-free reactions are optimum at an extract protein concentration of 10 mg/ml (determined by Bradford assay). Higher extract concentrations have been also used that give similar protein production[5].

[c] Free *E. coli* core RNA polymerase not bound to DNA was estimated in[6]. A same estimation is made from[1] using Table 3 in part V chapter 96. In a cell-free expression reaction, the concentration of core RNA polymerase was calculated from the protein dilution (20-30) and the amount of active core RNA polymerase present in *E. coli*.

[d] Considering that all σ_{70} are free during extract preparation. σ_{70} in a cell-free extract was calculated from the protein dilution (20-30) and the concentration *in vivo*[7]. The *in vivo* concentration of the other sigma factors were also obtained from[7] and diluted by 20 to get the concentrations in cell-free reaction.

[e] The *in vivo* concentration of NtrC was obtained from[8].

[f] *In vivo*, the average mRNA elongation rate with the *E. coli* RNA polymerase is 39-55 nuc/s[1]. The average mRNA elongation rate with the *E. coli* RNA polymerase has not been estimated in a cell-free system. Our measurements in this work show that the first fluorescent deGFP proteins are measured after 2.5 minutes of incubation **(Supplementary Figure S2)**. The length of transcription for that gene is about 750 bases, we conclude that transcription speed is at least 5 nuc/s. Some *in vitro* measurements have been performed, for example in[9], the elongation rate with the *E. coli* RNA polymerase was estimated: 10-30 nuc/s.

[g] *In vivo* from[10], *in vitro* from this work.

[h] The concentration of ribosomes in a cell-free extract was estimated by Underwood and colleagues[11]. This concentration can be also obtained from the concentration of ribosomes *in vivo*[1] corrected from a dilution of 20-30, considering that the fraction of ribosomes lost during extract preparation is negligible.

[i] *In vivo*, the average peptide elongation rate is 18 aa/s[1]. *In vitro*, the average peptide elongation rate is 1-2 aa/s[11]. In this work, the first fluorescent deGFP proteins are measured after 2.5 minutes of incubation **(Supplementary Figure S2)**. The length of translation for that gene is 226 aa, we conclude that translation speed is greater than 1.5 aa/s.

[j] The doubling time of a cell-free reaction refers to the time required to synthesize a protein amount equal to the amount of protein contained in the extract at the beginning of the reaction (e.g. If the protein concentration of a cell-free reaction is 10 mg/ml at the beginning of cell-free expression, the doubling time is the time required to synthesize 10 mg/ml of protein). Although no cell-free system has been shown to produce as much protein as in the extract, some estimation about the doubling time can be made from the protein production and the rate of protein production in semi-continuous mode[5] and this work.

eGFP	deGFP (eGFP modified in N and C-terminus)
ATGGTGAGCAAGGGCGAGGAGCTGTTCACCGGGGTGGTGCCCATCCTGGTC GAGCTGGACGGCGACGTAAACGGCCACAAGTTCAGCGTGTCCGGCGAGGGC GAGGGCGATGCCACCTACGGCAAGCTGACCCTGAAGTTCATCTGCACCACCG GCAAGCTGCCCGTGCCCTGGCCCACCCTCGTGACCACCCTGACCTACGGCGT GCAGTGCTTCAGCCGCTACCCCGACCACATGAAGCAGCACGACTTCTTCAAGT CCGCCATGCCCGAAGGCTACGTCCAGGAGCGCACCATCTTCTTCAAGGACGA CGGCAACTACAAGACCCGCGCCGAGGTGAAGTTCGAGGGCGACACCCTGGT GAACCGCATCGAGCTGAAGGGCATCGACTTCAAGGAGGACGGCAACATCCTG GGGCACAAGCTGGAGTACAACTACAACAGCCACAACGTCTATATCATGGCCGA CAAGCAGAAGAACGGCATCAAGGTGAACTTCAAGATCCGCCACAACATCGAG GACGGCAGCGTGCAGCTCGCCGACCACTACCAGCAGAACACCCCCATCGGC GACGGCCCCGTGCTGCTGCCCGACAACCACTACCTGAGCACCCAGTCCGCCC TGAGCAAAGACCCCAACGAGAAGCGCGATCACATGGTCCTGCTGGAGTTCGT GACCGCCGCCGGGATCACTCTCGGCATGGACGAGCTGTACAAGTAA	ATGGAGCTTTTCACTGGCGTTGTTCCCATCCTGGTCGAGCTGGACGGCGACG TAAACGGCCACAAGTTCAGCGTGTCCGGCGAGGGCGAGGGCGATGCCACCT ACGGCAAGCTGACCCTGAAGTTCATCTGCACCACCGGCAAGCTGCCCGTGCC CTGGCCCACCCTCGTGACCACCCTGACCTACGGCGTGCAGTGCTTCAGCCGC TACCCCGACCACATGAAGCAGCACGACTTCTTCAAGTCCGCCATGCCCGAAG GCTACGTCCAGGAGCGCACCATCTTCTTCAAGGACGACGGCAACTACAAGAC CCGCGCCGAGGTGAAGTTCGAGGGCGACACCCTGGTGAACCGCATCGAGCT GAAGGGCATCGACTTCAAGGAGGACGGCAACATCCTGGGGCACAAGCTGGA GTACAACTACAACAGCCACAACGTCTATATCATGGCCGACAAGCAGAAGAACG GCATCAAGGTGAACTTCAAGATCCGCCACAACATCGAGGACGGCAGCGTGCA GCTCGCCGACCACTACCAGCAGAACACCCCCATCGGCGACGGCCCCGTGCT GCTGCCCGACAACCACTACCTGAGCACCCAGTCCGCCCTGAGCAAAGACCCC AACGAGAAGCGCGATCACATGGTCCTGCTGGAGTTCGTGACCGCCGCCGGGA TCTAA

eCFP	deCFP (eCFP modified in N and C-terminus)
ATGGTGAGCAAGGGCGAGGAGCTGTTCACCGGGGTGGTGCCCATCCTGGTC GAGCTGGACGGCGACGTAAACGGCCACAAGTTCAGCGTGTCCGGCGAGGGC GAGGGCGATGCCACCTACGGCAAGCTGACCCTGAAGTTCATCTGCACCACCG GCAAGCTGCCCGTGCCCTGGCCCACCCTCGTGACCACCCTGACCTGGGGCG TGCAGTGCTTCAGCCGCTACCCCGACCACATGAAGCAGCACGACTTCTTCAAG TCCGCCATGCCCGAAGGCTACGTCCAGGAGCGCACCATCTTCTTCAAGGACG ACGGCAACTACAAGACCCGCGCCGAGGTGAAGTTCGAGGGCGACACCCTGG TGAACCGCATCGAGCTGAAGGGCATCGACTTCAAGGAGGACGGCAACATCCT GGGGCACAAGCTGGAGTACAACTACATCAGCCACAACGTCTATATCACCGCC GACAAGCAGAAGAACGGCATCAAGGCCAACTTCAAGATCCGCCACAACATCG AGGACGGCAGCGTGCAGCTCGCCGACCACTACCAGCAGAACACCCCCATCG GCGACGGCCCCGTGCTGCTGCCCGACAACCACTACCTGAGCACCCAGTCCG CCCTGAGCAAAGACCCCAACGAGAAGCGCGATCACATGGTCCTGCTGGAGTT CGTGACCGCCGCCGGGATCACTCTCGGCATGGACGAGCTGTACAAGCTGTAC AAGTAA	ATGGAGCTTTTCACTGGCGTTGTTCCCATCCTGGTCGAGCTGGACGGCGACG TAAACGGCCACAAGTTCAGCGTGTCCGGCGAGGGCGAGGGCGATGCCACCT ACGGCAAGCTGACCCTGAAGTTCATCTGCACCACCGGCAAGCTGCCCGTGCC CTGGCCCACCCTCGTGACCACCCTGACCTGGGGCGTGCAGTGCTTCAGCCGC TACCCCGACCACATGAAGCAGCACGACTTCTTCAAGTCCGCCATGCCCGAAG GCTACGTCCAGGAGCGCACCATCTTCTTCAAGGACGACGGCAACTACAAGAC CCGCGCCGAGGTGAAGTTCGAGGGCGACACCCTGGTGAACCGCATCGAGCT GAAGGGCATCGACTTCAAGGAGGACGGCAACATCCTGGGGCACAAGCTGGA GTACAACTACATCAGCCACAACGTCTATATCACCGCCGACAAGCAGAAGAACG GCATCAAGGCCAACTTCAAGATCCGCCACAACATCGAGGACGGCAGCGTGCA GCTCGCCGACCACTACCAGCAGAACACCCCCATCGGCGACGGCCCCGTGCT GCTGCCCGACAACCACTACCTGAGCACCCAGTCCGCCCTGAGCAAAGACCCC AACGAGAAGCGCGATCACATGGTCCTGCTGGAGTTCGTGACCGCCGCCGGGA TCTAA

YFP	deYFP (eYFP modified in N and C-terminus)
ATGGTGAGCAAGGGCGAGGAGCTGTTCACCGGGGTGGTGCCCATCCTGGTC GAGCTGGACGGCGACGTAAACGGCCACAAGTTCAGCGTGTCCGGCGAGGGC GAGGGCGATGCCACCTACGGCAAGCTGACCCTGAAGTTCATCTGCACCACCG GCAAGCTGCCCGTGCCCTGGCCCACCCTCGTGACCACCTTCGGCTACGGCCT GCAGTGCTTCGCCCGCTACCCCGACCACATGAAGCAGCACGACTTCTTCAAG TCCGCCATGCCCGAAGGCTACGTCCAGGAGCGCACCATCTTCTTCAAGGACG ACGGCAACTACAAGACCCGCGCCGAGGTGAAGTTCGAGGGCGACACCCTGG TGAACCGCATCGAGCTGAAGGGCATCGACTTCAAGGAGGACGGCAACATCCT GGGGCACAAGCTGGAGTACAACTACAACAGCCACAACGTCTATATCATGGCC GACAAGCAGAAGAACGGCATCAAGGTGAACTTCAAGATCCGCCACAACATCG AGGACGGCAGCGTGCAGCTCGCCGACCACTACCAGCAGAACACCCCCATCG GCGACGGCCCCGTGCTGCTGCCCGACAACCACTACCTGAGCTACCAGTCCGC CCTGAGCAAAGACCCCAACGAGAAGCGCGATCACATGGTCCTGCTGGAGTTC GTGACCGCCGCCGGGATCACTCTCGGCATGGACGAGCTGTACAAGTAA	ATGGAGCTTTTCACTGGCGTTGTTCCCATCCTGGTCGAGCTGGACGGCGACG TAAACGGCCACAAGTTCAGCGTGTCCGGCGAGGGCGAGGGCGATGCCACCT ACGGCAAGCTGACCCTGAAGTTCATCTGCACCACCGGCAAGCTGCCCGTGCC CTGGCCCACCCTCGTGACCACCTTCGGCTACGGCCTGCAGTGCTTCGCCCGC TACCCCGACCACATGAAGCAGCACGACTTCTTCAAGTCCGCCATGCCCGAAG GCTACGTCCAGGAGCGCACCATCTTCTTCAAGGACGACGGCAACTACAAGAC CCGCGCCGAGGTGAAGTTCGAGGGCGACACCCTGGTGAACCGCATCGAGCT GAAGGGCATCGACTTCAAGGAGGACGGCAACATCCTGGGGCACAAGCTGGA GTACAACTACAACAGCCACAACGTCTATATCATGGCCGACAAGCAGAAGAACG GCATCAAGGTGAACTTCAAGATCCGCCACAACATCGAGGACGGCAGCGTGCA GCTCGCCGACCACTACCAGCAGAACACCCCCATCGGCGACGGCCCCGTGCT GCTGCCCGACAACCACTACCTGAGCTACCAGTCCGCCCTGAGCAAAGACCCC AACGAGAAGCGCGATCACATGGTCCTGCTGGAGTTCGTGACCGCCGCCGGGA TCTAA

mVenus	dmVenus (mVenus modified in N and C-terminus)
ATGGTGAGCAAGGGCGAGGAGCTGTTCACCGGGGTGGTGCCCATCCTGGTC GAGCTGGACGGCGACGTAAACGGCCACAAGTTCAGCGTGTCCGGCGAGGGC GAGGGCGATGCCACCTACGGCAAGCTGACCCTGAAGCTGATCTGCACCACCG GCAAGCTGCCCGTGCCCTGGCCCACCCTCGTGACCACCCTGGGCTACGGCC TGCAGTGCTTCGCCCGCTACCCCGACCACATGAAGCAGCACGACTTCTTCAA GTCCGCCATGCCCGAAGGCTACGTCCAGGAGCGCACCATCTTCTTCAAGGAC GACGGCAACTACAAGACCCGCGCCGAGGTGAAGTTCGAGGGCGACACCCTG GTGAACCGCATCGAGCTGAAGGGCATCGACTTCAAGGAGGACGGCAACATCC TGGGGCACAAGCTGGAGTACAACTACAACAGCCACAACGTCTATATCACCGCC GACAAGCAGAAGAACGGCATCAAGGCCAACTTCAAGATCCGCCACAACATCG AGGACGGCGGCGTGCAGCTCGCCGACCACTACCAGCAGAACACCCCCATCG GCGACGGCCCCGTGCTGCTGCCCGACAACCACTACCTGAGCTACCAGTCCAA GCTGAGCAAAGACCCCAACGAGAAGCGCGATCACATGGTCCTGCTGGAGTTC GTGACCGCCGCCGGGATCACTCTCGGCATGGACGAGCTGTACAAGTAA	ATGGAGCTTTTCACTGGCGTTGTTCCCATCCTGGTCGAGCTGGACGGCGACG TAAACGGCCACAAGTTCAGCGTGTCCGGCGAGGGCGAGGGCGATGCCACCT ACGGCAAGCTGACCCTGAAGCTGATCTGCACCACCGGCAAGCTGCCCGTGCC CTGGCCCACCCTCGTGACCACCCTGGGCTACGGCCTGCAGTGCTTCGCCCGC TACCCCGACCACATGAAGCAGCACGACTTCTTCAAGTCCGCCATGCCCGAAG GCTACGTCCAGGAGCGCACCATCTTCTTCAAGGACGACGGCAACTACAAGAC CCGCGCCGAGGTGAAGTTCGAGGGCGACACCCTGGTGAACCGCATCGAGCT GAAGGGCATCGACTTCAAGGAGGACGGCAACATCCTGGGGCACAAGCTGGA GTACAACTACAACAGCCACAACGTCTATATCACCGCCGACAAGCAGAAGAACG GCATCAAGGTGAACTTCAAGATCCGCCACAACATCGAGGACGGCAGCGTGCA GCTCGCCGACCACTACCAGCAGAACACCCCCATCGGCGACGGCCCCGTGCT GCTGCCCGACAACCACTACCTGAGCTACCAGTCCGCCCTGAGCAAAGACCCC AACGAGAAGCGCGATCACATGGTCCTGCTGGAGTTCGTGACCGCCGCCGGGA TCTAA

mCherry	mmCherry (mCherry modified in N-terminus)
ATGGTGAGCAAGGGCGAGGAGGATAACATGGCCATCATCAAGGAGTTCATGC GCTTCAAGGTGCACATGGAGGGCTCCGTGAACGGCCACGAGTTCGAGATCGA GGGCGAGGGCGAGGGCCGCCCCTACGAGGGCACCCAGACCGCCAAGCTGA AGGTGACCAAGGGTGGCCCCCTGCCCTTCGCCTGGGACATCCTGTCCCCTCA GTTCATGTACGGCTCCAAGGCCTACGTGAAGCACCCCGCCGACATCCCCGAC TACTTGAAGCTGTCCTTCCCCGAGGGCTTCAAGTGGGAGCGCGTGATGAACTT CGAGGACGGCGGCGTGGTGACCGTGACCCAGGACTCCTCCCTGCAGGACGG CGAGTTCATCTACAAGGTGAAGCTGCGCGGCACCAACTTCCCCTCCGACGGC CCCGTAATGCAGAAGAAGACCATGGGCTGGGAGGCCTCCTCCGAGCGGATGT ACCCCGAGGACGGCGCCCTGAAGGGCGAGATCAAGCAGAGGCTGAAGCTGA AGGACGGCGGCCACTACGACGCTGAGGTCAAGACCACCTACAAGGCCAAGAA GCCCGTGCAGCTGCCCGGCGCCTACAACGTCAACATCAAGTTGGACATCACC TCCCACAACGAGGACTACACCATCGTGGAACAGTACGAACGCGCCGAGGGCC GCCACTCCACCGGCGGCATGGACGAGCTGTACAAGTAA	ATGGTGAGCAAGGGCGAAGAAGATAACATGGCCATCATCAAGGAGTTCATGC GCTTCAAGGTGCACATGGAGGGCTCCGTGAACGGCCACGAGTTCGAGATCGA GGGCGAGGGCGAGGGCCGCCCCTACGAGGGCACCCAGACCGCCAAGCTGA AGGTGACCAAGGGTGGCCCCCTGCCCTTCGCCTGGGACATCCTGTCCCCTCA GTTCATGTACGGCTCCAAGGCCTACGTGAAGCACCCCGCCGACATCCCCGAC TACTTGAAGCTGTCCTTCCCCGAGGGCTTCAAGTGGGAGCGCGTGATGAACTT CGAGGACGGCGGCGTGGTGACCGTGACCCAGGACTCCTCCCTGCAGGACGG CGAGTTCATCTACAAGGTGAAGCTGCGCGGCACCAACTTCCCCTCCGACGGC CCCGTAATGCAGAAGAAGACCATGGGCTGGGAGGCCTCCTCCGAGCGGATGT ACCCCGAGGACGGCGCCCTGAAGGGCGAGATCAAGCAGAGGCTGAAGCTGA AGGACGGCGGCCACTACGACGCTGAGGTCAAGACCACCTACAAGGCCAAGAA GCCCGTGCAGCTGCCCGGCGCCTACAACGTCAACATCAAGTTGGACATCACC TCCCACAACGAGGACTACACCATCGTGGAACAGTACGAACGCGCCGAGGGCC GCCACTCCACCGGCGGCATGGACGAGCTGTACAAGTAA

dTomato (not modified)	TagRFP-T (not modified)
ATGGTGAGCAAGGGCGAGGAGGTCATCAAAGAGTTCATGCGCTTCAAGGTG CGCATGGAGGGCTCCATGAACGGCCACGAGTTCGAGATCGAGGGCGAGGG CGAGGGCCGCCCCTACGAGGGCACCCAGACCGCCAAGCTGAAGGTGACCA AGGGCGGCCCCCTGCCCTTCGCCTGGGACATCCTGTCCCCCCAGTTCATGT ACGGCTCCAAGGCGTACGTGAAGCACCCCGCCGACATCCCCGATTACAAGA AGCTGTCCTTCCCCGAGGGCTTCAAGTGGGAGCGCGTGATGAACTTCGAGG ACGGCGGTCTGGTGACCGTGACCCAGGACTCCTCCCTGCAGGACGGCACG CTGATCTACAAGGTGAAGATGCGCGGCACCAACTTCCCCCCCGACGGCCCC GTAATGCAGAAGAAGACCATGGGCTGGGAGGCCTCCACCGAGCGCCTGTAC CCCCGCGACGGCGTGCTGAAGGGCGAGATCCACCAGGCCCTGAAGCTGAA GGACGGCGGCCACTACCTGGTGGAGTTCAAGACCATCTACATGGCCAAGAA GCCCGTGCAACTGCCCGGCTACTACTACGTGGACACCAAGCTGGACATCAC CTCCCACAACGAGGACTACACCATCGTGGAACAGTACGAGCGCTCCGAGGG CCGCCACCACCTGTTCCTGTACGGCATGGACGAGCTGTACAAGTAA	ATGGTGTCTAAGGGCGAAGAGCTGATTAAGGAGAACATGCACATGAAGCTGTAC ATGGAGGGCACCGTGAACAACCACCACTTCAAGTGCACATCCGAGGGCGAAGG CAAGCCCTACGAGGGCACCCAGACCATGAGAATCAAGGTGGTCGAGGGCGGC CCTCTCCCCTTCGCCTTCGACATCCTGGCTACCAGCTTCATGTACGGCAGCAGA ACCTTCATCAACCACACCCAGGGCATCCCCGACTTCTTTAAGCAGTCCTTCCCT GAGGGCTTCACATGGGAGAGAGTCACCACATACGAAGACGGGGGCGTGCTGA CCGCTACCCAGGACACCAGCCTCCAGGACGGCTGCCTCATCTACAACGTCAAG ATCAGAGGGGTGAACTTCCCATCCAACGGCCCTGTGATGCAGAAGAAAACACTC GGCTGGGAGGCCAACACCGAGATGCTGTACCCCGCTGACGGCGGCCTGGAAG GCAGAACCGACATGGCCCTGAAGCTCGTGGGCGGGGGCCACCTGATCTGCAA CTTCAAGACCACATACAGATCCAAGAAACCCGCTAAGAACCTCAAGATGCCCGG CGTCTACTATGTGGACCACAGACTGGAAAGAATCAAGGAGGCCGACAAAGAGA CCTACGTCGAGCAGCACGAGGTGGCTGTGGCCAGATACTGCGACCTCCCTAGC AAACTGGGGCACAAACTTAATGGCATGGACGAGCTGTACAAGTAA

mApple (not modified)	mRuby (not modified)
ATGGTGAGCAAGGGCGAGGAGAATAACATGGCCATCATCAAGGAGTTCATG CGCTTCAAGGTGCACATGGAGGGCTCCGTGAACGGCCACGAGTTCGAGATC GAGGGCGAGGGCGAGGGCCGCCCCTACGAGGCCTTTCAGACCGCTAAGCT GAAGGTGACCAAGGGTGGCCCCCTGCCCTTCGCCTGGGACATCCTGTCCCC TCAGTTCATGTACGGCTCCAAGGTCTACATTAAGCACCCAGCCGACATCCCC GACTACTTCAAGCTGTCCTTCCCCGAGGGCTTCAGGTGGGAGCGCGTGATG AACTTCGAGGACGGCGGCATTATTCACGTTAACCAGGACTCCTCCCTGCAG GACGGCGTGTTCATCTACAAGGTGAAGCTGCGCGGCACCAACTTCCCCTCC GACGGCCCCGTAATGCAGAAGAAGACCATGGGCTGGGAGGCCTCCGAGGA GCGGATGTACCCCGAGGACGGCGCCCTGAAGAGCGAGATCAAGAAGAGGC TGAAGCTGAAGGACGGCGGCCACTACGCCGCCGAGGTCAAGACCACCTAC AAGGCCAAGAAGCCCGTGCAGCTGCCCGGCGCCTACATCGTCGACATCAAG TTGGACATCGTGTCCCACAACGAGGACTACACCATCGTGGAACAGTACGAA CGCGCCGAGGGCCGCCACTCCACCGGCGGCATGGACGAGCTGTACAAGTA A	ATGAACAGCCTGATCAAAGAAAACATGCGGATGAAGGTGGTGCTGGAAGGCAG CGTGAACGGCCACCAGTTCAAGTGCACCGGCGAGGGCGAGGGCAACCCCTAC ATGGGCACCCAGACCATGCGGATCAAAGTGATCGAGGGCGGACCTCTGCCCTT CGCCTTCGACATCCTGGCCACATCCTTCATGTACGGCAGCCGGACCTTCATCAA GTACCCCAAGGGCATCCCCGATTTCTTCAAGCAGAGCTTCCCCGAGGGCTTCA CCTGGGAGAGAGTGACCAGATACGAGGACGGCGGCGTGATCACCGTGATGCA GGACACCAGCCTGGAAGATGGCTGCCTGGTGTACCATGCCCAGGTCAGGGGC GTGAATTTTCCCAGCAACGGCGCCGTGATGCAGAAGAAAACCAAGGGCTGGGA GCCCAACACCGAGATGATGTACCCCGCTGACGGCGGACTGAGAGGCTACACCC ACATGGCCCTGAAGGTGGACGGCGGAGGGCACCTGAGCTGCAGCTTCGTGAC CACCTACCGATCCAAGAAAACCGTGGGCAACATCAAGATGCCCGGCATCCACG CCGTGGACCACCGGCTGGAAAGGCTGGAAGAGTCCGACAACGAGATGTTCGTG GTGCAGCGGGAGCACGCCGTGGCCAAGTTCGCCGGCCTGGGCGGAGGGTAA

Table S2. DNA sequences of the nine reporter genes tested. deGFP, deCFP, deYFP, and dmVenus have been modified in their N- and C-terminus based on previous observations[12] to be more translatable in cell-free systems. The most important modification is in N-terminus, where a ribosome-like sequence has been removed. mmCherry was modified in N-terminus in a similar manner to deGFP. dTomato, TagRFP-T, mApple and mRuby were not modified.

Protein	Excitation (nm)	Emission (nm)	Relative Intensity
deCFP	440	480	22
deGFP	488	510	100
deYFP	514	532	93
dmVenus	516	533	78
dTomato	554	583	13
TagRFPT1	557	588	2
mApple	569	597	9
mRuby	558	601	9
mmCherry	587	616	4

Table S3. Excitation and emission wavelengths at peak of the nine reporter proteins synthesized with Toolbox 2.0. The relative intensity is given with respect to deGFP, which is set to 100. The relative intensities are specific to the wavelength settings as well as to the device that was used (plate reader Biotek H1m).

The following plasmids have been constructed from parts shown in **Supplementary Table S7**. Examples of construction are given in **Supplementary Table S4**. Short names are given in the first column, the full name should read as: pTXTL-P70a-S19 (the corresponding short name is: P70a-S19).

Nomenclature:

• P70a: promoter specific to *E. coli* sigma factor 70, 'a' indicates the first in the list. The same notation is used for other promoters, for example P28a is a promoter specific to the *E. coli* sigma factor 28, 'a' indicates the first in the list. All of the circuits shown in this work were done with the 'a' series of promoters and with T7p14 for T7. The P70a-d series was constructed from the OR_2-OR_1-Pr promoter by mutating the -35 and/or the -10 without altering the two operators.

• The *E. coli* strain KL740 can be found at the *E. coli* resources at Yale, CGSC.

• All of the plasmids listed are Ampicillin resistant.

• MGapt (and MGapt1): the malachite green aptamer[13].

Relative strengths of some part series:

Promoters	Relative strength
P70a	100
P70b	25
P70c	2
P70d	30
T7p7	48
T7p8	7
T7p11	3
T7p14	100
T7p16	24
UTRs	**Relative strength**
UTR1	100
UTR3	25
UTR4	50
UTR5	10

Name	UTR	Expressed gene	TX term.	Ori.	Size (bp)	*E. coli* host
P70a-S19	UTR1	fecI (sigma 19)	T500	p15A	3306	KL740
P70a-S28	UTR1	rpoF (sigma 28)	T500	p15A	3265	KL740
P70a-S24	UTR1	RpoE (sigma 24)	T500	p15A	3349	KL740
P70a-S32	UTR1	RpoH (sigma 32)	T500	p15A	3628	KL740
P70a-S38	UTR1	RpoS (sigma 38)	T500	p15A	3525	KL740
P70a-S54	UTR1	RpoN (sigma 54)	T500	p15A	4207	KL740
P70a-NtrC	UTR1	NtrC	T500	p15A	4183	KL740
P70a-deGFP	UTR1	deGFP	T500	ColE1	3202	KL740 or DH5alpha
P70a-deGFP-ssrA	UTR1	deGFP-ssrA	T500	ColE1	3235	KL740 or DH5alpha
P70a-S19-ssrA	UTR1	S19-ssrA	T500	p15A	3080	KL740
P70a-OmpA-S24	UTR1	OmpA-S24	T500	p15A	3427	KL740
P70a-S28-YbaQ	UTR1	S28-YbaQ	T500	p15A	3295	KL740
P70a-S28-ssrA	UTR1	S28-ssrA	T500	p15A	3294	KL740
P70a-S32-ssrA	UTR1	S32-ssrA	T500	p15A	3670	KL740
P70a-OmpA-S38	UTR1	OmpA-S38	T500	p15A	3844	KL740
P70a-mmCherry	UTR1	mmCherry	T500	ColE1	3235	KL740 or DH5alpha
P70a-deCFP	UTR1	deCFP	T500	ColE1	3202	KL740 or DH5alpha
P70a-mCherry	UTR1	mCherry	T500	ColE1	3235	KL740 or DH5alpha
P70a-dmVenus	UTR1	dmVenus	T500	ColE1	3202	KL740 or DH5alpha
P70a-dTomato	UTR1	dTomato	T500	ColE1	3229	KL740 or DH5alpha
P70a-mRuby	UTR1	mRuby	T500	ColE1	3208	KL740 or DH5alpha
P70a-mApple	UTR1	mApple	T500	ColE1	3235	KL740 or DH5alpha
P70a-TagRFPT1	UTR1	TagRFPT1	T500	ColE1	3259	KL740 or DH5alpha
P70a-deYFP	UTR1	deYFP	T500	ColE1	3202	KL740 or DH5alpha
P70a-Venus	UTR1	Venus	T500	ColE1	3241	KL740 or DH5alpha
P70a-cI-ssrA	UTR1	cI-ssrA	T500	ColE1	3515	KL740
P70a-ClpPX	UTR1	ClpPX	T500	p15A	4676	KL740
P70a-MGapt	none	MG aptamer	T500	ColE1	2544	KL740
P70a-MGapt-deGFP	UTR1	deGFP	T500	ColE1	3241	KL740

P70a-T7rnap	UTR1	T7rnap	T500	p15A	5425	KL740
P70a-T3rnap	UTR1	T3rnap	T500	p15A	5428	KL740
P70a-U3-deGFP	UTR3	deGFP	T500	ColE1	3202	KL740 or DH5alpha
P70a-U4-deGFP	UTR4	deGFP	T500	ColE1	3202	KL740 or DH5alpha
P70a-U5-deGFP	UTR5	deGFP	T500	ColE1	3202	KL740 or DH5alpha
P70b-deGFP	UTR1	deGFP	T500	ColE1	3202	KL740 or DH5alpha
P70b-MGapt1	none	MG aptamer	T500	ColE1	2544	KL740 or DH5alpha
P70b-MGapt-deGFP	UTR1	deGFP	T500	ColE1	3241	KL740 or DH5alpha
P70b-U3-deGFP	UTR3	deGFP	T500	ColE1	3202	KL740 or DH5alpha
P70b-U4-deGFP	UTR5	deGFP	T500	ColE1	3202	KL740 or DH5alpha
P70c-deGFP	UTR1	deGFP	T500	ColE1	3202	KL740 or DH5alpha
P70c-MGapt1	none	MG aptamer	T500	ColE1	2544	KL740 or DH5alpha
P70c-MGapt-deGFP	UTR1	deGFP	T500	ColE1	3241	KL740 or DH5alpha
P70c-U3-deGFP	UTR3	deGFP	T500	ColE1	3202	KL740 or DH5alpha
P70c-U4-deGFP	UTR5	deGFP	T500	ColE1	3202	KL740 or DH5alpha
P70d-deGFP	UTR1	deGFP	T500	ColE1	3202	KL740 or DH5alpha
P28a-deGFP	UTR1	deGFP	T500	ColE1	3231	JM109
P28a-mApple	UTR1	mApple	T500	ColE1	3264	JM109
P28a-Luc	UTR1	Luc	T500	ColE1	4261	JM109
P28a-deCFP	UTR1	deCFP	T500	ColE1	3231	JM109
P28a-deYFP	UTR1	deYFP	T500	ColE1	3231	JM109
P28a-deGFP-ssrA	UTR1	deGFP-ssrA	T500	ColE1	3264	JM109
P28a-flgM	UTR1	FlgM	none	ColE1	2694	JM109
P28a-flgM-ssrA	UTR1	FlgM-ssrA	none	ColE1	2730	JM109
P28a-S19-ssA	UTR1	S19-ssrA	none	ColE1	3072	JM109
P28a-S19	UTR1	S19	none	ColE1	3298	JM109
P28a-OmpA-S24	UTR1	OmpA-S24	none	ColE1	3419	JM109
P28a-S24-ssrA	UTR1	S24-ssrA	none	ColE1	3419	JM109

P28a-S38	UTR1	S38	none	ColE1	3803	JM109
P28a-S54	UTR1	S54	T500	ColE1	4117	JM109
P28a-NtrC	UTR1	NtrC	T500	ColE1	4093	JM109
P28a-TetR	UTR1	TetR	T500	ColE1	3177	JM109
P28a-CI-ssrA	UTR1	cI-ssrA	T500	ColE1	3332	JM109
P28a-MazF-ssrA	UTR1	MazF-ssrA	none	ColE1	3143	JM109
P28a-MazE-ssrA	UTR1	MazE-ssrA	none	ColE1	3057	JM109
P19a-deGFP	UTR1	deGFP	T500	ColE1	3255	JM109
P19a-deCFP	UTR1	deCFP	T500	ColE1	3255	JM109
P19a-deYFP	UTR1	deYFP	T500	ColE1	3255	JM109
P19a-S28-ssrA	UTR1	S28-ssrA	T500	p15A	3319	JM109
P19a-S28	UTR1	S28-ssrA	T500	p15A	3290	JM109
P19a-OmpA-S24	UTR1	OmpA-S24	T500	ColE1	3361	JM109
P19a-S24	UTR1	S24	T500	ColE1	3283	JM109
P19a-S38	UTR1	S38	T500	p15A	3550	JM109
P19a-NtrC	UTR1	NtrC	T500	p15A	4208	JM109
P54a-deGFP	UTR1	deGFP	T500	ColE1	3418	JM109
P54a-S38	UTR1	S38	T500	p15A	3713	JM109
P54a-S28	UTR1	S28	T500	p15A	3453	JM109
P54a-S19	UTR1	S19	T500	p15A	3494	JM109
P54a-S24	UTR1	S24	T500	p15A	3537	JM109
P32a-deGFP	UTR1	deGFP	T500	ColE1	3240	JM109
P24a-deGFP	UTR1	deGFP	T500	ColE1	3228	JM109
P24a-OmpA-S38	UTR1	OmpA-S38	T500	ColE1	3751	JM109
P24a-S38	UTR1	S38	T500	ColE1	3432	JM109
P24a-S28	UTR1	S28	T500	ColE1	3172	JM109
P24a-S28-ssrA	UTR1	S28-ssrA	T500	ColE1	3201	JM109

P38a-deGFP	UTR1	deGFP	T500	ColE1	3232	JM109
P38a-S19	UTR1	S19	T500	ColE1	3217	JM109
P38a-S19-ssrA	UTR1	S19-ssrA	T500	ColE1	2991	JM109
P38a-S28	UTR1	S28	T500	ColE1	3176	JM109
P38a-S28-ssrA	UTR1	S28-ssrA	T500	ColE1	3206	JM109
P38a-S54	UTR1	S54	T500	ColE1	4118	JM109
P38a-NtrC	UTR1	NtrC	T500	ColE1	4094	JM109
PLtet01-deGFP-ssrA	UTR1	deGFP-ssrA	T500	p15A	3326	DH5aZ1
PLtet01-deGFP-YbaQ	UTR1	deGFP-YbaQ	T500	p15A	3323	DH5aZ1
PLtet01-deGFP	UTR1	deGFP	T500	p15A	3293	DH5aZ1
T7P11-deGFP		deGFP	T7	ColE1	4077	JM109
T7P11-MGapt		MG aptamer	T7	ColE1	3423	JM109
T7P14-deGFP		deGFP	T7	ColE1	4137	JM109
T7P14-MGapt		MG aptamer	T7	ColE1	3427	JM109
T7P16-deGFP		deGFP	T7	ColE1	4124	JM109
T7P16-MGapt		MG aptamer	T7	ColE1	3424	JM109
T7P7-deGFP		deGFP	T7	ColE1	4118	JM109
T7P7-MGapt		MG aptamer	T7	ColE1	3425	JM109
T7P8-deGFP		deGFP	T7	ColE1	4110	JM109
T7P8-MGapt		MG aptamer	T7	ColE1	3424	JM109
pCa-deGFP		deGFP	T500	p15A	3303	JM109
pC-MGapt		MG aptamer	T500	ColE1	2513	JM109
T3P-deGFP		deGFP	T7	ColE1	4137	JM109
P28a-MreB	UTR1	MreB	T500	ColE1	3668	JM109
P28a-MreC	UTR1	MreC	T500	ColE1	3898	JM109
P28a-Venus-MreB	UTR1	Venus-Mreb	T500	ColE1	4389	JM109
P28a-venus-MreB-18L	UTR1	Venus-MreB-18L	T500	ColE1	4450	JM109

P28a-AH	UTR1	αHemolysin	none	ColE1	3438	JM109
P28a-AH-eGFP	UTR1	αHemolysin-eGFP	none	ColE1	4422	JM109
T7p14-AH	UTR1	αHemolysin	T7	ColE1	4419	JM109
T7p14-AH-eGFP	UTR1	αHemolysin-eGFP	T7	ColE1	5156	JM109

Table S4. List of plasmids designed for Toolbox 2.0. Plasmids are sorted by promoters.

σ factor / promoter	σ_{70}	σ_{19}	σ_{24}	σ_{28}	σ_{32}	σ_{38}	σ_{54}/NtrC
P_{70a}	7.65	7.47	7.24	5.95	6.73	7.09	5.99
P_{19a}	0.04	0.27	0.02	0.02	0.01	0.02	0.05
P_{24a}	0.04	0.03	0.21	0.02	0.02	0.03	0.02
P_{28a}	0.01	0.02	0.01	5.69	0.02	0.01	0.02
P_{32a}	0.41	0.44	0.40	0.31	3.65	0.40	0.27
P_{38a}	0.02	0.04	0.05	0.01	0.02	0.40	0.01
P_{54a}	0.02	0.02	0.02	0.01	0.00	0.01	0.15

Table S5. Crosstalk between transcriptional activation units measured in the linear regime of plasmid concentration (0.1 nM of plasmid encoding the sigma factor and 1 nM reporter plasmid, σ_{70} salt conditions, see **Table 1**). Values (deGFP [μM]) are from the end-point deGFP production for seven *E. coli* sigma factors (non-degradable versions). Except for the endogenous σ_{70} present in the reaction, the transcription factors were expressed as shown in the **Figure S8a-g**. Expression through the promoter P_{70a} is high in all of the cases because the endogenous σ_{70} is present in the extract.

Promoter	Description	Source - references
P_{70a}	Lambda phage promoter OR_2-OR_1-Pr specific to *E. coli* σ_{70}	GenBank: J02459.1, [12]
P_{19a}	Promoter of the *fec* transporter genes (*E. coli*) specific to σ_{19}	GenBank: U00096.2, [14]
P_{24a}	Promoter of the *htrA* gene (*E. coli*) specific to σ_{24}	GenBank: U00096.2, [15]
P_{28a}	Promoter of the *tar* gene (*E. coli*) specific to σ_{28}	GenBank: U00096.2, [16]
P_{32a}	Promoter of the *groE* gene (*E. coli*) specific to σ_{32}	GenBank: U00096.2, [17]
P_{38a}	Promoter of the *osmY* gene (*E. coli*) specific to σ_{38}	GenBank: U00096.2, [18]
P_{54a}	Promoter of the *glna* gene (*E. coli*) specific to σ_{54}	GenBank: U00096.2, [19]
T3P	Promoter of bacteriophage T3	GenBank: NC_003298
$T7P_{14}$	Promoter of bacteriophage T7	GenBank: NC_001604
araBAD	Promoter specific to *E. coli* σ_{70} and regulated by the *araC* gene	[20]
melAB	Promoter specific to *E. coli* σ_{70} and regulated by the *melR* gene	[21]
$P_{L\text{-}tetO1}$	Promoter specific to *E. coli* σ_{70} and regulated by the *tetR* gene	[22]
Untranslated region	**Description**	**Source – references**
UTR1	The untranslated region containing the T7 g10 leader sequence for highly efficient translation initiation	GenBank: M35614.1, [12, 23]
Transcription terminator	**Description**	**Source – references**
T500	Transcription terminator for *E. coli* RNA polymerase	[24]
T7	Transcription terminator for T7 RNA polymerase	GenBank: NC_001604
Riboregulator	**Description**	**Source – references**
Raj11, Raj 31	Synthetic riboregulator of translation	[25]
Genes	**Description**	**Source – references**
deGFP	eGFP truncated and modified in N- and C- terminus	[12]
deCFP	eCFP truncated and modified in N- and C- terminus	[12]
deYFP	eYFP truncated and modified in N- and C- terminus	This work
dmVenus	Venus YFP A206K protein truncated and modified in N- and C-terminus	This work
mmCherry	mCherry truncated and modified in N- and C- terminus	This work
dTomato	The fluorescent protein dTomato	GenBank: AY678268.1
TagRFP-T	The fluorescent protein TagRFP-T	GenBank: EU582019.1
mApple	The fluorescent protein mApple	GenBank: DK336160.2
mRuby	The fluorescent protein mRuby	[26]

σ_{19}	*fecI* (*E. coli* σ_{19})	GenBank: U00096.2
σ_{19}-*ssrA*	*fecI* tagged with *ssrA*	[27]
σ_{24}	*rpoE* (*E. coli* σ_{24})	GenBank: U00096.2
ompA-σ_{24}	*rpoE* tagged with *ompA*	[27]
σ_{28}	*rpoF* (*E. coli* σ_{28})	GenBank: U00096.2
σ_{28}-*ssrA*	*rpoF* tagged with *ssrA*	[27]
σ_{32}	*rpoH* (*E. coli* σ_{32})	GenBank: U00096.2
σ_{32}-*ssrA*	*rpoH* tagged with *ssrA*	[27]
σ_{38}	*rpoS* (*E. coli* σ_{38})	GenBank: U00096.2
ompA-σ_{38}	*rpoS* tagged with *ompA*	[27]
σ_{54}	*rpoN* (*E. coli* σ_{54})	GenBank: U00096.2
clpXP	*E. coli* clpXP tandem proteins (same operon)	GenBank: J05534.1, L18867.1
ntrC	Co-activator of σ^{54} promoters	GenBank: U00096.2
mazF	*E. coli* interferase MazF (*chpA* gene)	GenBank: CDJ74047.1
T7 RNAP	T7 bacteriophage RNA polymerase	GenBank: FJ881694.1
T3 RNAP	T3 bacteriophage RNA polymerase	GenBank: X02981.1
araC	Arabinose operon regulatory gene	GenBank: AAC73175.1
asia	T4 protein Asia, inhibitor of *E. coli* σ_{70}	GenBank: AAA32480.1
mSA	Monomeric streptavidin	[28]
tetR	Tet operon regulatory gene	GenBank: BAG71042.1
αHemolysin	*Staphylococcus aureus* pore forming protein αHemolysin	GenBank: M90536.1
αHemolysin-eGFP	Fusion of the pore forming encoding gene *αHemolysin* and *eGFP*	[29]
cI	Lambda phage repressor protein CI	GenBank: CAB96428.1
ssrA	SsrA peptide for degradation by AAA+ proteases	[30]
Synthetic operon	**Description**	**Source – references**
vioABCDE	Engineered vioABCDE operon (*Chromobacterium violaceum*)	Addgene: #40782
Genomes	**Description**	**Source – references**
T7	T7 phage complete dsDNA genome	GenBank: NC_001604
ΦX174	ΦX174 phage complete dsDNA genome	GenBank: J02482.1, [31]
MS2	MS2 phage complete RNA genome	GenBank: NC_001417.2

Table S7. DNA parts used in this work.

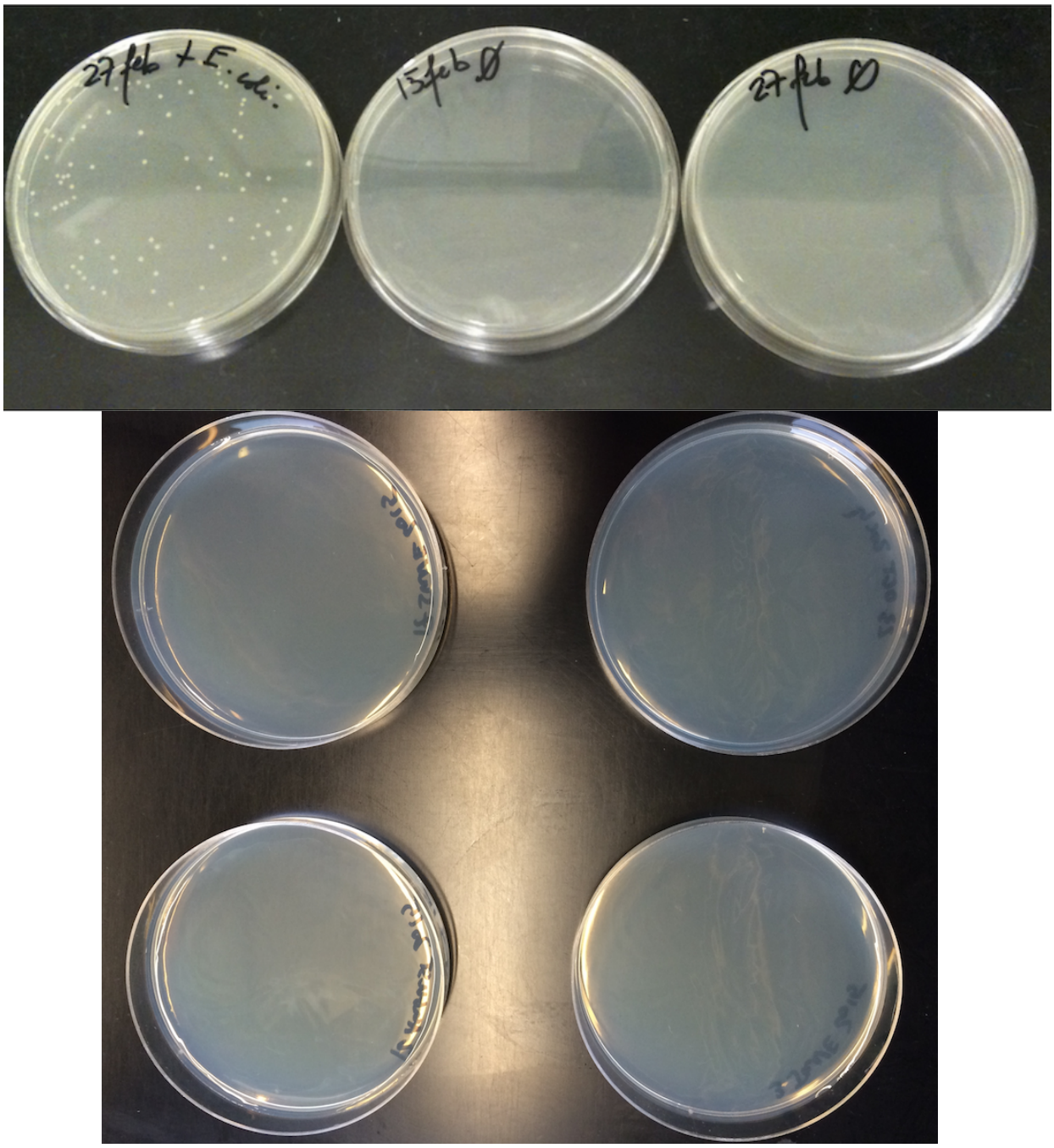

Figure S1. Cytoplasmic extract control plates. All the LB-agar (no antibiotic) plates were incubated at 37°C for 16 h. 30 µl of *E. coli* extract corresponds to seven reactions of 12 µl. **Top:** 50 µl of *E. coli* cytoplasmic extract were plated on each of the three plates. About 50 *E. coli* cells were added to the plate on the left, as a positive control. The two other plates show no living *E. coli* in two different extracts prepared in February 2013. **Bottom:** 60µl of four different *E. coli* cytoplasmic extracts were plated on each of the four plates. One extract was prepared in 2014 and three in 2015. No *E. coli* colonies grew on either plate for those six extracts.

To determine the maturation of deGFP, we used an RNAse A based assay. We previously showed that addition of RNAseA instantaneously stops TX-TL in the reaction[32]. We modified this assay to determine the maturation time more accurately compared to our previous approach. We first determined that no deGFP is produced in the first 2 minutes of the reaction (no increase of fluorescence was observed when RNAse A was added 2 minutes after the reaction start, plasmid P_{70a}-deGFP was set to 5 nM in those experiments). Then, we monitored the time course of fluorescence of the first burst of deGFP produced in cell-free reaction, between 2 minutes and 3 minutes by adding RNAseA after 3 minutes of incubation. We modeled this increase of fluorescence with a first order chemical kinetics fit using Mathematica:

$$\frac{d[\text{deGFP}_{\text{mat}}]}{dt} = k[\text{deGFP}_{\text{dark}}], \text{ with solution: } [\text{deGFP}_{\text{mat}}](t) = [\text{deGFP}_{\text{mat}}]_0 + [\text{deGFP}_{\text{dark}}]_0 \left(1 - e^{-kt}\right)$$

$[\text{deGFP}_{\text{mat}}](t)$	mature (fluorescent) deGFP as a function of time
$[\text{deGFP}_{\text{mat}}]_0$	initial mature (fluorescent) deGFP, measured at transcription arrest (which we call time point zero). For 2 minutes incubation, this value is zero.
$[\text{deGFP}_{\text{dark}}]_0$	initial dark deGFP, corresponding to concentration of dark deGFP (not matured) at transcription arrest. This value is fit by the software. (For 2 minutes incubation, this value is at the saturation level deGFPmat as t → infinity)
κ	protein maturation rate. Inverse (maturation time) is 16.2 minutes.

The experiment was repeated twice, a value of $1/k_1$ = 16.5 min and $1/k_2$ = 15.9 min was determined. The characteristic time of deGFP maturation was averaged to 16.2 ± 0.42 min.

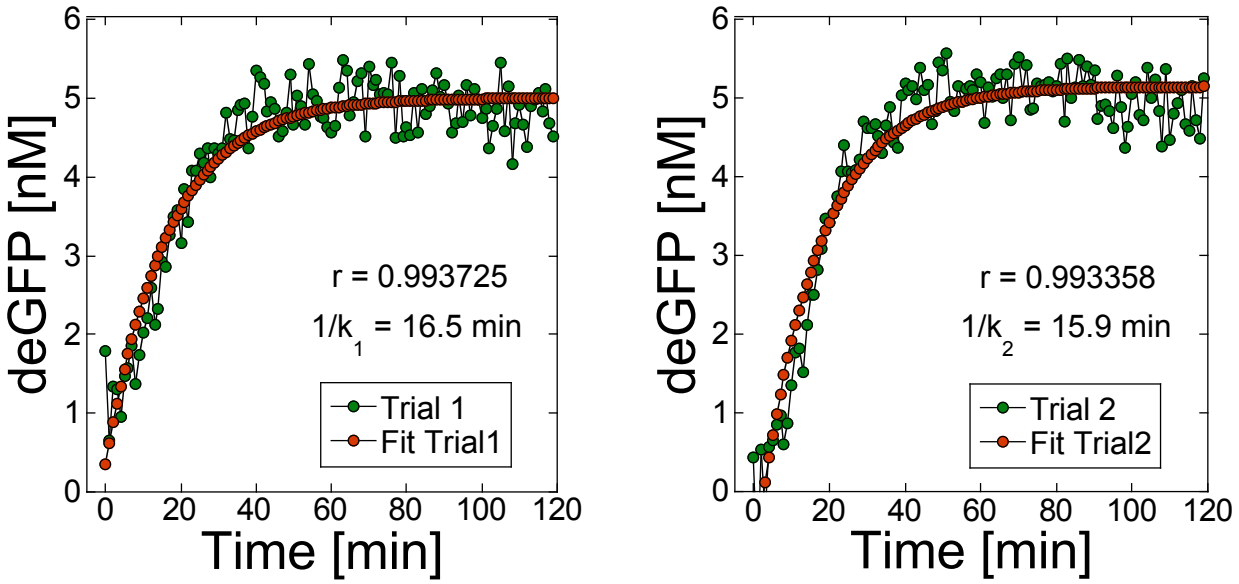

Figure S2. Two trials were made to estimate deGFP maturation time based on the RNAseA assay.

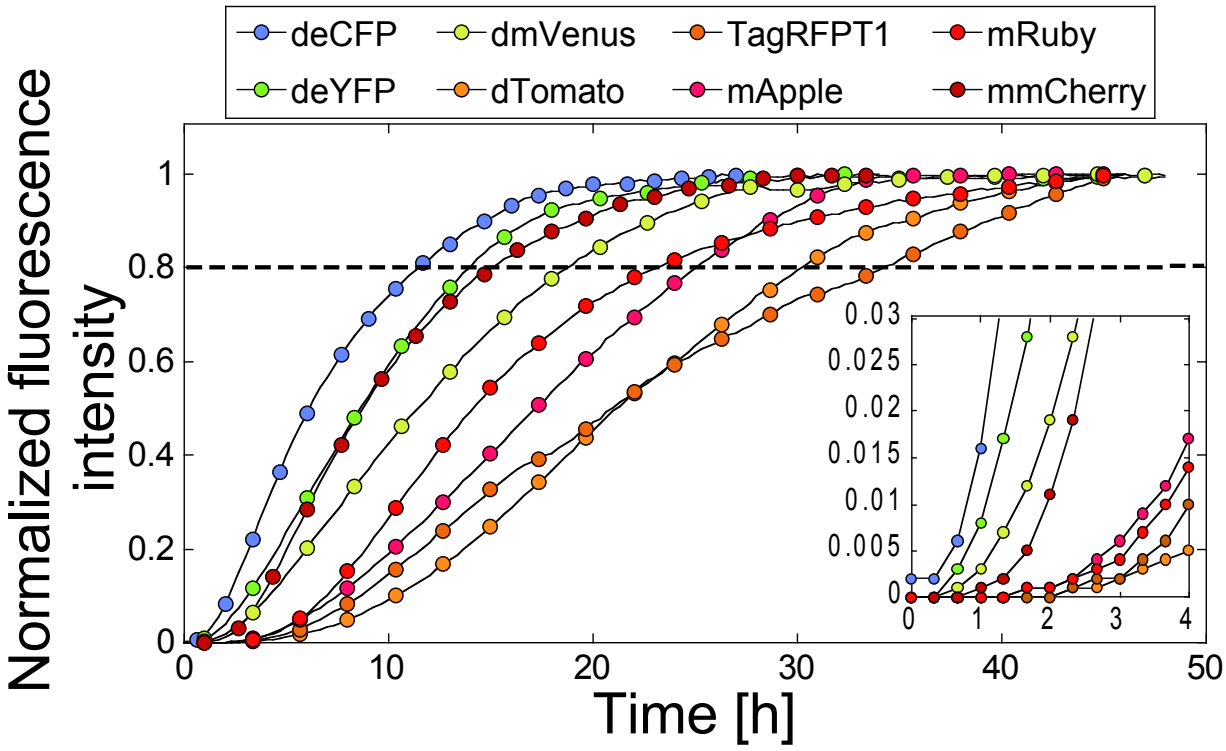

Figure S3. Kinetics of expression of eight reporter proteins in batch mode reactions (for deGFP see **Figure 2** or **Supplementary Figure S8a**). All of the reporter proteins were expressed through the promoter P_{70a} (e.g. P_{70a}-deCFP for deCFP), at a plasmid concentration of 5 nM. In agreement with literature[33], red fluorescent proteins are slower to mature, which explains the slow kinetics. The inset shows the first four hours of the kinetic measurement. From left to right, the kinetics crossing the dashed line are: deCFP, deYFP, mmCherry, dmVenus, mRuby, mApple, dTomato, TagRFPT1.

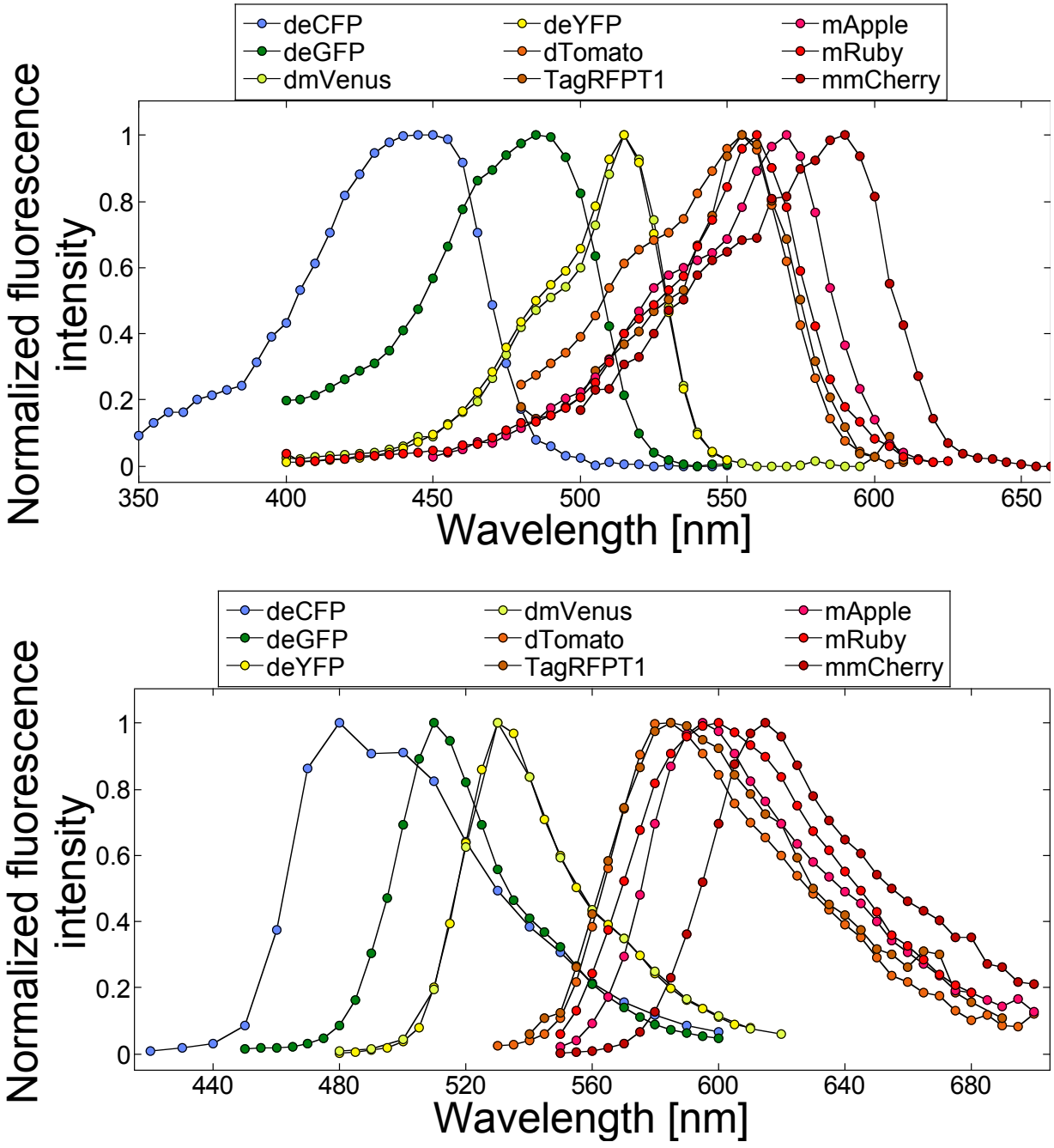

Figure S4. Top: excitation spectra of the nine reporter proteins expressed in Toolbox 2.0. **Bottom:** emission spectra of the nine reporter proteins expressed in Toolbox 2.0.

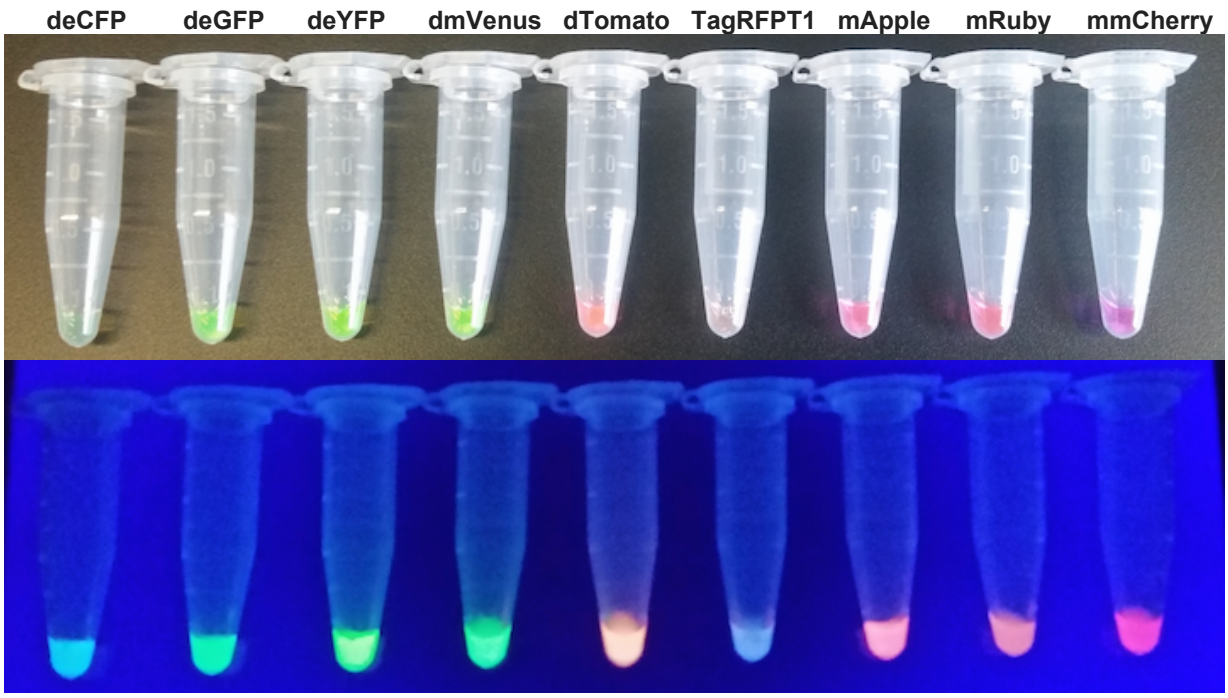

Figure S5. Photos of the nine reporter proteins produced in batch mode cell-free reaction. **Top:** with ambient light. **Bottom:** with a UV excitation (260 nm).

pTXTL-P70a-S28:

• pTXTL: plasmid series name
• P70a: promoter specific to sigma70, ‘a’ marks the first in the series
• S28: gene for the *E. coli* sigma factor 28

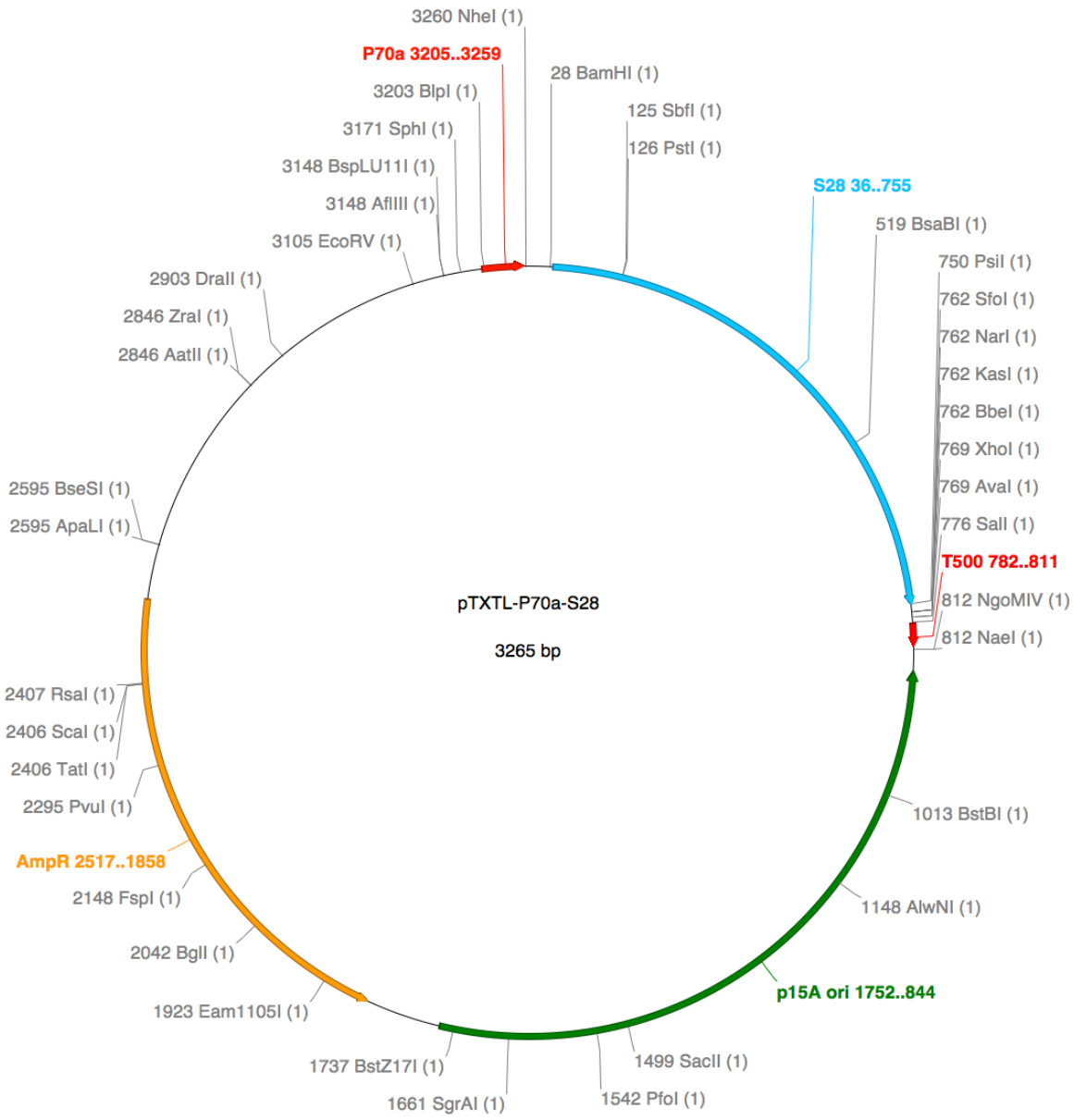

pTXTL-P28a-deGFP:
• pTXTL: plasmid series name
• P28a: promoter specific to sigma28, ‘a’ marks the first in the series
• deGFP: gene for the reporter protein deGFP

Figure S6. Maps of two pTXTL plasmids.

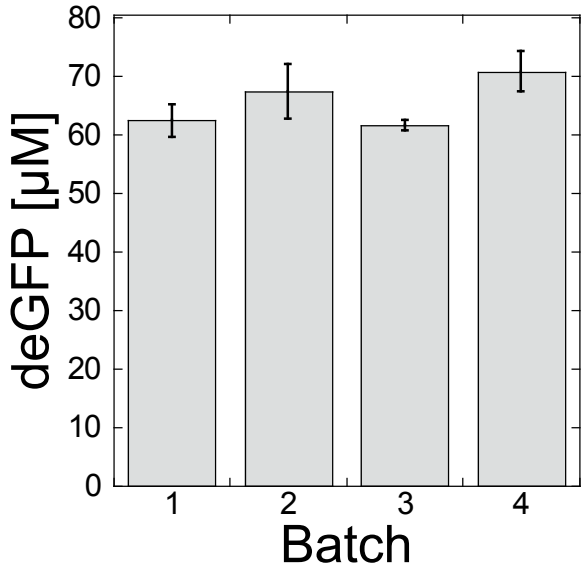

Figure S7. deGFP expression performance of four different lysates using the plasmid P_{70a}-deGFP (5 nM) in batch mode. The four different lysates were prepared over a period of three months.

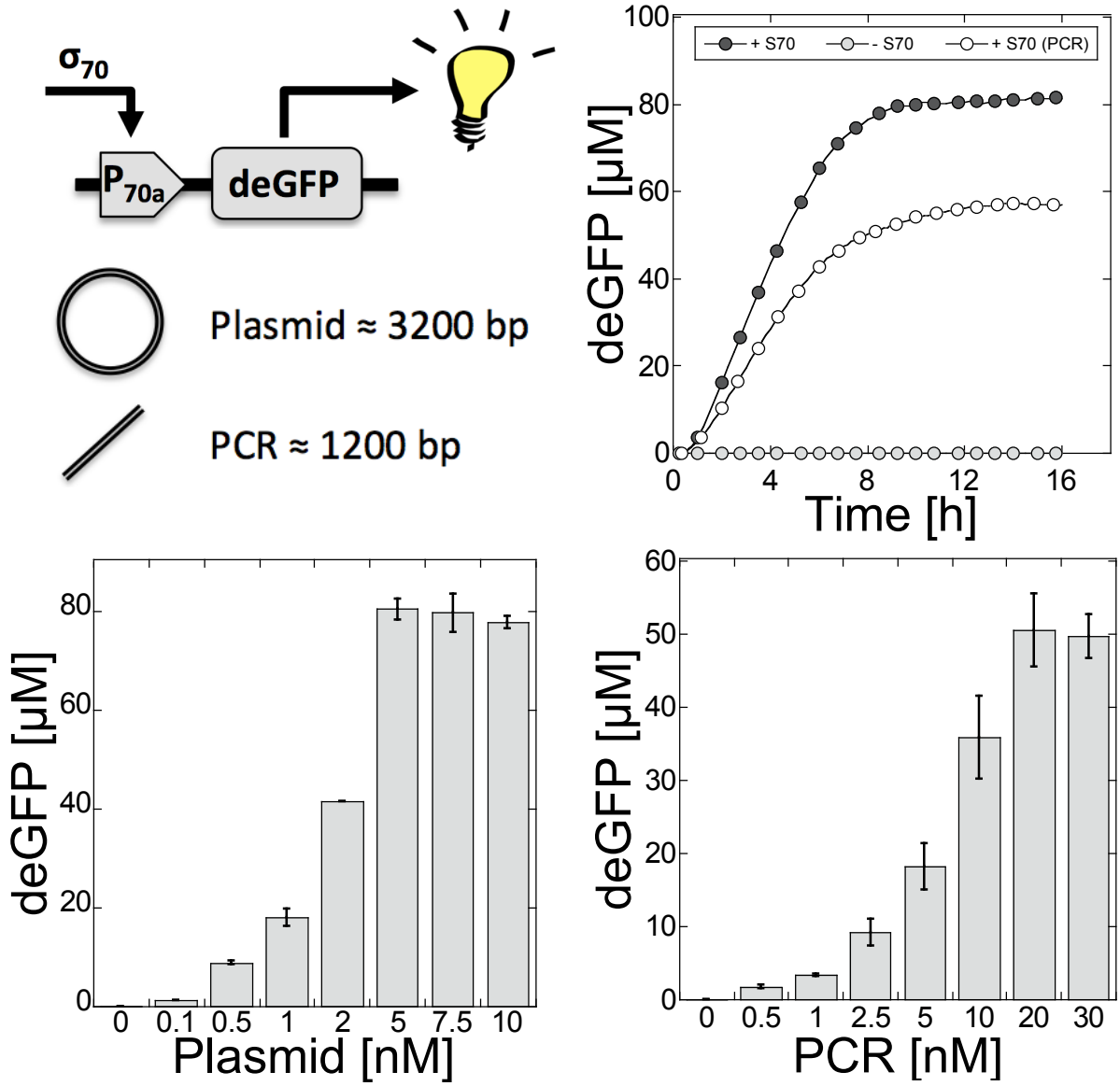

Figure S8a. Characterization of cell-free expression with an *E. coli* promoter specific to the housekeeping σ_{70}. **Top left:** Schematic of the gene circuit. Both plasmid and PCR product of the plasmid can be used as template. **Top right:** Kinetics of deGFP expression. Plasmid P_{70a}-deGFP was set at 5 nM, whereas the linear PCR product was used at 20 nM. Negative control: addition of Rifampicin (50 μM), an inhibitor of the *E. coli* RNA polymerase. **Bottom left:** Synthesis of active fluorescent deGFP vs plasmid concentration. Response is linear up to 2-3 nM plasmid and saturates above 5 nM. **Bottom right:** Synthesis of active fluorescent deGFP vs PCR product concentration. Response is linear up to 10 nM PCR and saturates above 20 nM.

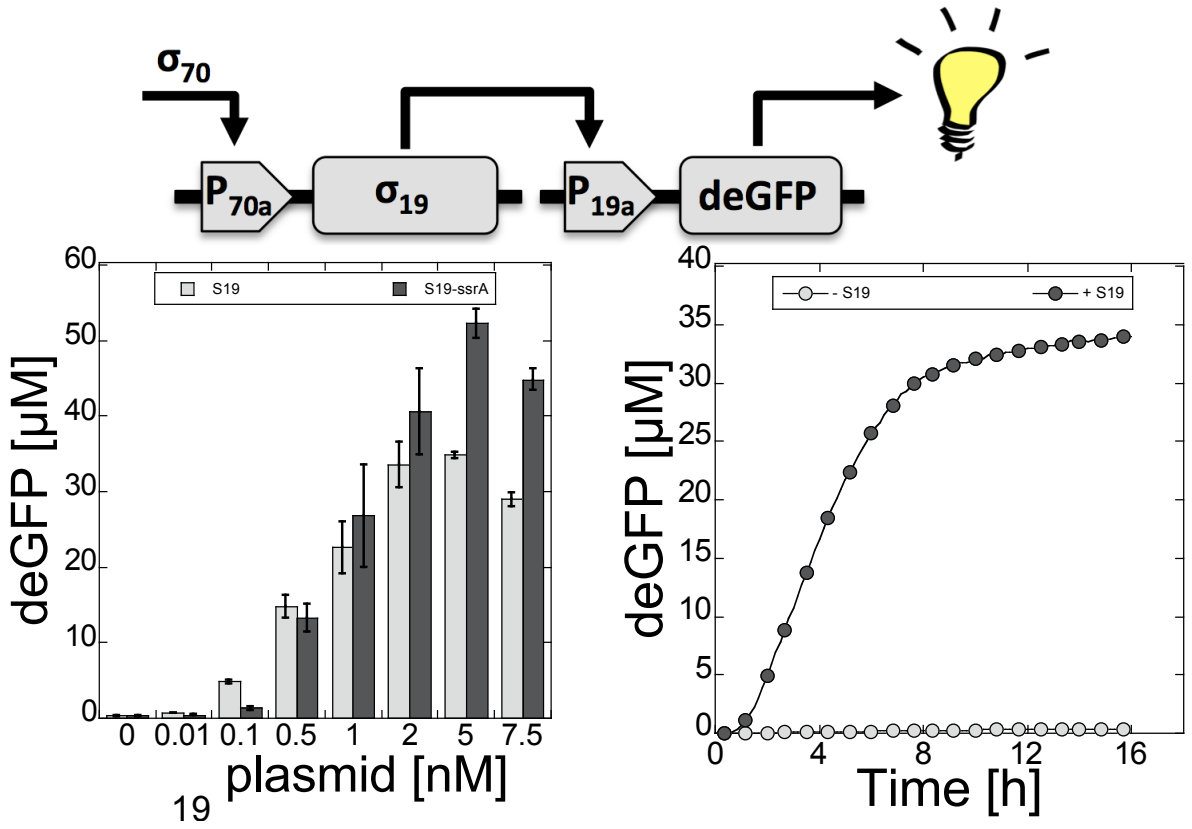

Figure S8b. Two-stage transcriptional activation cascade using *E. coli* σ_{19}. **Top:** schematic of the circuit (only closed circular plasmids were used). **Bottom left:** endpoint deGFP fluorescence measurement of the circuit performance for σ_{19} and σ_{19}-ssrA. The reporter plasmid concentration was set to the optimum (**Table 1**). **Bottom right:** kinetics of the circuit with and without the σ_{19} plasmid.

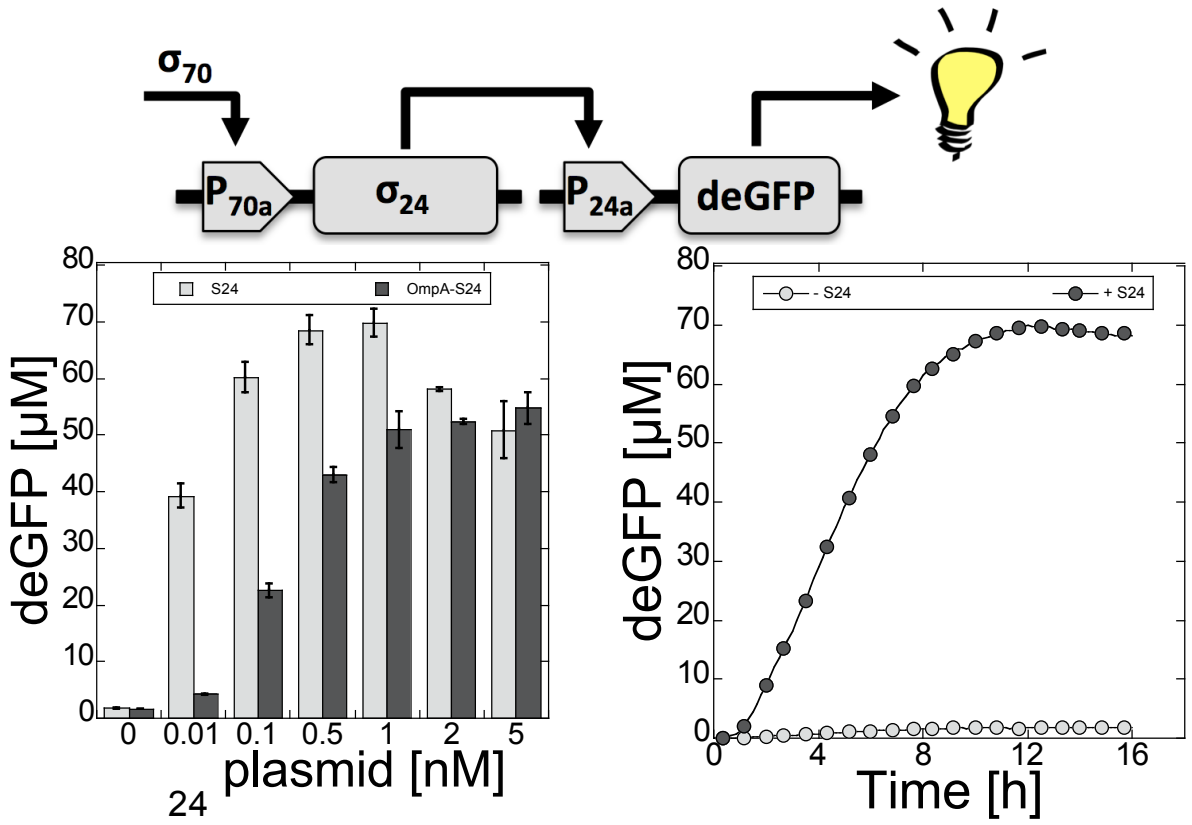

Figure S8c. Two-stage transcriptional activation cascade using *E. coli* σ_{24}. **Top:** schematic of the circuit (only closed circular plasmids were used). **Bottom left:** endpoint deGFP fluorescence measurement of the circuit performance for σ_{24} and OmpA-σ_{24}. The reporter plasmid concentration was set to the optimum (**Table 1**). **Bottom right:** kinetics of the circuit with and without the σ_{24} plasmid.

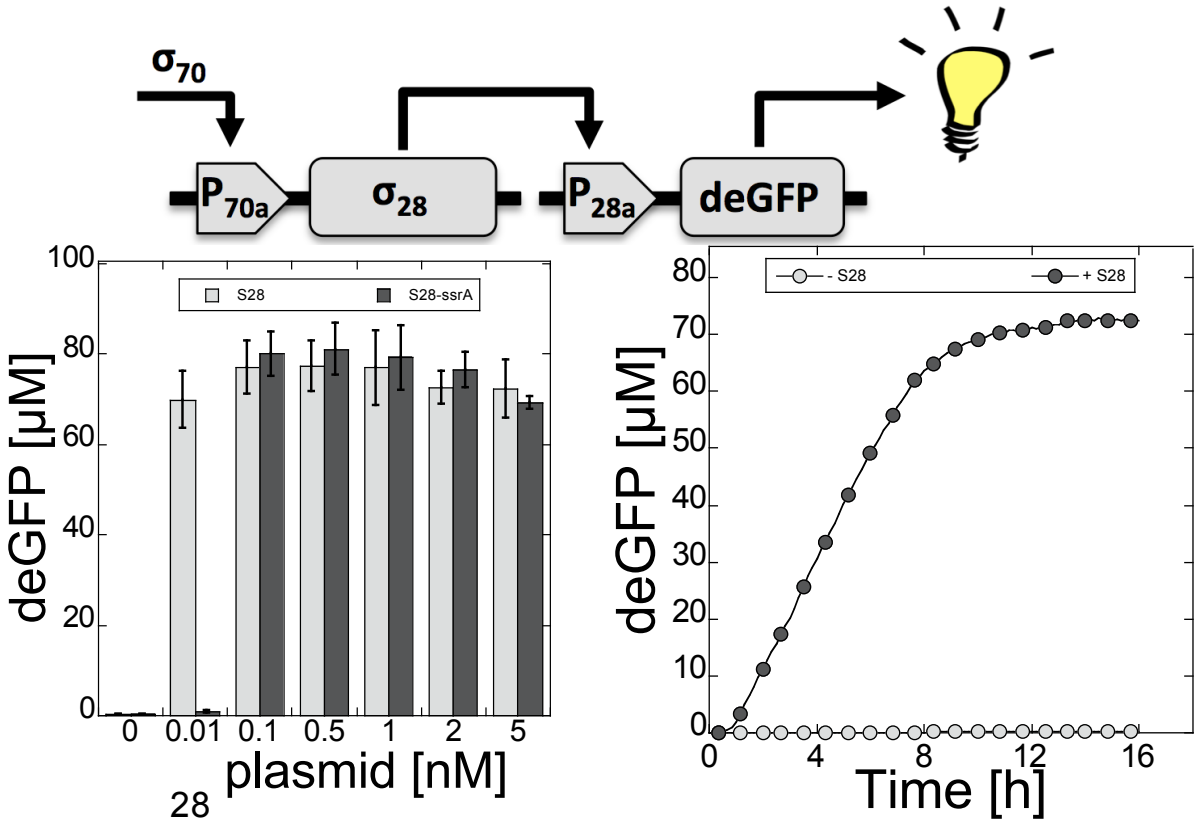

Figure S8d. Two-stage transcriptional activation cascade using *E. coli* σ_{28}. **Top:** schematic of the circuit (only closed circular plasmids were used). **Bottom left:** endpoint deGFP fluorescence measurement of the circuit performance for σ_{28} and σ_{28}-ssrA. The reporter plasmid concentration was set to the optimum (**Table 1**). **Bottom right:** kinetics of the circuit with and without the σ_{28} plasmid.

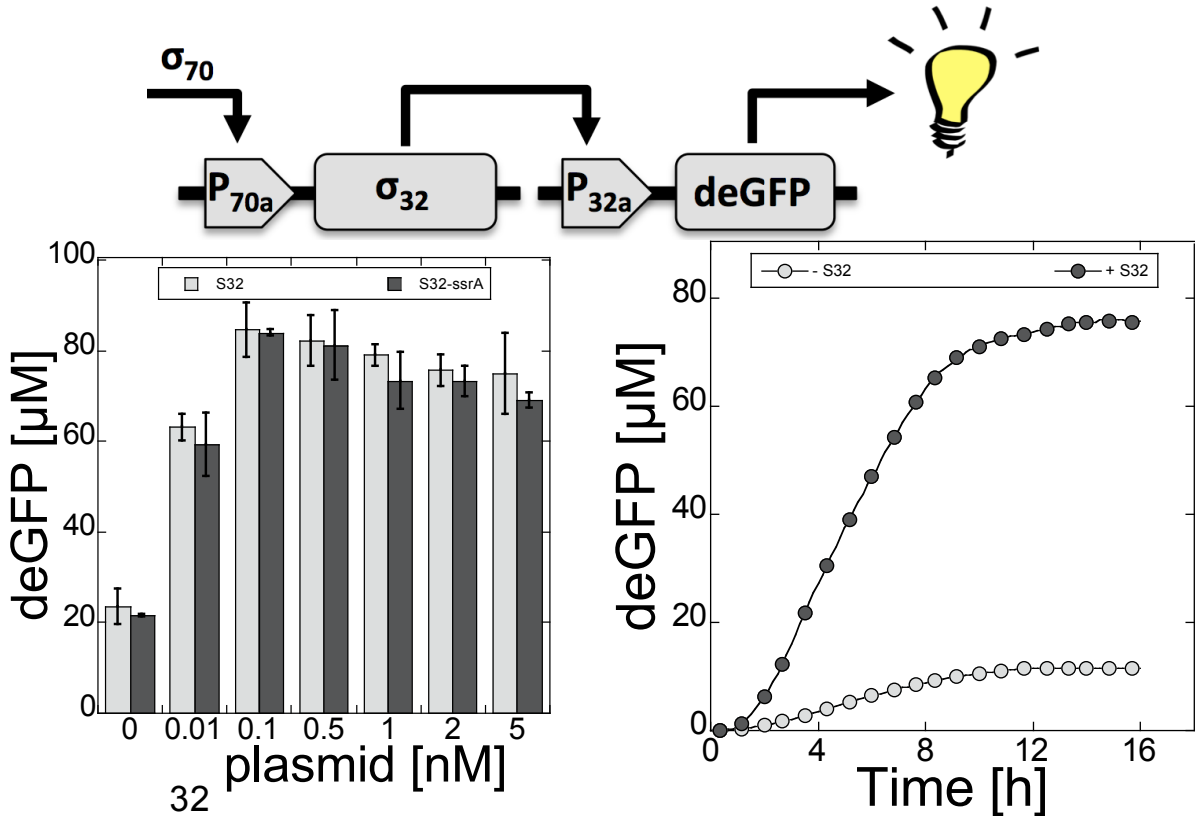

Figure S8e. Two-stage transcriptional activation cascade using *E. coli* σ_{32}. **Top:** schematic of the circuit (only closed circular plasmids were used). **Bottom left:** endpoint deGFP fluorescence measurement of the circuit performance for σ_{32} and σ_{32}-ssrA. The reporter plasmid concentration was set to the optimum (**Table 1**). **Bottom right:** kinetics of the circuit with and without the σ_{32} plasmid.

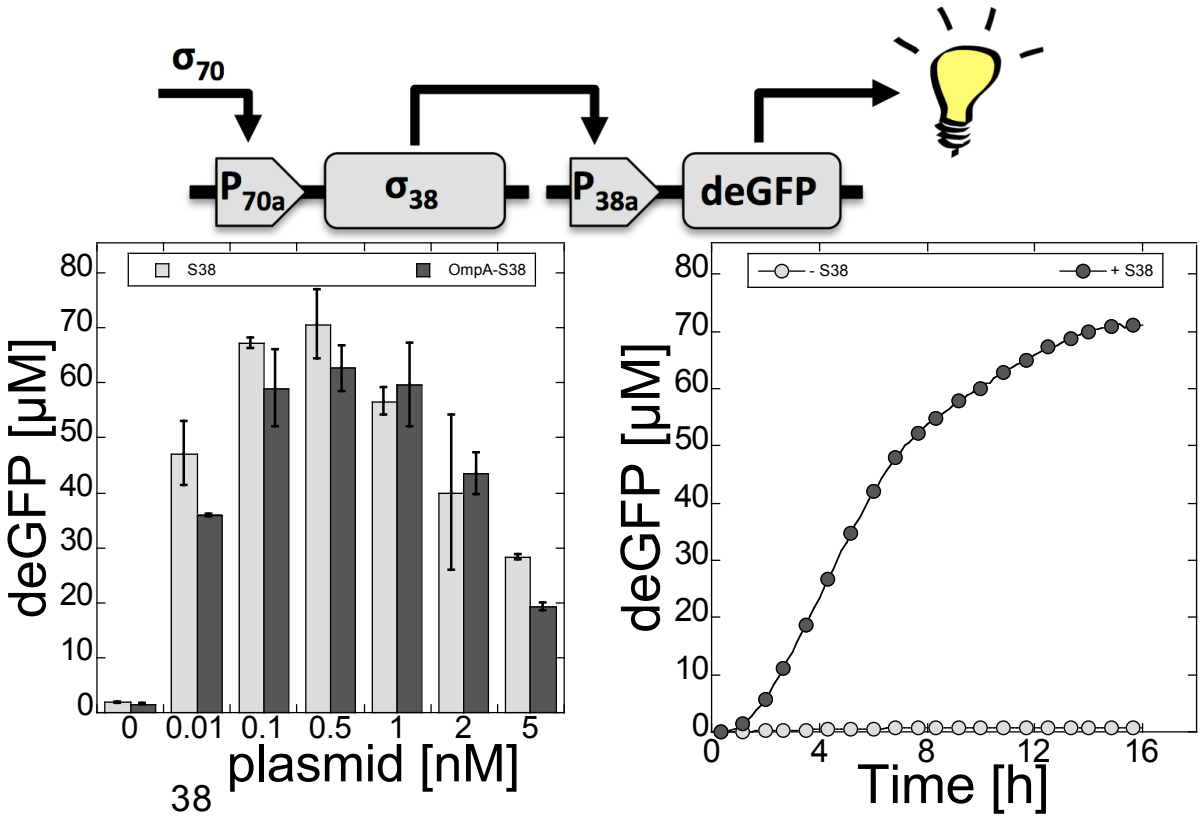

Figure S8f. Two-stage transcriptional activation cascade using *E. coli* σ_{38}. **Top:** schematic of the circuit (only closed circular plasmids were used). **Bottom left:** endpoint deGFP fluorescence measurement of the circuit performance for σ_{38} and OmpA-σ_{38}. The reporter plasmid concentration was set to the optimum (**Table 1**). **Bottom right:** kinetics of the circuit with and without the σ_{38} plasmid.

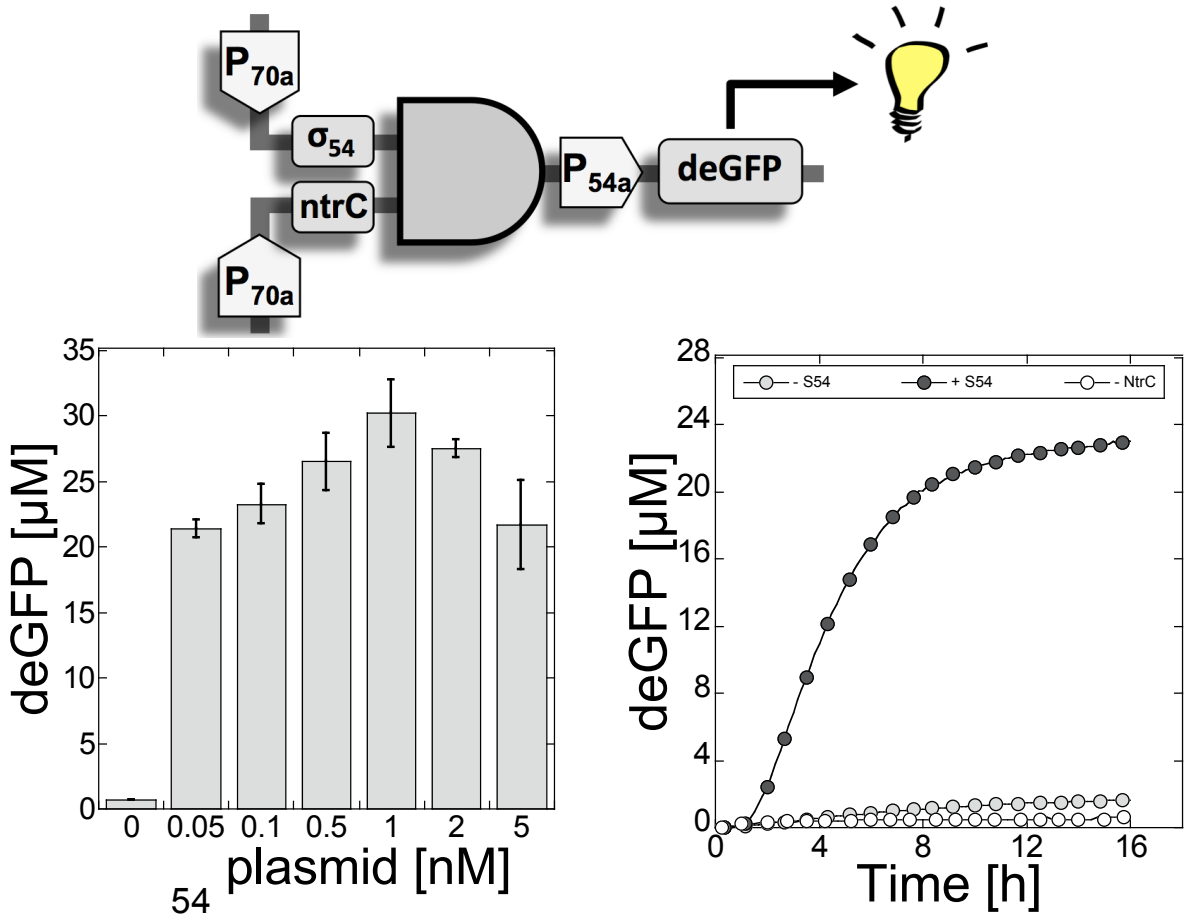

Figure S8g. Two-stage transcriptional activation cascade using *E. coli* σ_{54} and NtrC. **Top:** schematic of the circuit (only closed circular plasmids were used). **Bottom left:** endpoint deGFP fluorescence measurement of the circuit performance for σ_{54}-NtrC. The reporter plasmid concentration was set to the optimum (**Table 1**). **Bottom right:** kinetics of the circuit with and without the σ_{54} and NtrC plasmid.

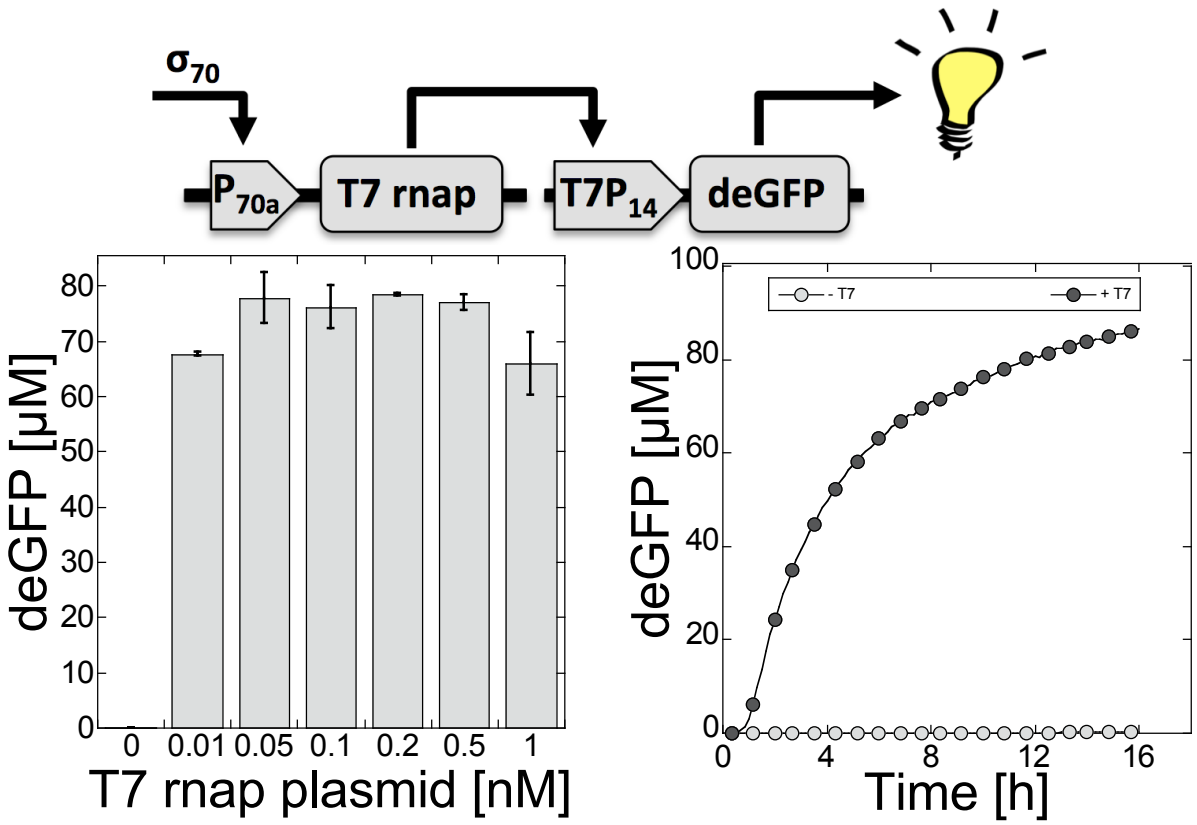

Figure S8h. Two-stage transcriptional activation cascade using bacteriophage T7 RNA polymerase. **Top:** schematic of the circuit (only closed circular plasmids were used). **Bottom left:** endpoint deGFP fluorescence measurement of the circuit performance for T7 rnap. The reporter plasmid concentration was set to the optimum (**Table 1**). **Bottom right:** kinetics of the circuit with and without the T7 rnap plasmid.

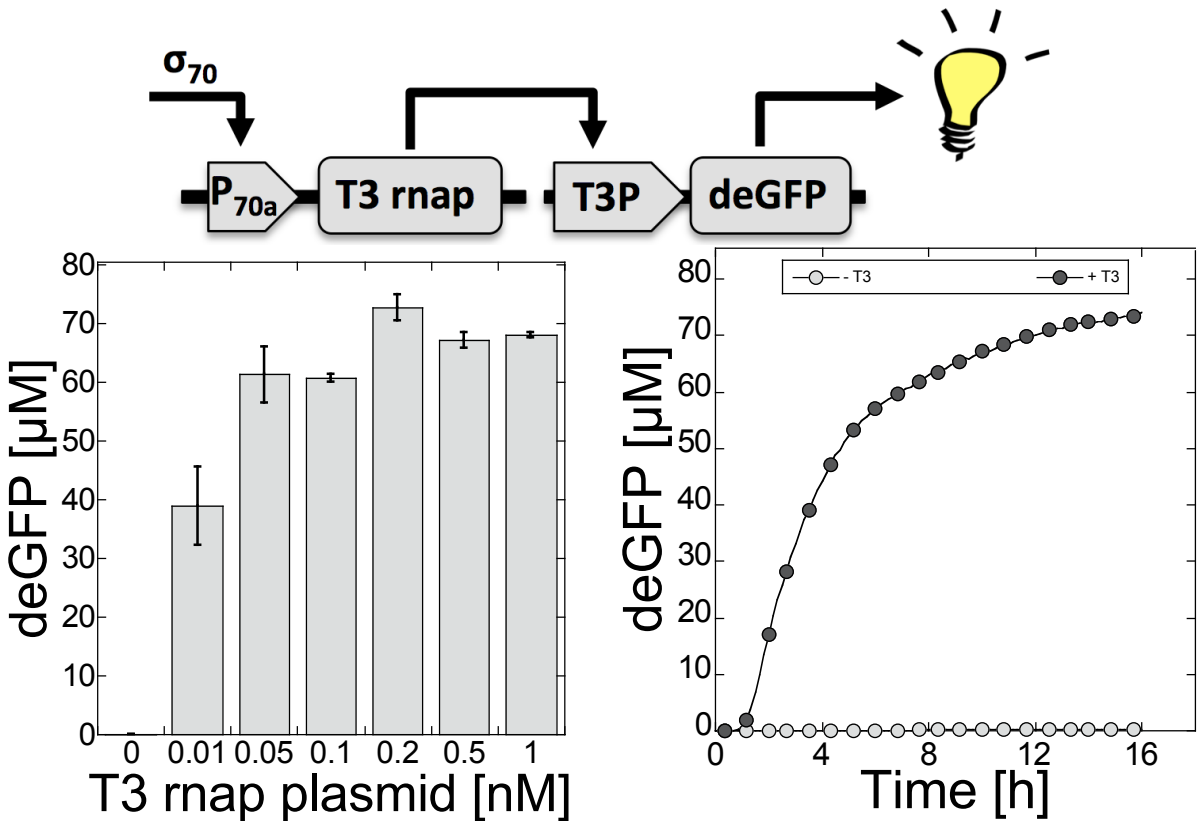

Figure S8i. Two-stage transcriptional activation cascade using bacteriophage T3 RNA polymerase. **Top:** schematic of the circuit (only closed circular plasmids were used). **Bottom left:** endpoint deGFP fluorescence measurement of the circuit performance for T3 rnap. The reporter plasmid concentration was set to the optimum (**Table 1**). **Bottom right:** kinetics of the circuit with and without the T3 rnap plasmid.

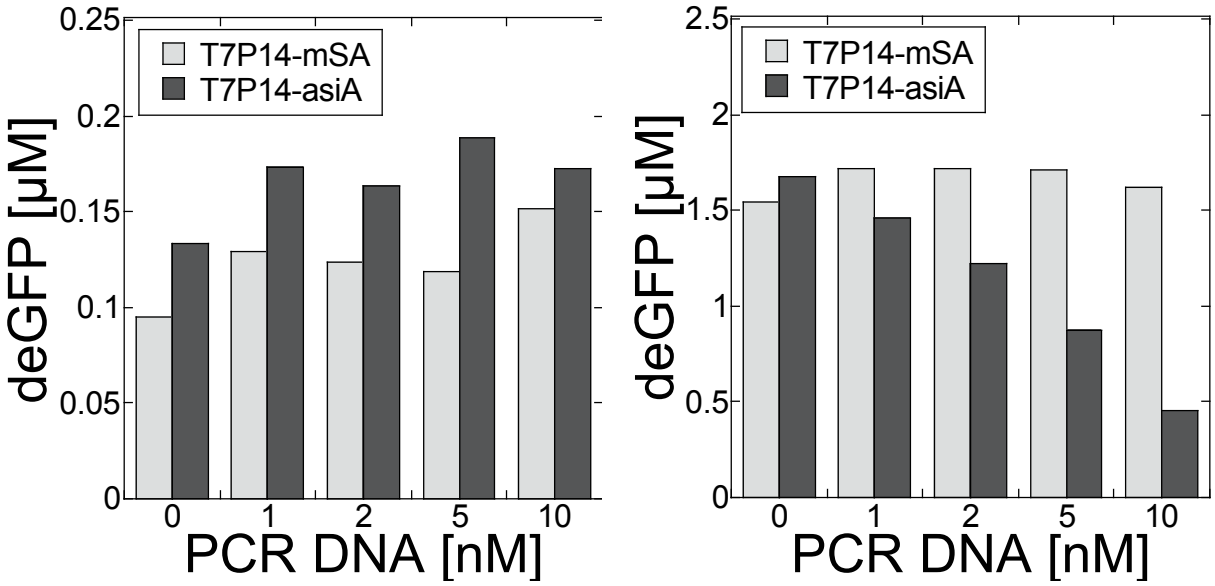

Figure S9. Inhibition of σ_{70} by the protein AsiA. The bacteriophage T4 protein AsiA was expressed through a T7 promoter using linear PCR (0.2 nM P_{70a}-T7rnap plasmid was added to the reaction). The protein mSA (monomeric streptavidin, comparable in size to Asia) was used as a control. **Left:** inhibition of σ_{70} is observed (P_{70a}-deGFP set to 0.25 nM). **Right:** no inhibition is observed for σ_{32} (P_{32a}-deGFP set to 1 nM).

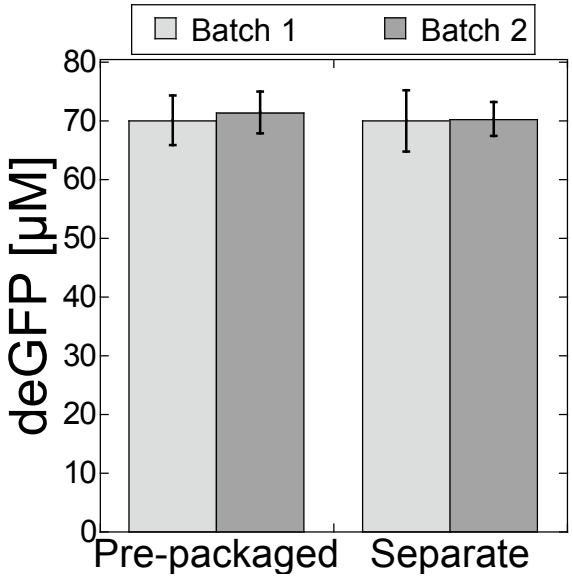

Figure S10. Performance of pre-packaged and separate cell-free reactions for two different batches (using 5 nM P_{70a}-deGFP). Pre-packaged: DNA and water are added to a reaction containing all of the components pre-mixed (stored pre-mixed at -80°C). Separate: the reaction is prepared from the separate components (extract, energy mixture, amino acid mixture, potassium, magnesium, PEG). deGFP production is measured after 10-12 h of incubation.

We estimated deGFP mRNA mean lifetimes with and without MazF in cell-free reactions by modeling cell-free expression with the following set of equations, the fourth equation being the solution of the first three:

$$\frac{d[m]}{dt} = -b[m]$$

$$\frac{d[deGFP_{dark}]}{dt} = a[m] - k[deGFP_{dark}]$$

$$\frac{d[deGFP_{mat}]}{dt} = k[deGFP_{dark}]$$

$$[deGFP_{mat}](t) = [deGFP_{mat}]_0 + [deGFP_{dark}]_0 \left(1 - e^{-kt}\right) + \frac{am_0}{b(b-k)}\left[b\left(1 - e^{-kt}\right) + k\left(e^{-bt} - 1\right)\right]$$

$[deGFP_{mat}](t)$	mature (fluorescent) deGFP as a function of time
$[deGFP_{mat}]_0$	initial mature (fluorescent) deGFP, measured at transcription arrest (which we call time zero)
$[deGFP_{dark}]_0$	initial dark deGFP, corresponding to concentration of dark deGFP at transcription arrest. This value is fit by the computer.
k	protein maturation rate. Inverse (maturation time) is 16.2 minutes.
b	mRNA inactivation rate. This value is fit by the computer.
a	protein synthesis/translation constant
m_0	initial mRNA at transcription arrest (product am_0 we measure using slope of deGFP kinetics in linear regime)

We used the RNA polymerase inhibitor Rifampicin to stop transcription and measured the time course of deGFP protein after transcription arrest, so we do not have an mRNA synthesis term in the first equation. First, the concentration of Rifampicin necessary to stop transcription completely was determined by adding Rifampicin at different concentrations at the beginning of expression. With 50 μM Rifampicin, the deGFP fluorescent signal stayed at background level. We added the RNAP inhibitor after 2 hours of incubation so that our reaction was in the regime of linear protein synthesis. In this regime, the slope of the fluorescent signal is equal to the parameter a[m], so we used the previously measured slope of the kinetic at the two hour point (shown in the table below) for the term am_0 in the model equation.

MazF [nM]	nM/min in linear regime	stdev (nM/min)
0	146.7	3.6
25	81.2	5.3
50	44.5	0.9
75	23.7	2.2
100	19.3	0.5
150	7.5	0.1

Table S6. Rate of deGFP synthesis after 2 hours of expression as a function of MazF added to the reaction.

The reference time point t = 0 is set to transcription arrest (addition of Rifampicin). The inverse of the parameter b, which was fit using Mathematica, is the mRNA mean lifetime. With no addition of MazF to the reaction, and a deGFP maturation time of 16.2 minutes, we found that

the deGFP mRNA inactivation rate b = 0.0573 min^{-1}, corresponding to a lifetime of 17.4 minutes. Then, we measured the lifetime for various concentrations of the toxin MazF, added at the beginning of the reaction. The fluorescent signal in time, for reactions containing MazF, after adding Rifampicin are seen in the **Supplementary Figure S11**.

The *E. coli* interferase MazF can be used to decrease the mRNA lifetime in a cell-free reaction. When MazF is added at the beginning of a reaction with 5 nM P_{70a}-deGFP, the endpoint expression is only a fraction of the saturation value with no MazF **(Figure 4a)**. The corresponding deGFP mRNA mean lifetimes are also shown in the table **(Figure 4a)**.

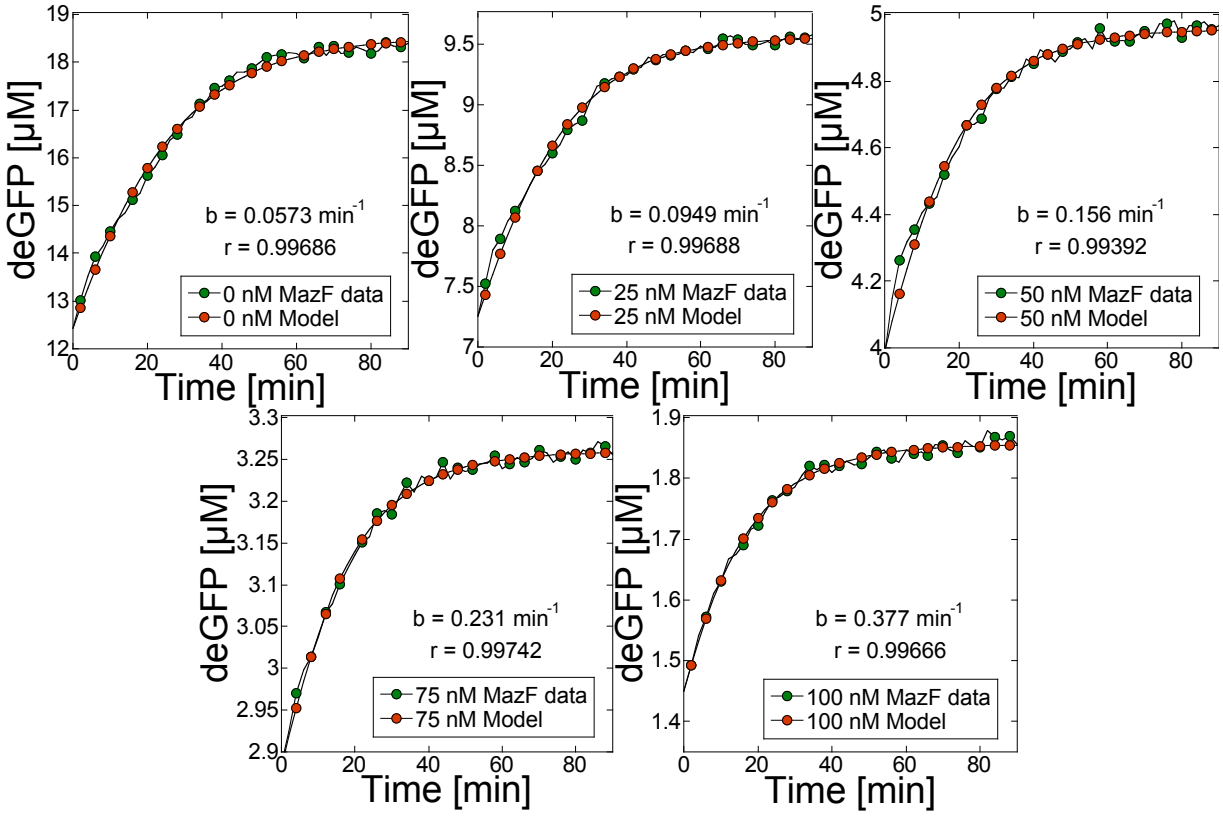

Figure S11. Kinetics of deGFP expression for five different concentrations of MazF added in cell-free reactions, after addition of Rifampicin (added 2 hours after the beginning of the reaction). The experimental curves were fit to determine the mRNA lifetime based on the model. Results are reported in **Figure 4a**.

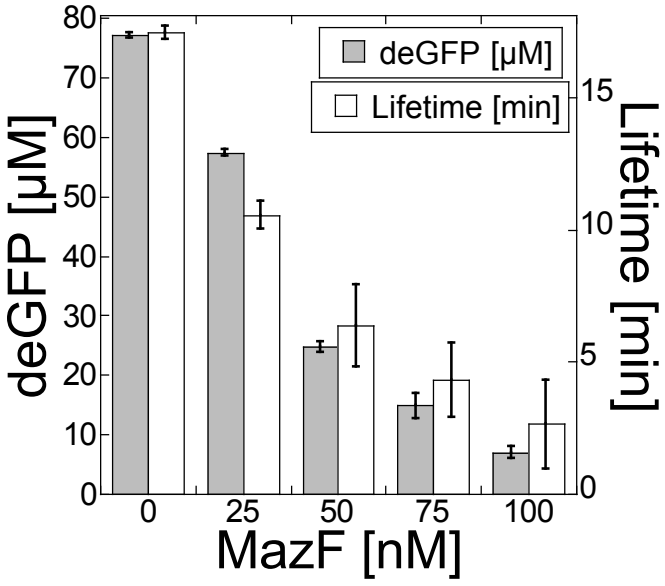

Figure S12. Synthesis of deGFP vs mRNA mean lifetime as a function of the concentration of MazF added to a cell-free reaction. Data are from **Figure 4a.** In first approximation, the amount of MazF used is a cell-free reaction is directly related to the mRNA mean lifetime.

There is a good agreement between the amount of deGFP produced and the mean lifetime as a function of the MazF concentration **(Supplementary Figure S12)**. It is therefore relatively straightforward to set the mean lifetime at a desired value, using deGFP as a reference.

Example of application: to decrease the mRNA mean lifetime from 17.5 minutes down to 6.5 minutes, 50 nM MazF have to be used. A volume of 2.25 µl MazF extract (2 µM MazF) is added to a reaction of total volume 90 µl.

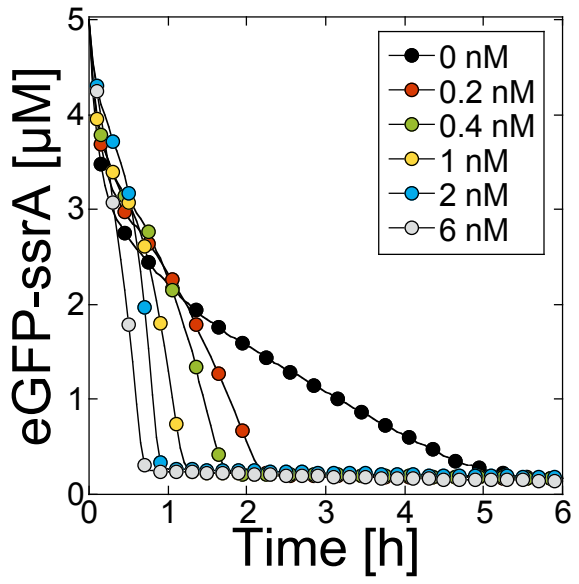

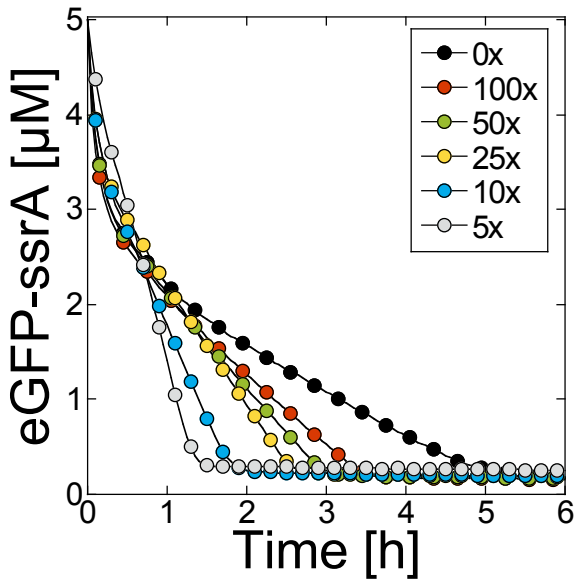

clpXP [nM]	deGFP degradation rate (nM/min)
0 nM	9.3
0.2 nM	29.4
0.4 nM	47.3
1 nM	80.1
2 nM	128.9
6 nM	128.4

clpXP [nM]	deGFP degradation rate (nM/min)
0 nM	9.3
0.2 nM	13.7
0.4 nM	16.6
1 nM	21.3
2 nM	32.7
6 nM	54.0

Figure S13. Degradation of His-eGFP-ssrA (added as pure protein in cell-free reaction) by the clpXP complex. **Left:** clpXP was co-expressed (P_{70a}-clpXP, concentrations given in the plot and table) in the cell-free reaction without pre-incubation. **Right:** clpXP was first expressed (P_{70a}-clpXP, 3 nM) in a cell-free reaction. Serial dilution of this reaction was made into a cell-free reaction containing pure His-eGFP-ssrA (5 µM).

Example of application using the method shown in Supplementary Figure S13 Left (expression of ClpXP with no pre-incubation): to accelerate the degradation of an ssrA-tagged protein by a factor of about 9 (for deGFP: from 9.3 nM/min up to 80.1 nM/min), 1 nM of plasmid P_{70a}-clpXP have to be added to the cell-free reaction.

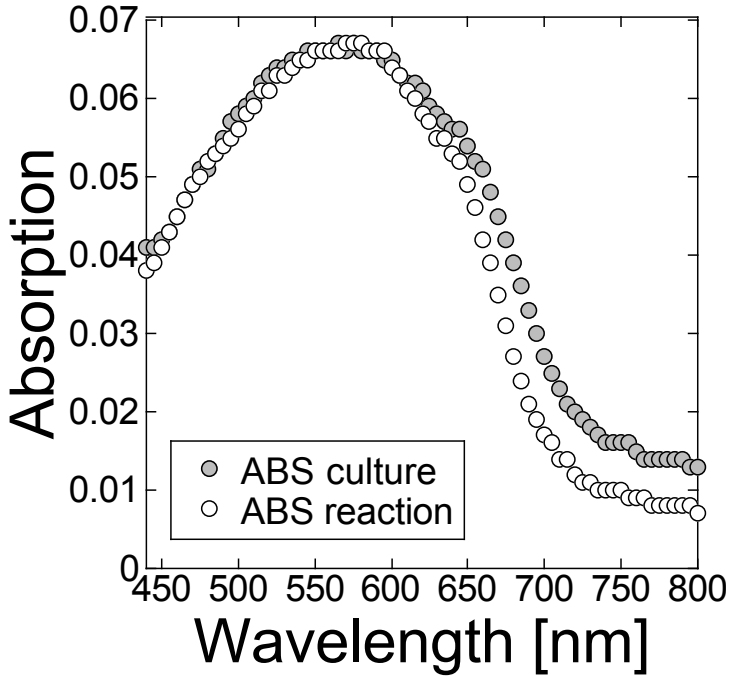

Figure S14. Absorbance spectrum of violacein. Spectrum from an *E. coli* cell cultures and from a cell-free reaction producing violacein. Both absorption maxima are at 575 nm. Only a slight difference is observed above 650 nm.

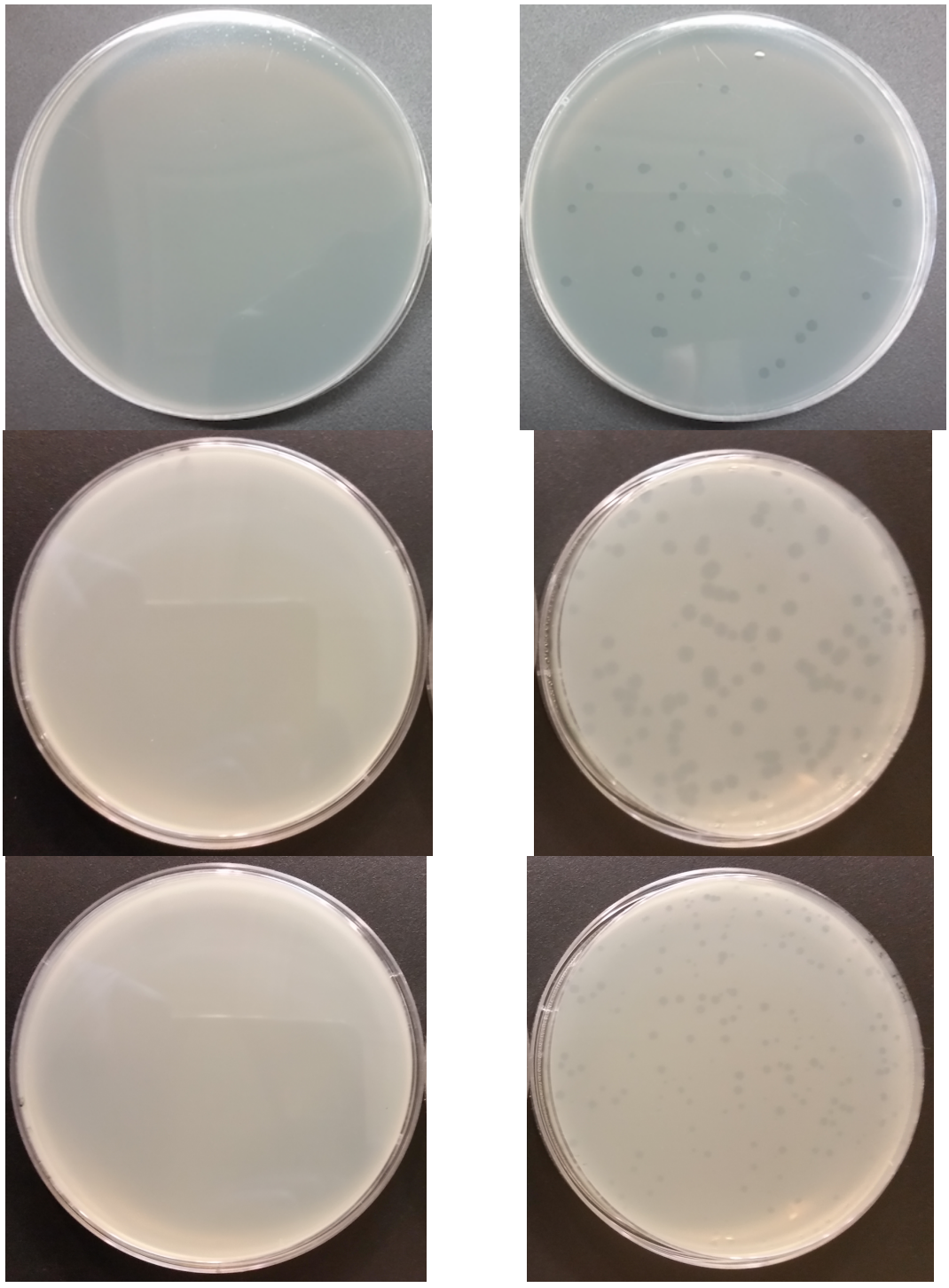

Figure S15. Photos of bacteriophage plaque forming assay. **Top:** phage T7 (left: negative control). **Middle:** ΦX174 (left: negative control). **Bottom:** MS2 (left: negative control). The negative control consisted of performing the plaque assay from cell-free reactions (containing phage genomes) incubated less than five minutes and doing no dilution to the reaction, as opposed to the reactions that were incubated 8-12 h.

deGFP was expressed overnight and quantified via fluorescence. It was encapsulated in liposomes at concentrations of 2, 4, and 8 μM. Liposomes were photographed on an inverted microscope with a GFP filter (473 nm excitation, 520 nm emission) at 100 ms exposure. Using Metamorph imaging software, area versus integrated intensity curves were linearly fit and their leading coefficients compared. Using these curves, deGFP concentration inside liposomes could be measured given the area and intensity. Since actual experiments involved much higher concentrations of deGFP and thus much greater intensities, the CCD camera was tested to verify linear scaling behavior with varying exposure times. Liposomes encapsulating 8 μM deGFP were photographed at 100, 33.3, and 10 ms. Again, area versus integrated intensity curves were linearly fit and the leading coefficients compared. The scaling was observed to be linear.

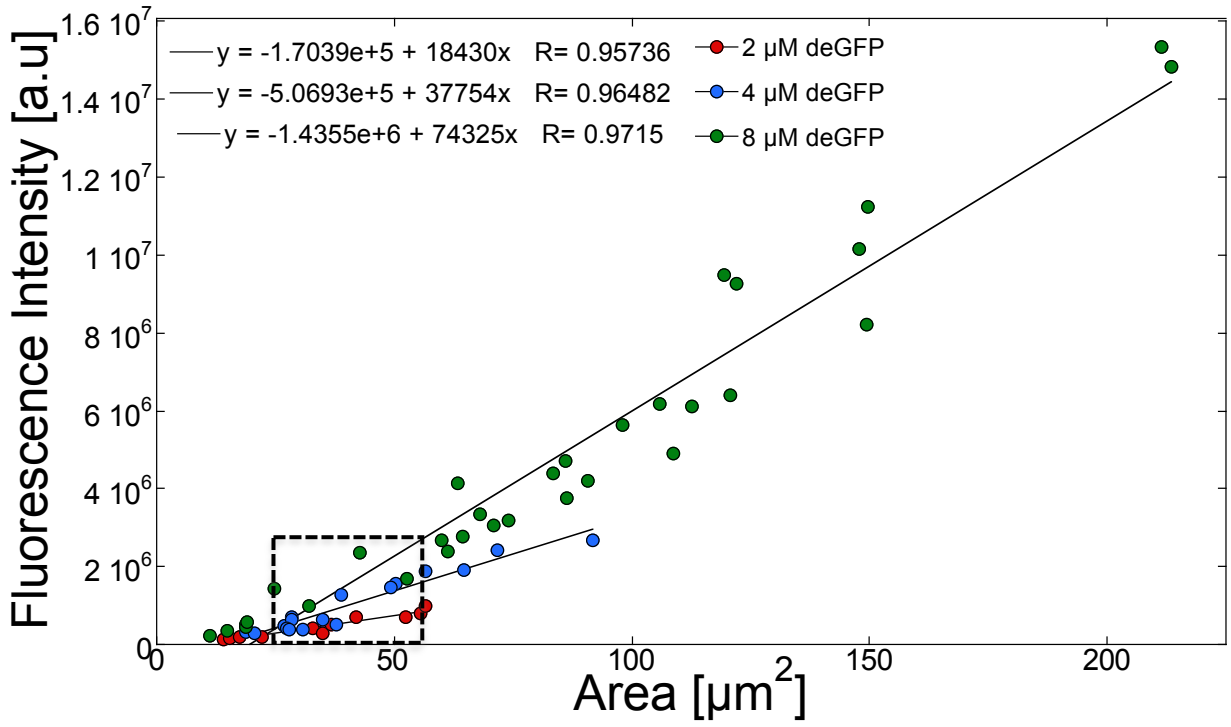

Figure S16. Calibration of deGFP fluorescence in liposomes for three different concentrations. Statistics of liposome populations **(Figure 7)** has been determined for sizes in the rectangular labeled region.

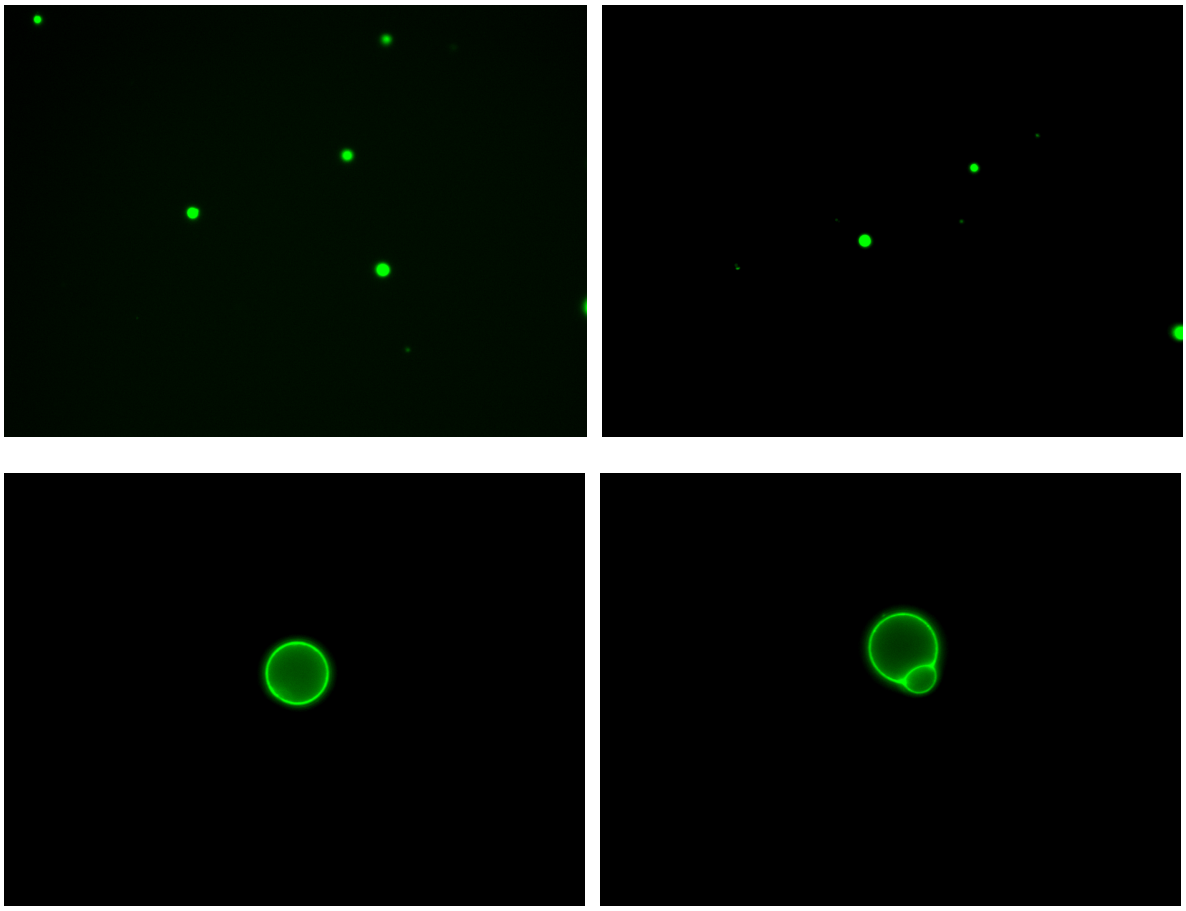

Figure S17. Fluorescence images inside liposomes. **Top:** deGFP expressed through the promoter P_{70a} (scale bar: 15 μm). **Bottom:** AH-eGFP express through the transcriptional activation cascade P_{70a}-T7rnap → $T7P_{14}$-AH-eGFP (scale bar: 15 μm).

Figure S18. SDS-PAGE (12%) analysis of alpha-hemolysin (AH, 33.4 kDa) synthesis. AH was expressed through the cascade P_{70a}-T7rnap → $T7P_{14}$-AH. The blank is the same reaction with no plasmid.

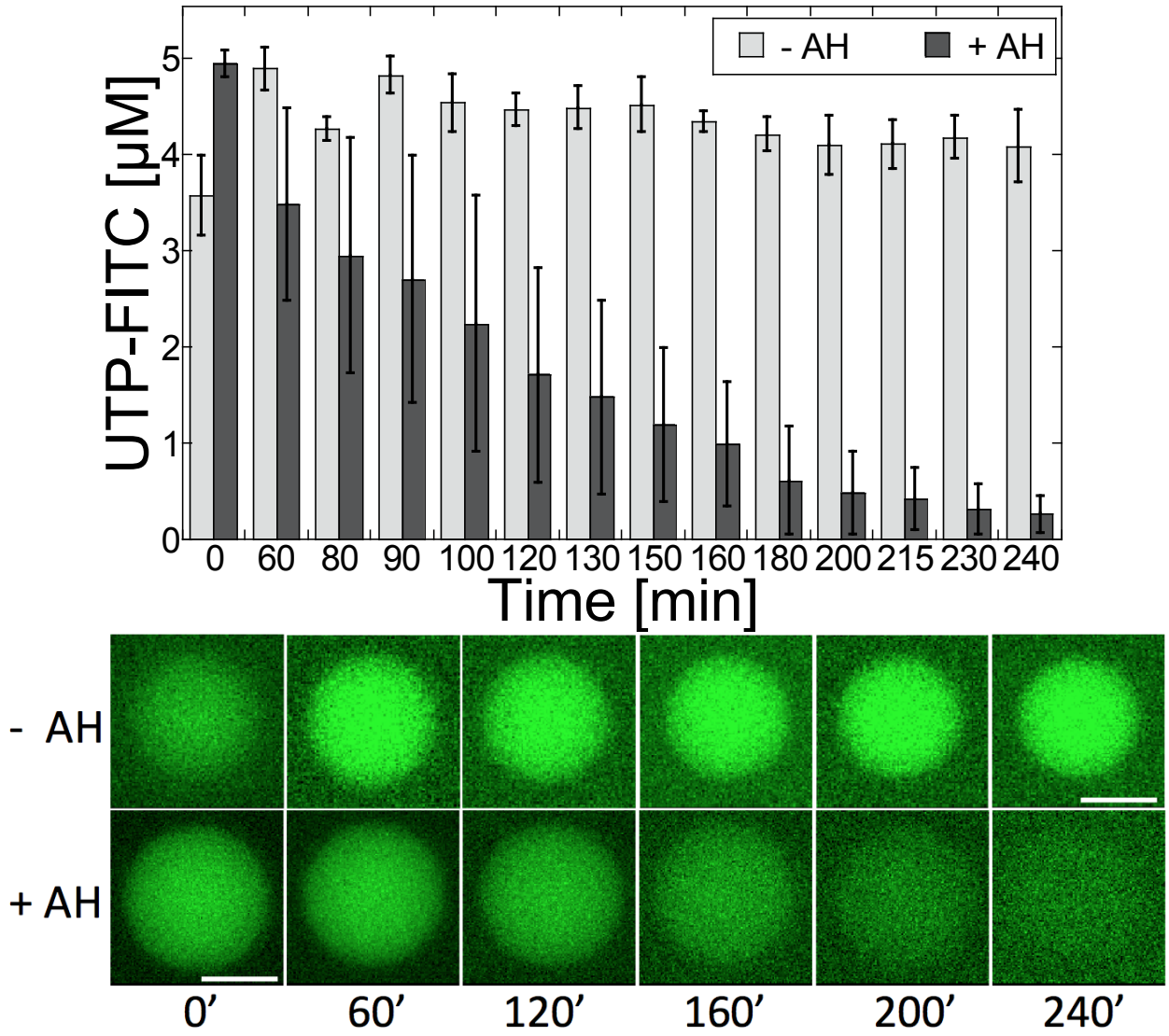

Figure S19. Leak of UTP-fluorescein from cell-sized liposomes through the pore-forming protein alpha-hemolysin (AH). Error bars represent the standard deviation from six liposomes **Top:** kinetics of the leak with and without AH. **Bottom:** fluorescence images of liposomes at different times (minutes), with (8 µm diameter) and without (6 µm diameter) AH. Scale bars: 4 µm.

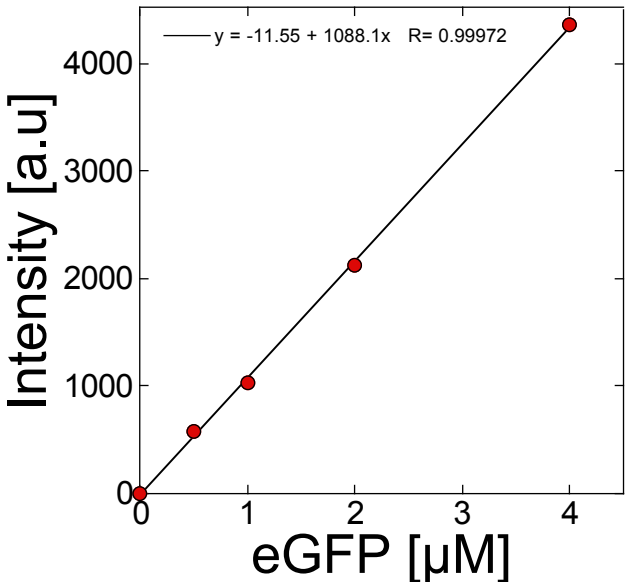

	Dilution 8x		Dilution 16x	
	Well 1	Well 2	Well 1	Well 2
Background	27	37	0	16
Reaction	11652	9014	4848	5192

	Dilution 10x			
	Well 1	Well 2	Well 3	Well 4
Background	30	24	28	27
Reaction	9904	10276	9025	8643

Figure S20. Fluorescence calibration and measurements. **Top:** calibration of plate reader with pure eGFP. Concentration of the His-eGFP protein stock was first re-estimated by absorption at 488 nm with an extinction coefficient of 55000 $M^{-1}cm^{-1}$. The calibration was made in the concentration range 0-4 µM by diluting the pure His-eGFP into a cell-free reaction. **Middle:** example of fluorescence measurement from a cell-free reaction (5 nM plasmid P_{70a}-His-deGFP, deGFP with an histag in N-terminus, MW = 27.2 kDa, 1 mg/ml = 36.76 µM). Two measurements (for two different dilutions of the reaction and background, 8x and 16x) of background and reaction were averaged. The final average concentration of the protein is 74.72 ± 8.26 µM, which corresponds to 2.03 ± 0.22 mg/ml. **Bottom:** example of data from a cell-free reaction (0.2 nM P_{70a}-T7rnap 2 nM plasmid $T7P_{14}$-His-deGFP). Four measurements of background and reaction were averaged (dilution 10x). The final average concentration of the protein is 86.82 ± 6.96 µM, which corresponds to 2.35 ± 0.19 mg/ml.

References

[1] Bremer, H., and Dennis, P. P. (1987) Modulation of chemical composition and other parameters of the cell by growth rate, In *Escherichia and Salmonella: Cellular and Molecular Biology* (Neidhardt, F. C., Ed.), pp 1527-1542, ASM Press, Washington, D.C.

[2] Elowitz, M. B., Surette, M. G., Wolf, P. E., Stock, J. B., and Leibler, S. (1999) Protein mobility in the cytoplasm of Escherichia coli, *J Bacteriol 181*, 197-203.

[3] Cayley, S., Lewis, B. A., Guttman, H. J., and Record, M. T., Jr. (1991) Characterization of the cytoplasm of Escherichia coli K-12 as a function of external osmolarity. Implications for protein-DNA interactions in vivo, *J Mol Biol 222*, 281-300.

[4] Zimmerman, S. B., and Trach, S. O. (1991) Estimation of macromolecule concentrations and excluded volume effects for the cytoplasm of Escherichia coli, *J Mol Biol 222*, 599-620.

[5] Iskakova, M. B., Szaflarski, W., Dreyfus, M., Remme, J., and Nierhaus, K. H. (2006) Troubleshooting coupled in vitro transcription-translation system derived from Escherichia coli cells: synthesis of high-yield fully active proteins, *Nucleic Acids Res 34*, e135.

[6] Shepherd, N., Dennis, P., and Bremer, H. (2001) Cytoplasmic RNA Polymerase in Escherichia coli, *J Bacteriol 183*, 2527-2534.

[7] Maeda, H., Fujita, N., and Ishihama, A. (2000) Competition among seven Escherichia coli sigma subunits: relative binding affinities to the core RNA polymerase, *Nucleic Acids Res 28*, 3497-3503.

[8] Mettke, I., Fiedler, U., and Weiss, V. (1995) Mechanism of Activation of a Response Regulator - Interaction of Ntrc-P Dimers Induces Atpase Activity, *J Bacteriol 177*, 5056-5061.

[9] Kassavetis, G. A., and Chamberlin, M. J. (1981) Pausing and Termination of Transcription within the Early Region of Bacteriophage-T7 DNA Invitro, *J Biol Chem 256*, 2777-2786.

[10] Selinger, D. W., Saxena, R. M., Cheung, K. J., Church, G. M., and Rosenow, C. (2003) Global RNA half-life analysis in Escherichia coli reveals positional patterns of transcript degradation, *Genome Res 13*, 216-223.

[11] Underwood, K. A., Swartz, J. R., and Puglisi, J. D. (2005) Quantitative polysome analysis identifies limitations in bacterial cell-free protein synthesis, *Biotechnol Bioeng 91*, 425-435.

[12] Shin, J., and Noireaux, V. (2010) Efficient cell-free expression with the endogenous E. Coli RNA polymerase and sigma factor 70, *J Biol Eng 4*, 8.

[13] Grate, D., and Wilson, C. (1999) Laser-mediated, site-specific inactivation of RNA transcripts, *Proc Natl Acad Sci U S A 96*, 6131-6136.

[14] Enz, S., Braun, V., and Crosa, J. H. (1995) Transcription of the region encoding the ferric dicitrate-transport system in Escherichia coli: similarity between promoters for fecA and for extracytoplasmic function sigma factors, *Gene 163*, 13-18.

[15] Lipinska, B., Sharma, S., and Georgopoulos, C. (1988) Sequence analysis and regulation of the htrA gene of Escherichia coli: a sigma 32-independent mechanism of heat-inducible transcription, *Nucleic Acids Res 16*, 10053-10067.

[16] Arnosti, D. N., and Chamberlin, M. J. (1989) Secondary Sigma-Factor Controls Transcription of Flagellar and Chemotaxis Genes in Escherichia-Coli, *P Natl Acad Sci USA 86*, 830-834.

[17] Wang, Y., and deHaseth, P. L. (2003) Sigma 32-dependent promoter activity in vivo: Sequence determinants of the groE promoter, *J Bacteriol 185*, 5800-5806.
[18] Yim, H. H., Brems, R. L., and Villarejo, M. (1994) Molecular Characterization of the Promoter of Osmy, an Rpos-Dependent Gene, *J Bacteriol 176*, 100-107.
[19] Reitzer, L. J., and Magasanik, B. (1985) Expression of Glna in Escherichia-Coli Is Regulated at Tandem Promoters, *P Natl Acad Sci USA 82*, 1979-1983.
[20] Guzman, L. M., Belin, D., Carson, M. J., and Beckwith, J. (1995) Tight Regulation, Modulation, and High-Level Expression by Vectors Containing the Arabinose P-Bad Promoter, *J Bacteriol 177*, 4121-4130.
[21] Webster, C., Kempsell, K., Booth, I., and Busby, S. (1987) Organisation of the regulatory region of the Escherichia coli melibiose operon, *Gene 59*, 253-263.
[22] Lutz, R., and Bujard, H. (1997) Independent and tight regulation of transcriptional units in Escherichia coli via the LacR/O, the TetR/O and AraC/I-1-I-2 regulatory elements, *Nucleic Acids Res 25*, 1203-1210.
[23] Olins, P. O., Devine, C. S., Rangwala, S. H., and Kavka, K. S. (1988) The T7 phage gene 10 leader RNA, a ribosome-binding site that dramatically enhances the expression of foreign genes in Escherichia coli, *Gene 73*, 227-235.
[24] Larson, M. H., Greenleaf, W. J., Landick, R., and Block, S. M. (2008) Applied force reveals mechanistic and energetic details of transcription termination, *Cell 132*, 971-982.
[25] Rodrigo, G., Landrain, T. E., and Jaramillo, A. (2012) De novo automated design of small RNA circuits for engineering synthetic riboregulation in living cells, *Proc Natl Acad Sci U S A 109*, 15271-15276.
[26] Kredel, S., Oswald, F., Nienhaus, K., Deuschle, K., Rocker, C., Wolff, M., Heilker, R., Nienhaus, G. U., and Wiedenmann, J. (2009) mRuby, a bright monomeric red fluorescent protein for labeling of subcellular structures, *PLoS One 4*, e4391.
[27] Shin, J., and Noireaux, V. (2012) An E. coli cell-free expression toolbox: application to synthetic gene circuits and artificial cells, *ACS Synth Biol 1*, 29-41.
[28] Lim, K. H., Huang, H., Pralle, A., and Park, S. (2013) Stable, high-affinity streptavidin monomer for protein labeling and monovalent biotin detection, *Biotechnol Bioeng 110*, 57-67.
[29] Noireaux, V., and Libchaber, A. (2004) A vesicle bioreactor as a step toward an artificial cell assembly, *Proc Natl Acad Sci U S A 101*, 17669-17674.
[30] Flynn, J. M., Neher, S. B., Kim, Y. I., Sauer, R. T., and Baker, T. A. (2003) Proteomic discovery of cellular substrates of the ClpXP protease reveals five classes of ClpX-recognition signals, *Mol Cell 11*, 671-683.
[31] Sanger, F., Coulson, A. R., Friedmann, T., Air, G. M., Barrell, B. G., Brown, N. L., Fiddes, J. C., Hutchison, C. A., 3rd, Slocombe, P. M., and Smith, M. (1978) The nucleotide sequence of bacteriophage phiX174, *J Mol Biol 125*, 225-246.
[32] Shin, J., and Noireaux, V. (2010) Study of messenger RNA inactivation and protein degradation in an Escherichia coli cell-free expression system, *J Biol Eng 4*, 9.
[33] Lentini, R., Forlin, M., Martini, L., Del Bianco, C., Spencer, A. C., Torino, D., and Mansy, S. S. (2013) Fluorescent proteins and in vitro genetic organization for cell-free synthetic biology, *ACS Synth Biol 2*, 482-489.